AD_____

Award Number: W81XWH-08-1-0462

TITLE: Influence of Tumor Microenvironment on the Molecular Regulation of Prostate Cancer Progession

PRINCIPAL INVESTIGATOR: Dr. Clayton Yates

CONTRACTING ORGANIZATION: Tuskegee University
Tuskegee Institute, AL 36068

REPORT DATE: August 2011

TYPE OF REPORT: Revised Final

PREPARED FOR: U.S. Army Medical Research and Materiel Command
Fort Detrick, Maryland 21702-5012

DISTRIBUTION STATEMENT: Approved for public release; distribution unlimited

REPORT DOCUMENTATION PAGE

Form Approved
OMB No. 0704-0188

1. REPORT DATE *(DD-MM-YYYY)*	**2. REPORT TYPE**	**3. DATES COVERED** *(From - To)*
August 2011	Revised Final	15 July 2008 - 14 July 2011

4. TITLE AND SUBTITLE

Influence of Tumor Microenvironment on the Molecular Regulation of Prostate Cancer Progession

5a. CONTRACT NUMBER

5b. GRANT NUMBER
W81XWH-08-1-0462

5c. PROGRAM ELEMENT NUMBER

6. AUTHOR(S)
Dr. Clayton Yates

E-Mail: cyates@mytu.tuskegee.edu

5d. PROJECT NUMBER

5e. TASK NUMBER

5f. WORK UNIT NUMBER

7. PERFORMING ORGANIZATION NAME(S) AND ADDRESS(ES)

Tuskegee University
Tuskegee Institute, AL 36068

8. PERFORMING ORGANIZATION REPORT NUMBER

9. SPONSORING / MONITORING AGENCY NAME(S) AND ADDRESS(ES)
U.S. Army Medical Research and Materiel Command
Fort Detrick, Maryland 21702-5012

10. SPONSOR/MONITOR'S ACRONYM(S)

11. SPONSOR/MONITOR'S REPORT NUMBER(S)

12. DISTRIBUTION / AVAILABILITY STATEMENT
Approved for Public Release; Distribution Unlimited

13. SUPPLEMENTARY NOTES

14. ABSTRACT

Please see next page.

15. SUBJECT TERMS

Tumor Microenvironment, Kaiso expression in Prostate Cancer

16. SECURITY CLASSIFICATION OF:			**17. LIMITATION OF ABSTRACT**	**18. NUMBER OF PAGES**	**19a. NAME OF RESPONSIBLE PERSON**
a. REPORT	**b. ABSTRACT**	**c. THIS PAGE**			USAMRMC
U	U	U	UU	66	**19b. TELEPHONE NUMBER** *(include area code)*

14. ABSTRACT

Background: Metastasis is a multi-step process wherein tumor cells detach from the primary mass, migrate through barrier matrices, gain access to conduits to disseminate, and subsequently survive and proliferate in an ectopic site. During the initial invasion stage, prostate carcinoma cells undergo epithelial–mesenchymal-like transition with gain of autocrine signaling and loss of E-cadherin, hallmarks that appear to enable invasion and dissemination. However, we have recently reported that some metastases express E-cadherin in bone or liver metastasis. These finding indicate that phenotypic plasticity occurs late in prostate cancer within the metastatic microenvironment. To determine the molecular signing mechanism responsible for this occurance, we have focused on Kaiso, a transcriptional repressor, is expressed in the cytoplasmic and nuclear compartments of cells. The objective of this award is to determine the influence of tumor microenvironment and the signaling mechanism through which tumor plasticity is accomplished.

Methods: HS-27a bone marrow stromal cells were cocultured with ARCaP prostate cancer cells for various time intervals in 2D or 3D culture situations. Growth and clonogenic survival was determined by the ability of prostate cells to form colonies or proliferation in the presence or absence of 4 Gy radiation treatment or inhibiting antibodies. The surviving fraction of colonies was calculated as a ratio of the number of colonies formed, divided by the total number of cells plated, times the plating efficiency [(# of colonies formed ÷ total # cells plated) x plating efficiency].

Additionally, Kaiso expression was determined in patients tumors utilizing immunohistochemistry. Kaiso expression and localization was determined utilizing qRT-PCR, immunoblotting, and immunofluorescence in prostate cancer cell lines. Functional analysis of Kaiso in shKaiso-DU-145 and PC-3 cells was determined by wound healing assay, and matrigel invasion assay. sh-Kaiso PC-3 cells, were subsequently analyzed for EMT markers expression by qRT-PCR, immunoblotting in the presence and absence of demethylation agent. Additionally direct binding of Kaiso to E-cadherin promoter was determined by Chromatin Immunoprecipitation assay.

Results: HS-27a human bone stromal cells, in 2D or 3D coultures, induced cellular plasticity in human prostate cancer EMT model $ARCaP_E$ and $ARCaP_M$ cells. Cocultured $ARCaP_E$ and $ARCaP_M$ cells developed increased survival and growth advantage, with $ARCaP_E$ exhibiting the most significant increases in presence of bone or prostate stroma. Prostate or bone stroma induced significant resistance to radiation treatment in $ARCaP_E$ cells compared to $ARCaP_M$ cells.

In separate, but linked set of experiments we further demonstrated enrichment of nuclear Kaiso expression was observed in primary and metastatic prostate tumors compared to normal prostate epithelium. Nuclear expression significantly correlates with clinicopathological features. EGF stimulation increases Kaiso expression, and causes a shift of Kaiso to the nucleus. sh-Kaiso abrogation in DU-145 and PC-3 cells blocks basal and EGF-induced cell migration and invasion, effects that are associated with re-establishment of cell-cell contacts and enhanced expression of the tumor suppressor, E-cadherin and a reversal of EMT. Lastly, Kaiso directly binds to methylated sequences with the E-cadherin promoter.

Conclusion: Our data demonstrate that the E-cadherin expressing cells have a growth and survival advantage over non-E-cadherin expressing cells within the tumor microenvironment. Furthermore, this is possibly due to growth factor regulation of a newly identified oncogene, Kaiso, in prostate cancer. .

Table of Contents

INTRODUCTION

The DoD funded Prostate Cancer New Investigator Award‟ (PC073977) entitled "The role of Tumor Microenvironment on Prostate Cancer Progression. We are pleased to report all aims are completed. As the aims are interrelated and interdependent, we have highlighted the accomplishments successively within the context of the entire text.

Overarching aims are to "Determine role of Tumor microenvironment on Prostate Progression" The work below represents work completed during Year 1 and 2 of the award. (*Final Publications included in Appendix*)To complete this aim we first determined the effect of tumor-stromal interactions on epithelial vs mesenchymal prostate cancer cell line ARCaP. The ARCaP model has been described to closely mimic the patho-physiology of advanced clinical human prostate cancer bone metastasis [10]. The $ARCaP_E$ cells were derived from single-cell dilutions of the ARCaP cells. These cells exhibit a cuboidal-shaped epithelial morphology with high expression of epithelial markers, such as cytokeratin 18 and E-cadherin. The lineage-derived $ARCaP_M$ cells have a spindle-shaped mesenchymal morphology and phenotype. $ARCaP_M$ cells have decreased expression of E-cadherin and cytokeratins 18 and 19, but increased expression of N-cadherin and vimentin. These cells have decreased cell adhesion and increased metastatic propensity to bone and adrenal glands [11]. The morphologic and phenotypic changes observed in the $ARCaP_M$ cells closely resemble that of cells undergoing EMT.

Figure 1

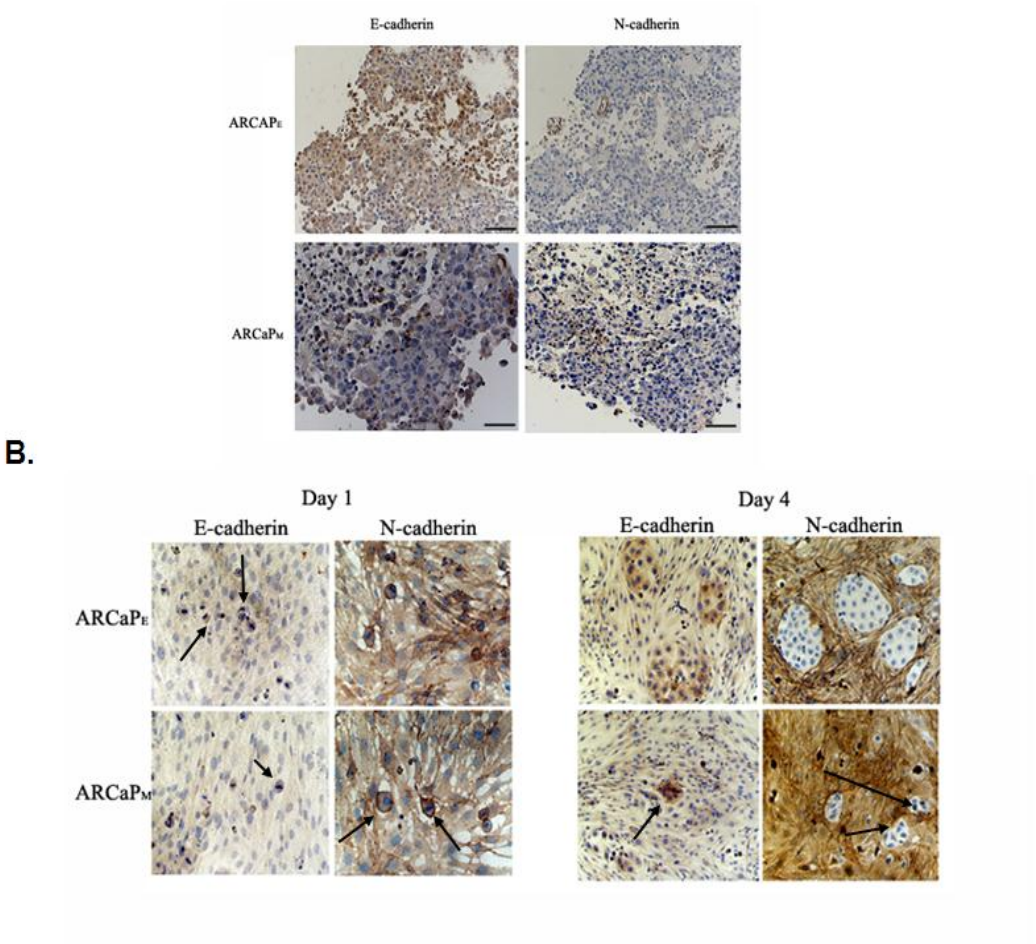

Figure 1. 3D co-culture of $ARCaP_E$ or $ARCaP_M$ with HS-27a cells show E-cadherin expression. (A) 1x 10^7 $ARCaP_E$ or $ARCaP_M$ were co-cultured with HS-27a cells in RWV for 3 days. Immunohistochemistry of organoids were stained with anti-E-cadherin or N-cadherin antibody. (B) 2D Cocultures of HS-27a were preformed utilizing a total of 50,000cm^2/ HS-27a fibroblasts, after which 20,000 cm^2 $ARCaP_E$ or $ARCaP_M$ were seeded on top of the fibroblast monolayer. The co-cultures were maintained in serum-free medium for 4 days. Immunocytochemistry of co-cultures over a 4 day period was performed utilizing anti-E-cadherin and N-cadherin antibodies. Shown are representative images of at least three experiments

Figure 1. 3D co-culture of $ARCaP_E$ or $ARCaP_M$ with HS-27a cells show E-cadherin expression. (A) 1x 10^7 $ARCaP_E$ or $ARCaP_M$ were co-cultured with HS-27a cells in RWV for 3 days. Immunohistochemistry of organoids were stained with anti-E-cadherin or N-cadherin antibody. (B) 2D Cocultures of HS-27a were preformed utilizing a total of 50,000cm^2/ HS-27a fibroblasts, after which 20,000 cm^2 $ARCaP_E$ or $ARCaP_M$ were seeded on top of the fibroblast monolayer. The co-cultures were maintained in serum-free medium for 4 days. Immunocytochemistry of co-cultures over a 4 day period was performed utilizing anti-E-cadherin and N-cadherin antibodies. Shown are representative images of at least three experiments

(MErT) of
me atients with
live tasis where
E-c e sought to
ide To assess
cellular plasticity of the ARCaP EMT model, we coultured ARCaP cells with HS-27a cells in 3D RWV (rotary wall vessel) system for 3 days. $ARCaP_E$ cells formed larger prostate organoids than $ARCaP_M$ cells, (data not shown). Upon immunohistochemical examination of organoids, we observed both $ARCaP_E$ and $ARCaP_M$ express E-cadherin and lack N-cadherin expression (Figure 1A). To further examine the influence of tumor-

stroma interactions over a multi-day period we utilized a similar 2D co-cultures method. Utilizing immunoctyochemical analysis, we observed a lack E-cadherin and robust N-cadherin staining after 1 day in both $ARCAP_E$ and $ARCaP_M$ cocultures. However by day 4, both $ARCaP_E$ and $ARCaP_M$ cells formed tumor nest that express E-cadherin and lack N-cadherin staining (Figure 1B). It is worthy to note that $ARCaP_M$ tumor nest appeared to develop at much smaller extent, compared to $ARCaP_E$ cocultures.

Since $ARCaP_E$ cells formed larger tumor nest and spheroids when co-cultured with HS-27a cells compared to $ARCaP_M$ cells, we sought to further assess if HS-27a cells preferentially stimulated the growth of $ARCaP_E$ cells versus $ARCaP_M$ cells. Utilizing GFP transfected HS-27a bone marrow stromal cells and RFP transfected $ARCaP_E$ or $ARCaP_M$ cells (Figure 2A), we examined the proliferative ability of ARCaP cells in homotypic and coculture conditions. Growth of RFP transfected $ARCaP_E$ and $ARCaP_M$ cells, respectively, was quantified by relative fluorescent unites (RFU) of transfected cell lines over a 6-day period in homotypic cultures and coculture conditions (Figure 2A). As previously reported, homotypic cultured $ARCaP_M$ shows significant growth compared to $ARCaP_E$ homotypic cultures, however cocultures reversed this trend with $ARCaP_E$ cells demonstrating the most significant growth (Figure 2B). We also confirmed these findings in $ARCaP_E$ cells in coculture using clongenic assay. Although $ARCaP_M$ cells have a higher plating efficiency than $ARCaP_E$ cells, $ARCaP_E$ cells exhibited an 8-fold increase in their ability to form colonies after coculture compared to 1.35 fold increase of cocultured $ARCaP_M$ cells (Figure 2C). Phase-contrast microscopy of colonies after co-culture show that $ARCaP_M$ colonies appear loosely adherent, while $ARCaP_E$ cells are compact and interact physically with few of the bone stromal fibroblast (Figure 2D). Taken together, these results demonstrate that $ARCaP_M$ cells re-express E-cadherin when grown with bone stromal cells for longer periods. Additionally, $ARCaP_E$ cells which have high levels of E-cadherin gain enhanced growth and self-renewal ability when cocultured with bone stromal cells.

Figure 2

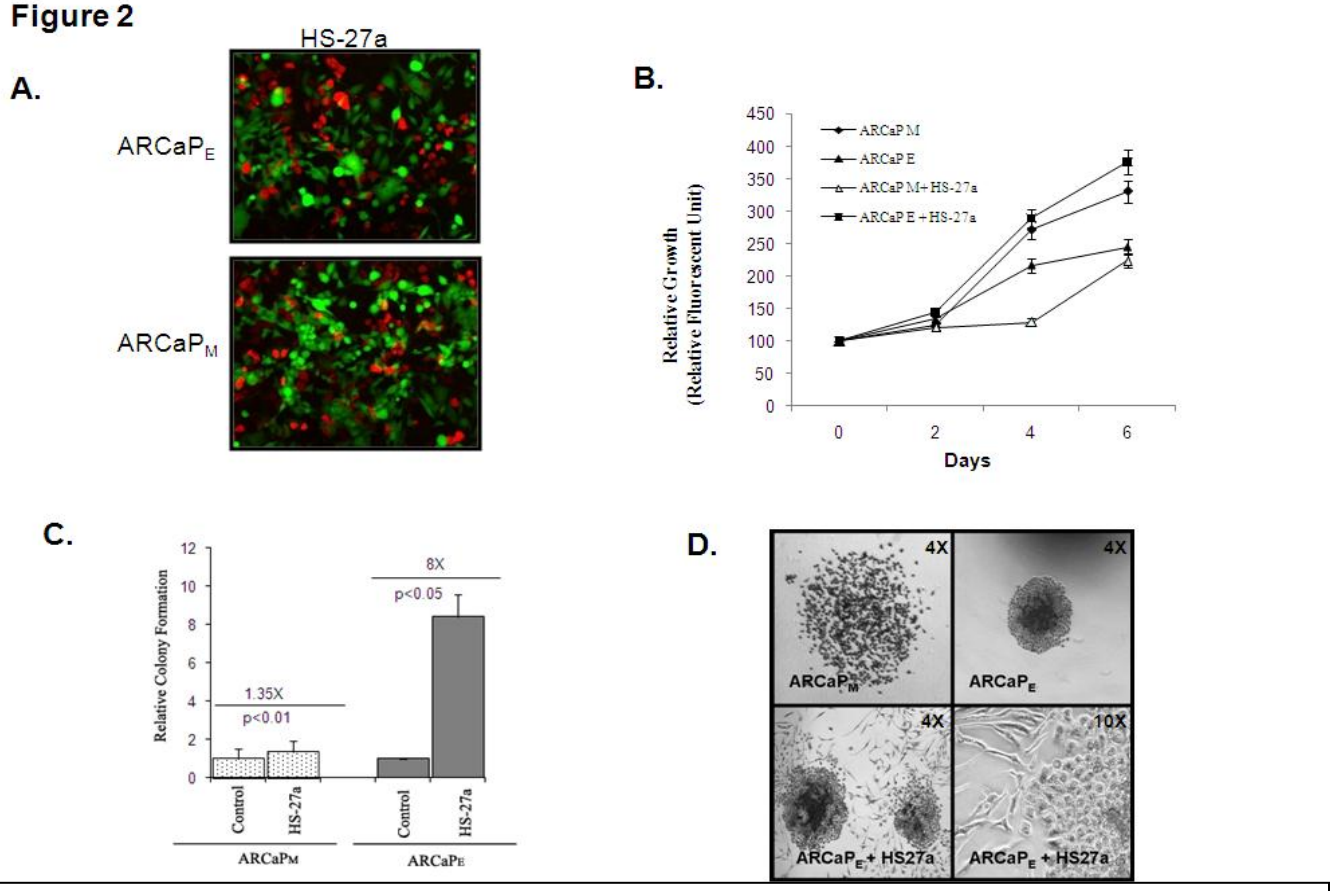

Figure 2. ARCaP$_E$ cells show a growth and colony forming capacity advantage in presence of HS-27a cells. (A) ARCaP$_M$ cells were cocultured in the presence of GFP-HS-27a cells over a 6-day period. Growth of RFP. ARCaP$_E$ or ARCaP$_M$ human prostate cancer cells was assessed by RFU (relative fluorescent units) in the presence cocultures over a 6-day period. Results are means ± SE of three independent experiments. *P , 0.05 (students t-test) compared to cell number at day 1 ±SEM (B) Clongenic colony forming capacity of ARCaP$_E$ and ARCaP$_M$ prostate cancer cell after coculture ±SEM. ARCaP$_M$ data was normalized to ARCaP$_M$ control, and ARCaP$_E$ data was normalized to ARCaP$_E$ control. (C) ARCaP$_E$ or ARCaP$_M$ cells were cocultured with HS-27a cells. Shown are phase contrast images of colonies formed in the clongenic assay.

Stromal Cells Influence Radiation Treatment in Prostate Cancer cells

Mesenchymal cancer cells have been thought to be more tumorigenic, aggressive and resistant to treatments when compared to epithelial cancer cells [15]. A similar trend was observed in both $ARCaP_E$ and $ARCaP_M$ cells after (4 Gy) irradiation treatment. $ARCaP_M$ homotypic cancer cells are more resistant to radiation treatment compared to $ARCaP_E$ homotypic cancer cells (Figure 3A). However, $ARCaP_M$ co-cultures did not affect the radiation sensitivity of $ARCaP_M$ cancer cells. The highly sensitive $ARCaP_E$ cells exhibit a significant increased resistance to radiation therapy, up to 3 fold, as result of their interaction with bone stromal cells

Figure 3

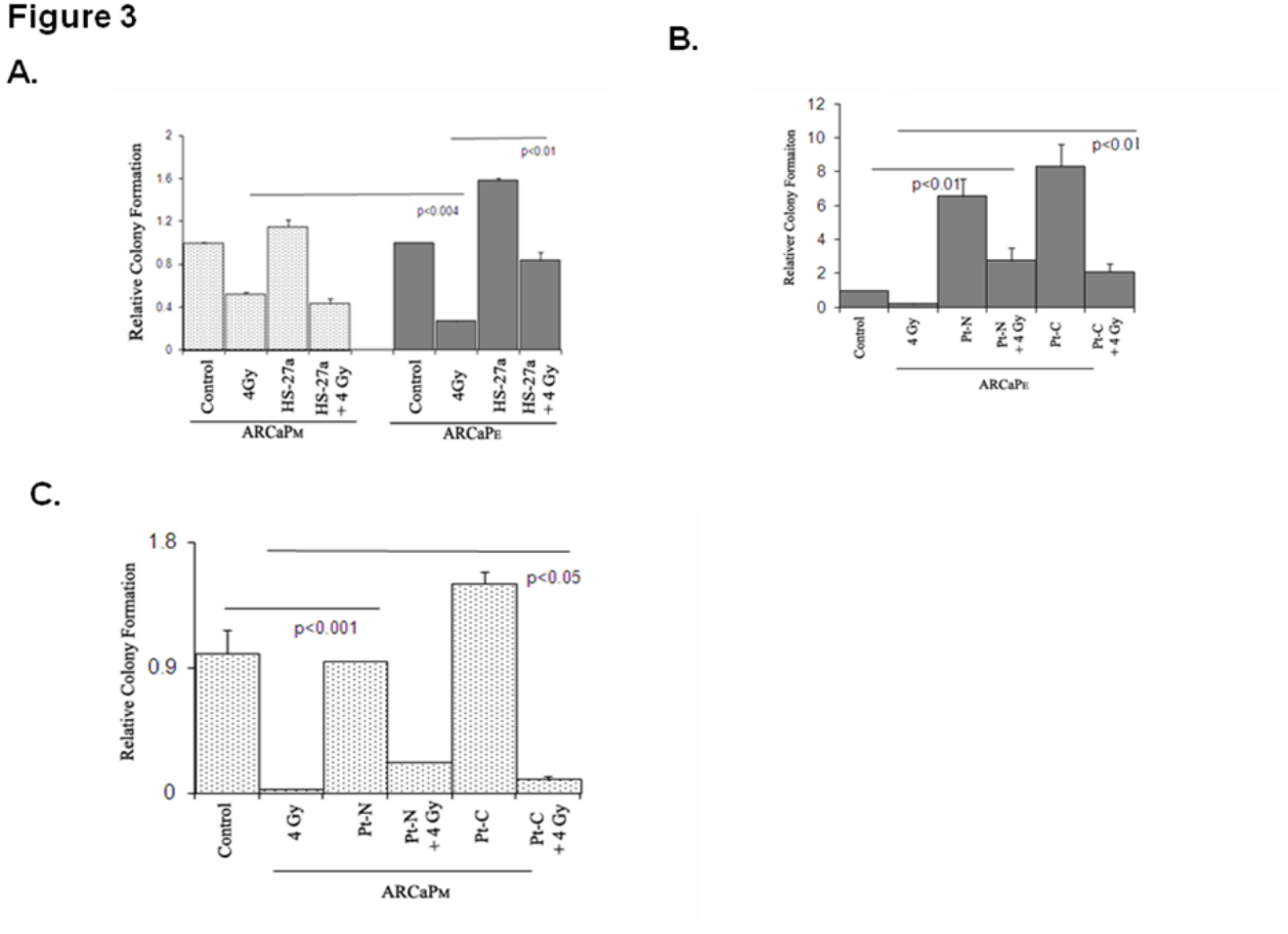

Figure 3. Cocultured $ARCaP_E$ cells gain cell colony forming capacity and radiation resistance when grown with bone and prostrate stromal cells. (A) $ARCaP_E$ or $ARCaP_M$ co-cultured cells were irradiated 24 hrs after coculture with HS-27a cells and cancer cell colony forming capacity was assayed using clongenic assay. Results are means ± SE of three independent experiments. $ARCaP_M$ experimental data normalized to $ARCaP_M$ control and $ARCaP_E$ experimental data normalized to $ARCaP_M$ control (B). $ARCaP_E$ cocultured with prostate fibroblasts Pt-C (Cancer associated fibroblast) or Pt-N (Normal fibroblast) were irradiated and compared to non-irradiated co-cultures. Cell colony forming capacity was assayed by clongenic assay. Data normalized to $ARCaP_E$ control levels. (C) $ARCaP_M$ cocultured with Pt-C or Pt-N were irradiated and compared to non-irradiated co-cultures. Cell colony forming capacity was assayed by clongenic assay. Data normalized to $ARCaP_M$ control levels

(Figure 3A, $p<0.01$). To further assess the role of the prostate stroma on tumor-interactions influencing ARCaP cellular behavior, we co-cultured paired prostate fibroblast cells isolated either from normal (Pt-N) or cancer associated regions (Pt-C) [16]. Again, $ARCaP_E$ cells co-cultured with (Pt-N) or (Pt-C) exhibited a 7-fold and 8-fold increase in colony formation, respectively (Figure 3B, $p<0.01$). We also saw a similar trend in a growth analysis assay (data not shown). However when measuring clongenic ability after radiation treatment, $ARCaP_E$ cells co-cultured with either Pt-N or Pt-C had increased radiation resistance, with a 2-fold difference observed between homotypic cultured cells. Although a significant increase in clongenic formation was observed in Pt-C versus Pt-N cocultures ($p<0.05$), this did not significantly effect of the radiation sensitivity of $ARCaP_M$ cells (Figures 3C). Taken together, both bone and prostate stroma have an inductive effect on $ARCaP_E$ cancer cells and mediate radiation resistance (up to 2-3 fold) in epithelial cancer phenotype, but not in $ARCaP_M$ mesenchymal cancer cells.

Figure 4

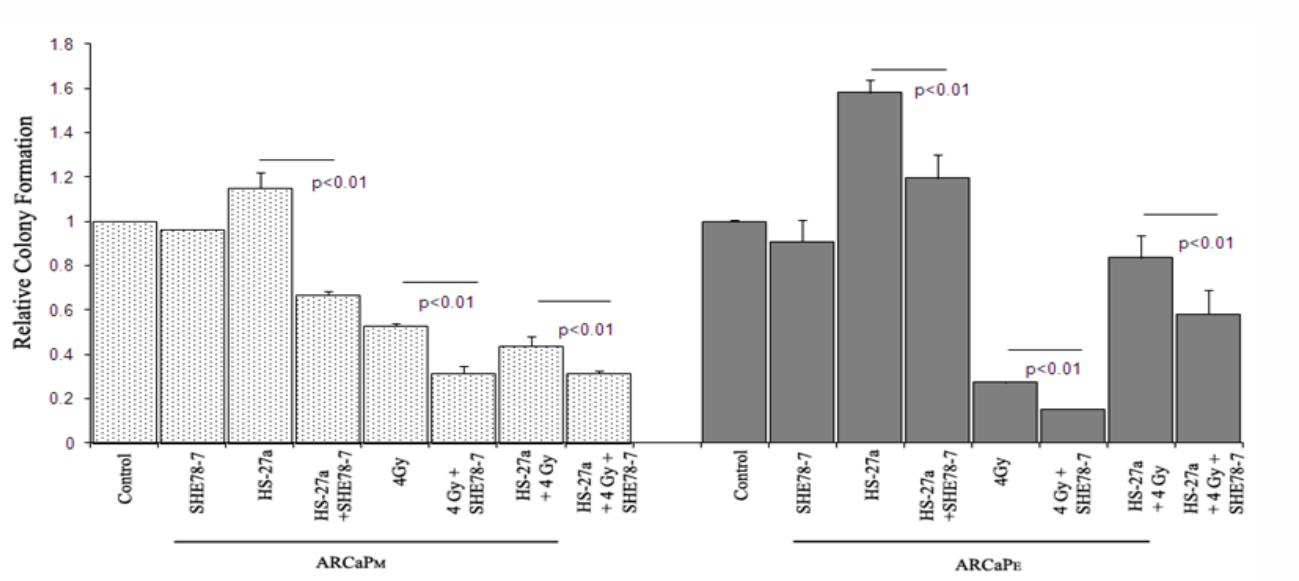

Figure 4 Effect of Anti-E-cadherin antibody on tumor-stroma interactions. A. $ARCaP_M$ and $ARCaP_E$, cells were pre-treated with Anti-E-cadherin antibody (SHEP8-7), cocultured with HS-27a stromal cells for 24 h and radiated with 4 Gy. Cell colony forming capacity was assayed using clongenic assay. $ARCaP_M$ data normalized to $ARCaP_M$ control levels, and $ARCaP_E$ data normalized to $ARCaP_E$ control levels.

Blocking Adhesive contact effects Radiation Sensitivity of Co-cultured ARCaP cells

The importance of cell adhesion (i.e. cell-cell and cell-ECM adhesion) on the survival of disseminated cancer cells has been well documented as a requirement for colonization and survival within the metastatic microenvironment [17-19]. Therefore we utilized a well known E-cadherin blocking antibody (SHEP8-7) and a pan-integrin antibody (CNT095) that targets human alpha-v-integrin, and also was shown to block prostate tumor growth within bone [20]. Since $ARCaP_E$ cells express high levels of the epithelial marker E-cadherin,

and $ARCaP_M$ cells can be microenvironmentally induced to express E-cadherin, we tested whether either of these blocking antibodies would affect the colony forming ability of either $ARCaP_E$ and $ARCaP_M$ bone stroma cocultured cells. Pretreatment with E-cadherin antibody did not affect the colony forming capacity of either $ARCaP_E$ or $ARCaP_M$ homotypic cultured cells, however significantly reduced the ability of $ARCaP_M$ ($p<0.001$)

Figure 5

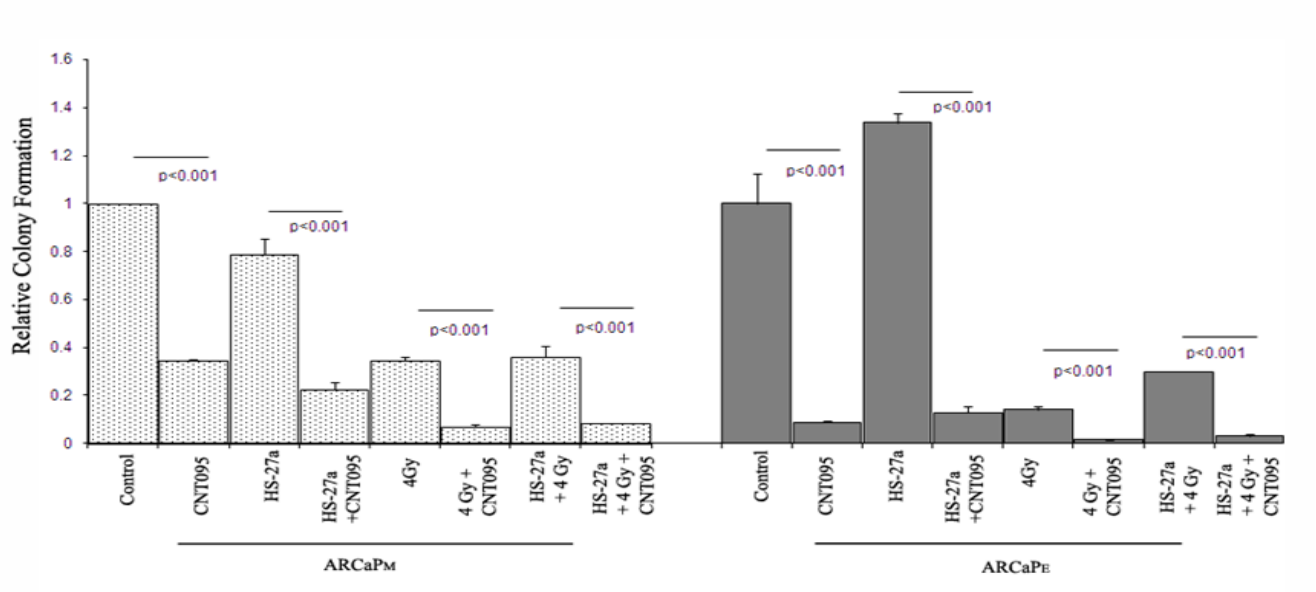

Figure 5 Effect of Anti-alpha v integrin (CNT095) on tumor-stroma interactions. $ARCaP_M$ and $ARCaP_E$, cells were pre-treated with CNT095 antibody were cocultured with HS-27a stromal cells for 24 h and radiated with 4 Gy. Cell colony forming capacity was assayed using clongenic assay. $ARCaP_M$ data normalized to $ARCaP_M$ control levels, and $ARCaP_E$ data normalized to $ARCaP_E$ control levels.

and $ARCaP_E$ ($p<0.01$) coultured cells to form colonies (Figure 4). Additionally, E-cadherin blocking antibody pretreatments further increased sensitivity to radiation treatment of $ARCaP_M$ cells in homotypic and co-cultured conditions, similarly ($p<.0.01$). E-cadherin blocking antibody pretreated $ARCaP_E$ cells showed the most significant increased sensitivity to radiation treatment in homotypic compared cocultured conditions ($p<0.001$), however a significant reduction in colony formation, to a lesser extent, was observed in $ARCaP_E$ cocultured cells (Figure 4, $p<0.01$). Therefore, targeting E-cadherin limited both epithelial and mesenchymal cells ability to form colonies after coculture with bone stromal cells.

To determine the influence of intergin alpha v cell adhesion with bone microenvironment, we performed similar clongenic formation assay. Pretreatment with CNT095 antibody significantly decreased the clongenic ability of both $ARCaP_M$ and $ARCaP_E$ cells in homotyic cultures (Figure 5, $p< 0.001$). Additionally, CNT095 significantly decreased bone stroma induced radiation resistance in cancer cells in both $ARCaP_M$ ($p<0.001$) and $ARCaP_E$ ($p<0.001$) cancer cells, with the most significant reduction in cocultured conditions ($p<0.001$) (Figure 5). Taken together, these results suggest that bone stroma induced radiation resistance is mediated through both E-cadherin and integrin alpha v beta signaling in epithelial and mesenchymal cells.

Thus, E-cadherin and integrin alpha v beta appear to present novel targets for metastatic and radiation resistant cells.

Aims 2 and 3 **Kaiso Expression in Relationship to E-cadherin expression. Completed during years 2 and 3 of the Award (*Final Publication included in Appendix*)**

Kaiso expression and subcellular localization.

To evaluate the expression and localization of Kaiso during prostate cancer progression, immunohistochemistry was used to evaluate samples from 172 patients, consisting of normal tissue (9 patients), benign prostatic hyperplasia (14 patients), adjacent normal tissue (17 patients), primary tumors (142 patients), and metastases (6 patients). There was low expression of the Kaiso protein in luminal cells of non-cancerous samples (Fig 6, panel A); expression was predominantly in the membrane or cytoplasm (Fig 6, panels B and C). There was, however, nuclear expression of Kaiso in the basal cells of adjacent normal tissue (panel B).

Figure 6

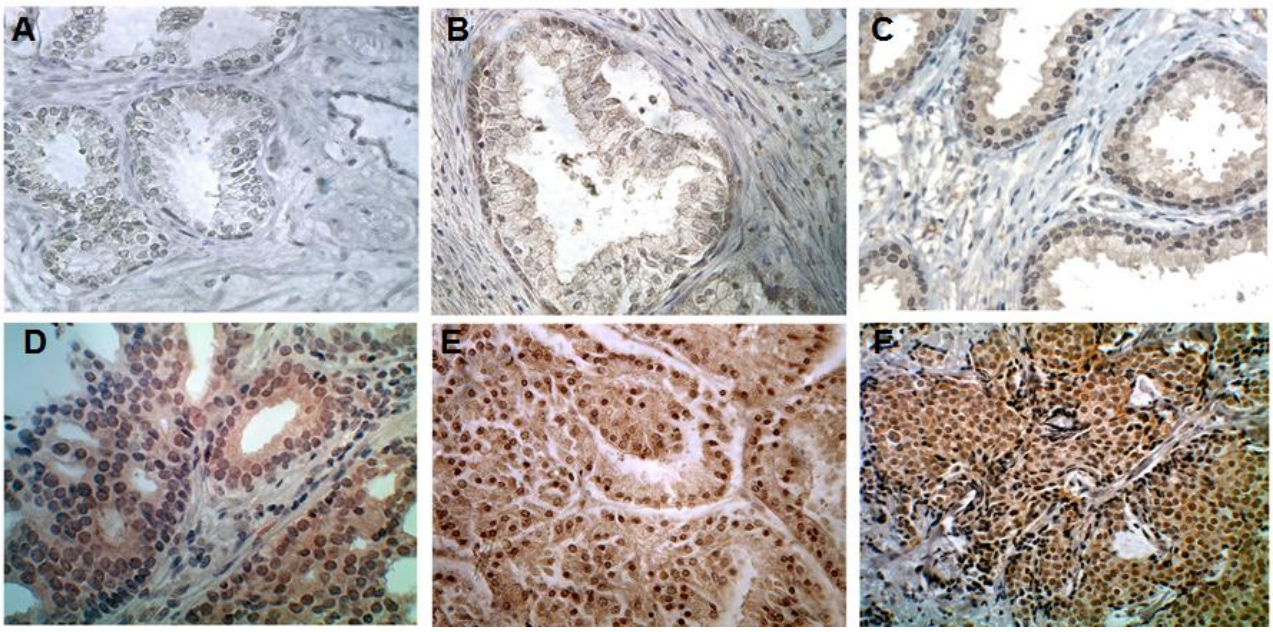

Fig 6 – ***Abnormal nuclear expression of Kaiso in Prostate Cancer Specimens***. Representative data from imunohistochemical studies of 172 PCa specimens are shown. *A,* Kaiso levels in a normal, healthy, prostate, with low staining seen in glandular epithelia. *B,* Kaiso expression in normal epithelia from adjacent PCa tumors, shows discernible cytoplasmic staining in epithelia, and nuclear positivity in the basal cells. *C,* Kaiso expression in Benign Prostatic Hyperplasia (BPH) show cytoplasmic with low nuclear positivity. *D,* Kaiso expression in low Grade 1 tumors exhibited a general up-regulation of Kaiso expression with cytoplasmic and nuclear positivity. *E-F,* High Grade 4 and lymph node metastasis exhibited uniform intense nuclear expression of Kaiso. All images were taken at a 400X magnification.

In contrast to previous reports, Kaiso expression was observed within the nucleus, with weak to moderate expression in tumors with low Gleason scores (panel D), and strong, intense expression in tumors with high Gleason scores and in metastases (panels E and F). Nuclear expression of Kaiso was found to significantly

Figure 7

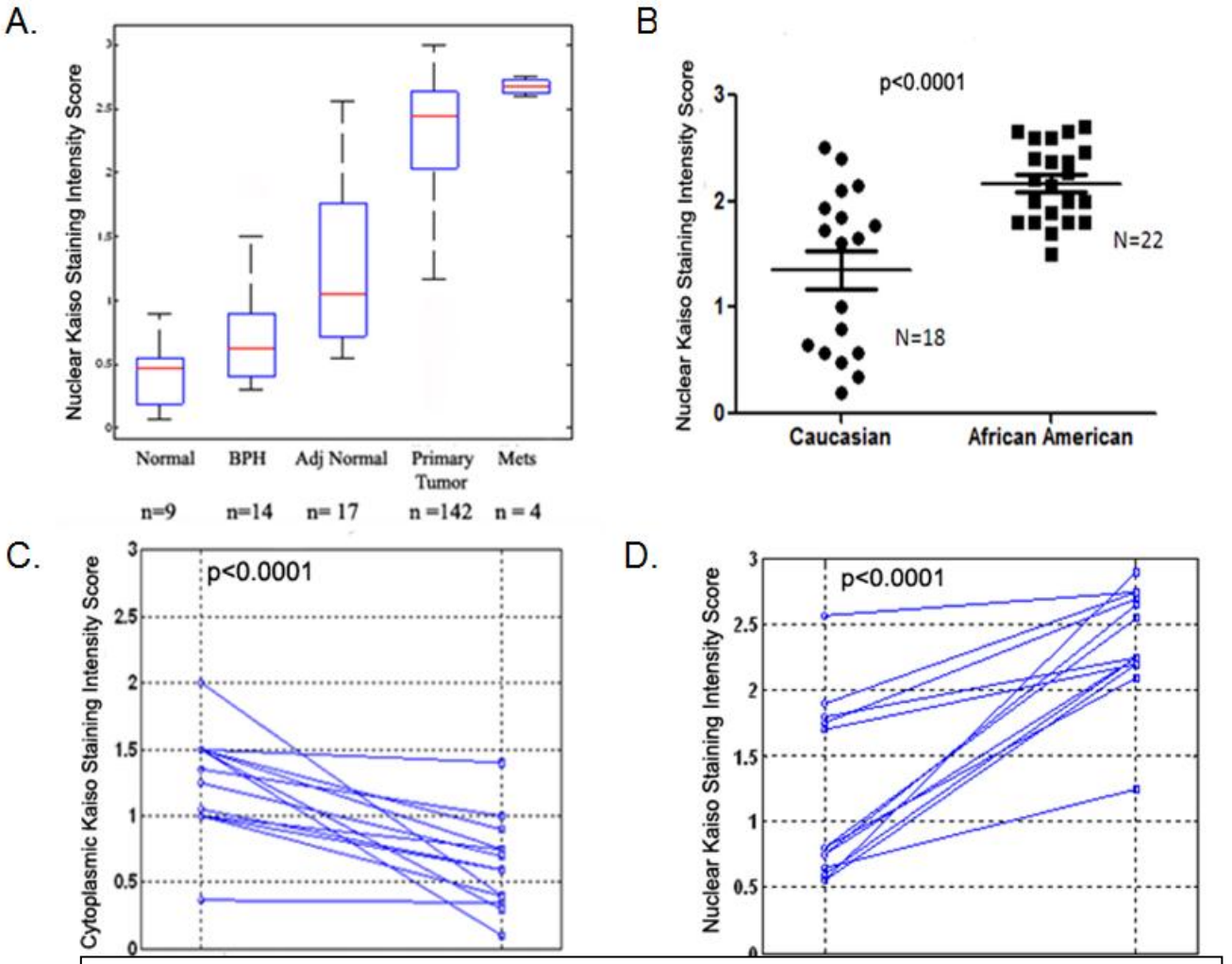

Fig 7 – ***Quantitative Analysis of Nuclear Kaiso in Prostate Tumor Progression.*** *A,* nuclear expression of Kaiso was analyzed and presented in box plot. Nuclear Kaiso levels increase monotonically from normal, BPH, adjacent normal, primary tumor, and metastasis, with all four p-values less than 0.05. (Normal and BPH is p=0.016; BPH and adjacent normal is p=0.01; adjacent normal and malignant is less than p<0.0001; malignant and metastasis p<0.0001). *B,* Points represent nuclear Kaiso staining intensity of individual African-American and Caucasian patients of similar age (67-80) and grade 3; bars represent the median value for the sample set. (p< .0001). *C,* Cytoplasmic Kaiso expression and *D,* Nuclear Kaiso expression in paired (surrounding non-tumor) normal and primary tumor tissues from n=13 prostate cancer patients.

correlate with tumor grade ≥ 2 (p <0.001) and Gleason score >7 (p <0.001) (Table 1). Cytoplasmic expression

was observed in tumors samples, however correlations with clinicalpathological features were not found to be significant. Increased nuclear expression occurred in a stage-specific manner, with the largest differential expression between metastatic tumors and normal samples, however difference between primary tumors and normal samples were significant as well. (Fig 7A). Further characterization of nuclear Kaiso expression in high grade of similar age African-Americans (n=22) and Caucasian (n=18) primary tumors, show that African-American patients express higher mean values of Kaiso ($p < 0.0001$): independent of grade and age (Fig 7B). Further Kaiso nuclear expression significantly correlated with race ($p=.0032$) (Table 2).

To determine if there is a shift in Kaiso localization in prostate tumors, matched normal and tumor samples were evaluated (n=13). Cytoplasmic expression was significantly decreased in paired primary tumors compared to normal samples ($p<0.0001$) (Fig 7C); however there were significant increases in nuclear expression within the same patients ($p<0.0001$) (Fig 7D). This analysis supports the idea that there is a progressive enhancement of abnormal Kaiso expression during prostate cancer progression and that the extent of abnormal expression correlates with progression.

Table 1 Correlation of Kaiso subcellular localization with Clinical Features

Characteristics	All patients	Cytoplasmic Kaiso Expression		p†	Nuclear Kaiso Expression	
		≤0.53(median)	>0.53		≤2.45(median)	>2.45
Total	142	70	72		73	69
Age						
≤69.5(median)	71	27	44	0.0072	35	36
>69.5	71	43	28		38	33
Grade						
≤2	70	39	31	0.1066	57	13
>2	69	29	40		13	56
Gleason score						
≤7	52	20	32	0.6394	29	23
>7	50	17	33		10	40
PSA(ng/mL)						
≤17(median)	15	4	11	0.1587	3	12
>17	15	5	10		8	7

†P value for the correlation of mean expression with clinical feature. p values were obtained with the χ^2 test
*Statistics were not preformed on samples without clinical information.

Table 2: Correlation of nuclear Kaiso expression and clinical features in 40 patients with prostate cancer

	All patients	Nuclear Kaiso Expression		p†
		≤1.87(median)	>1.87	
Total	40	23	23	
Age				
≤73(median)	19	11	8	0.555
>73	21	9	12	
African American	22	6	16	0.0032
Caucasian	18	12	6	

Expression and Subcellular Localization of Kaiso in Prostate Cancer Cell Lines

Figure 8

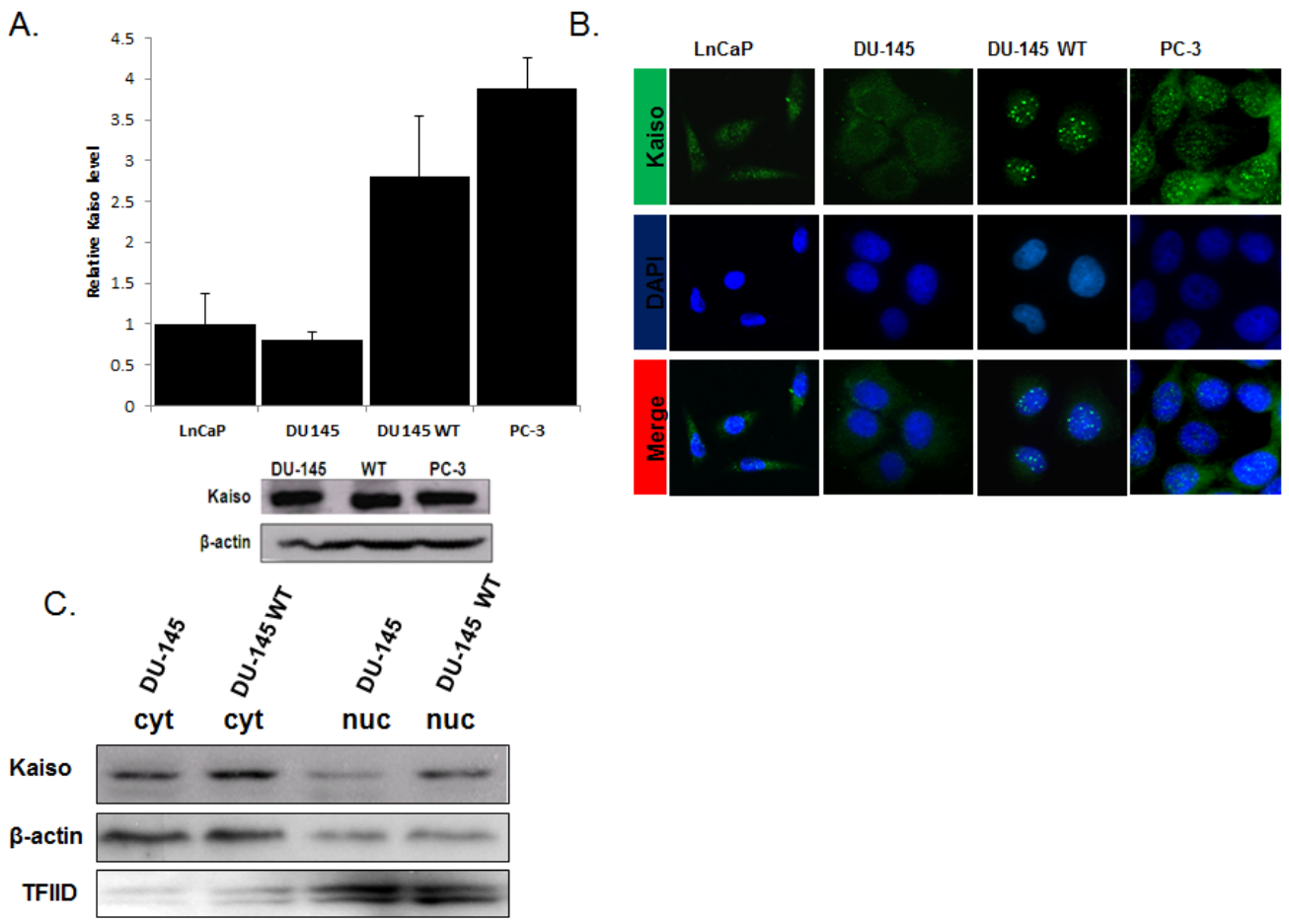

Figure 8. Endogenous Kaiso Expression and Localization in Prostate cancer progression model. **(A)** qRT-PCR analysis were used to compare the mRNA level of Kaiso in DU-145, DU-145 WT (EGFR overexpressing), and PC-3 cells. HRPT1 was used as loading control. **(B)** Immunofluorescence was utilzed to determine Kaiso localization in DU-145, DU-145 WT, and PC-3 cells. Anti-Kaiso 6F8 was utilized as primary antibody. Anti-Mouse HRP Anti-Mouse Alexa 488 was utilized as secondary antibody (Green). Dapi was utilzed as nuclear counter stain (Blue). **(C)** whole cell lysate and cytosolic and nuclear fractions were isolated by sequential extraction. As a loading control for the nuclear extracts, TFIID was used, and B-action used as a loading control for the whole-cell lysates and cytosolic fraction.

Since there have been no reports of Kaiso expression in prostate cancer cell lines, its expression and localization were evaluated in LnCaP, DU-145 and PC-3 cells, and in a DU-145 subline (DU-145WT) that was genetically engineered to over-express EGFR. DU-145 WT cells escape EGFR down-regulation and demonstrate enhanced invasiveness *in vitro* 12 and *in vivo* 13. qRT-PCR show that Kaiso levels were elevated at the mRNA in DU-145 WT and PC-3 cells compared to LnCaP and DU-145 cells (Supplemental Fig 8A). Confocal images show that Kaiso is located in both the cytoplasmic and nuclear compartments in all cell lines., However, the more aggressive DU-145WT and PC-3 cells showed increased presence of nuclear expression compared to LnCaP and DU-145 cells (Fig 8B), which was verified after quantification of fluorescent intensity in each compartment (Fig 8C). The influence of EGFR expression on Kaiso localization was further

demonstrated by the fact that subcellular fractions of DU-145 WT cells show elevated nuclear expression, while DU-145 cells exhibit low amounts of nuclear levels, which correlated with the confocal images (Supplemental Figure 8B). Thus, it appears that the subcellular localization of Kaiso is associated with EGFR expression.

Activation of EGFR signaling results in increased Kaiso expression and nuclear localization.

Various lines of evidence suggest the involvement of EGFR signaling in prostate cancer 14, 15. To identify EGFR as an upstream regulator of Kaiso, 10 ng/ml EGF, a concentration showing most significant fold increase (data not shown), was utilized in a time-dependent assay over 24 hours. DU-145, DU-145 WT, and PC-3 lines showed incremental increases in Kaiso expression at the RNA level; DU145WT cells show the greatest increase (4-fold) as early as 1 hour after EGF stimulation (Fig 9A). Increases in Kaiso expression were also observed at the protein level, as determined by immunoblots, with significant increases observed as early as 6 hours and sustained over 24 hours of exposure to EGF (Fig 9C).

Since we observed that increases in Kaiso expression are associated with a subcellular localization pattern in our patient cohort, we further determined if EGFR induced increases in Kaiso expression, coincided

Figure 9

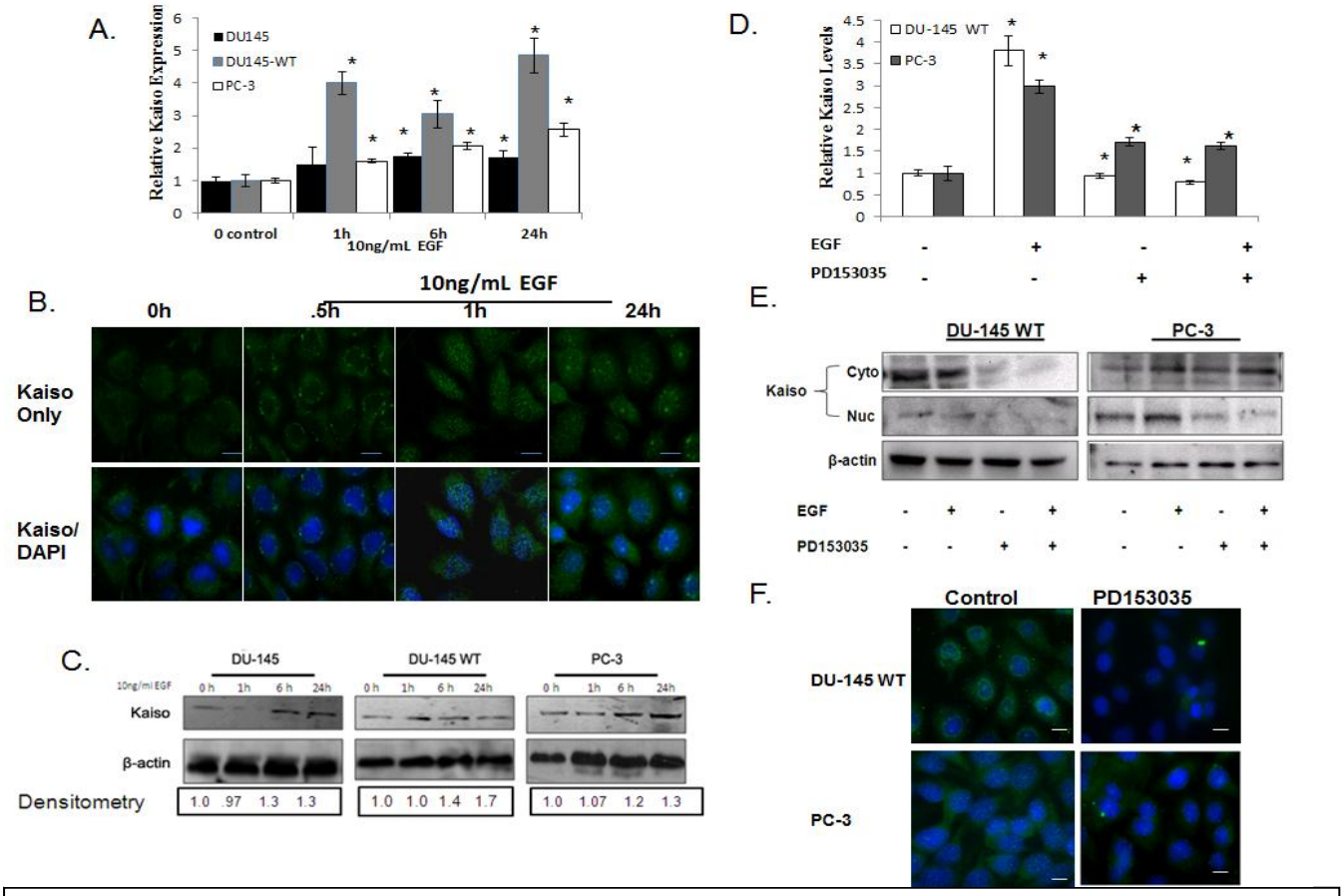

Fig 9 ***EGF induces Kaiso expression and cytoplasmic to nuclear localization in Prostate Cancer Cell lines.*** DU-145, DU-145 WT, and PC-3 prostate cancer cell lines were treated with 10ng/mL of EGF for 0, 1, 6, 24 hours and assayed for *A*, mRNA Kaiso levels by qRT-PCR with Kaiso-specific TaqMan primers and HPRT1 as the loading control . Data is normalized to control; n = 4 ± s.e. *B*, Kaiso protein levels in whole cell lysates by immunoblot utilizing, anti-Kaiso antibody and anti-β-actin antibody as loading control. Images shown are representative of three individual experiments. Densitometry was performed on individual time intervals and compared to control. *C*, Kaiso subcellular localization (Green) was determined by immunofluorescence. Note the colocalization of Kaiso in nucleus (Green) with nuclear stain Dapi (Blue) after EGF treatment in DU-145 cell. Images shown are representative of three individual experiments (Bar, 25 μM). *D.* Bar-graph quantification of Kaiso intensity in the individual cytoplasmic and nuclear compartments of DU-145 cells treated with 10ng/ml of EGFR compared to untreated control. Data is normalized to control; n =3 ± s.e *p<0.05. Kaiso mRNA levels, was determine by qRT-PCR, in the presence or absence of 10ng/ml EGF or EGFR specific kinase inhibitor, PD153035, in DU-145 WT and PC-3 cells utilizias the loading control. Data was normalized to control. *F*, Kaiso protein levels were determine by immunoblot in the cytoplasm and the nucleus in the presence or absence of 10ng/ml EGF or EGFR specific kinase inhibitor, PD153035, in DU-145 WT and PC-3 cells. β-actin served as loading control. Images shown are representative of three individual experiments. ng Kaiso specific TaqMan primers and HPRT1

with a subcellular localization in our cell culture model. After only 0.5 hours, EGF caused perinuclear accumulation of previously dispersed Kaiso in DU-145 cells, with visible nuclear accumulation at 1 hour. After 24 hours significant increases in both cytoplasmic and nuclear expression was observed, although nuclear expression was the most significant (Fig 9B). DU-145WT and PC-3 cells, which endogenously express high levels of nuclear Kaiso, demonstrated similar trends as DU-145 cells. Both cytoplasmic and nuclear Kaiso expression increased upon exposure to EGF, however nuclear expression remained significantly higher throughout the exposure times periods. To more clearly define the role of EGFR activation on increases in Kaiso expression and localization, we utilized an EGFR-specific kinase inhibitor, PD153035 (500 nM), in the presence or absence of EGF. PD153035 significantly reduced mRNA Kaiso expression levels even after EGF pretreatment (Fig 9 D). After subcellular fractionation and subsequent immunoblot of both DU-145 WT and PC-3 cells, we also observed that PD153035 significantly reduced expression of Kaiso in the cytoplasmic and nuclear compartments (Fig 9 E,F), which is a reversal of the expression pattern observed in endogenously expressing and EGF treated DU-145 WT and PC-3 cells. Thus, EGFR signaling positively affects Kaiso expression and subcellular localization.

Mediation by p120ctn of EGFR Induced Cytoplasmic-to-Nuclear Localization of Kaiso

Figure 10

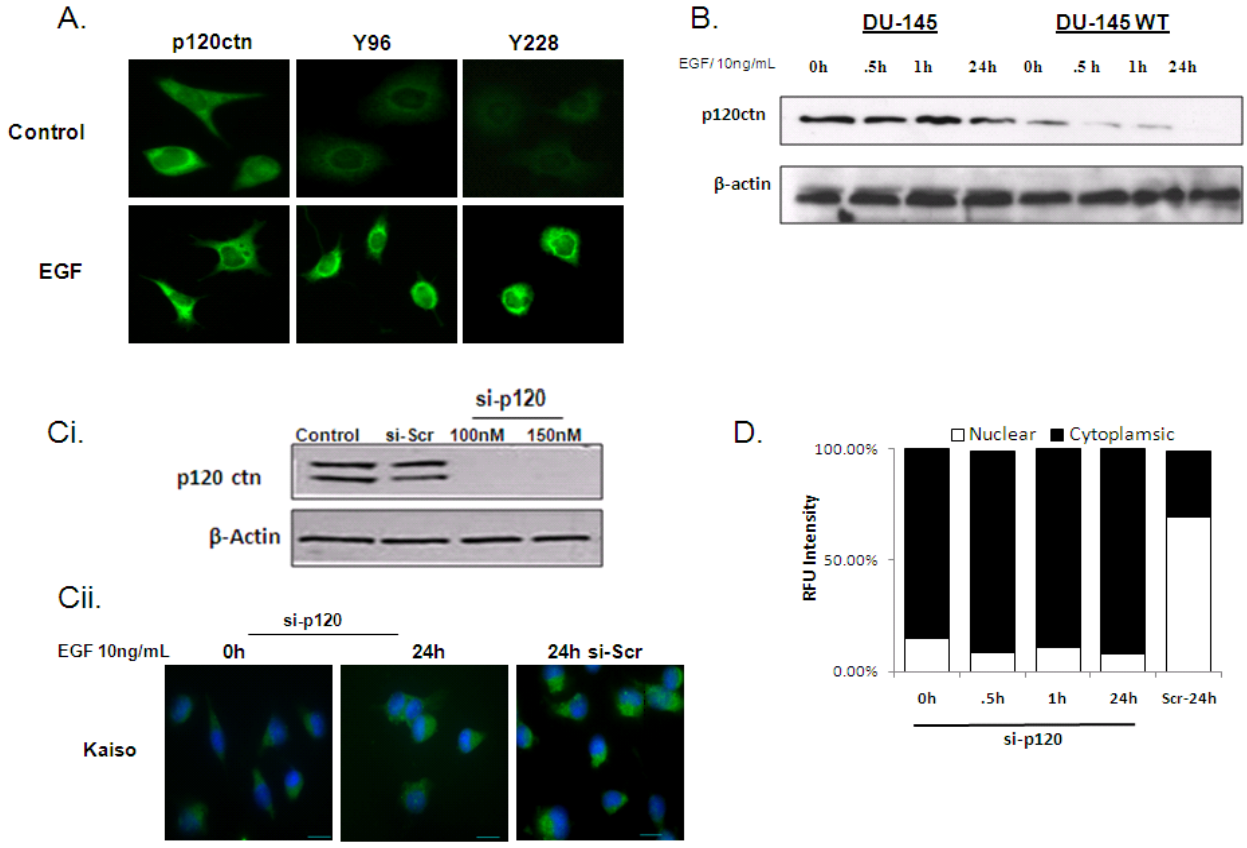

Fig 10. ***p120ctn is required for EGF induced nuclear localization of Kaiso.*** *A,* Activation of EGFR p120ctn tyrosine resides, Y228 and Y96 (Green) was determined by immunofluorescence utilizing specific antibodies to p120ctn tyrosine(s) Y228, and Y96. Images shown are representative of three individual experiments. *B,* DU-145 and DU-145 WT cells were treated with 10ng/ml for indicated time points and whole-cell lysates were immunoblotted for total p120ctn with β-actin served as loading control. *Ci,* p120ctn siRNA were exposed to DU-145 cells for 24 h and compared to the scrambled (si-Scr) control siRNA *Cii,* si-p120ctn pretreated cells were subsequently treated with 10ng/ml of EGF treatment for 24hrs and analyzed for Kaiso subcellular localization after 24hr by immunofluorescence utilizing anti-Kaiso antibody, Bar, 25 µM. *D,* relative intensity of fluorescence of the entire cell was measured in the cytoplasmic and nuclear subcellular compartments and quantified utilizing Metamorph imaging software.

p120^{ctn} has been demonstrated to specifically interact with Kaiso [4, 5, 25], however this has primarily been observed in the nucleus, where p120ctn inhibits Kaiso DNA binding [4, 26]. p120ctn contains multiple tyrosine residues located within its regulatory domain. Of these EGFR has been demonstrated to have specific phosphorylation of tyrosine Y228 [27], however a direct link between EGFR activation of p120ctn and Kaiso localization has not been demonstrated. Therefore, we sought to determine if cytoplasmic p120ctn mediates Kaiso nuclear localization. As determined by immunofluorescence, EGF induced the activation of full-length p120ctn as well as expression of

phosphorylated Y228 and Y96 (Fig 10A), which was maintained in the cytoplasm after 24 hours.We did not detect any levels of Y291 before or after EGF treatment (data not shown). In both DU-145 and DU-145WT cells, EGF stimulation also resulted in time-dependent decreases in total p120ctn expression (Figure 10B), which correlates with decreased p120ctn observed in prostate tumors [28].

To determine if p120ctn is required for EGFR-induced Kasio nuclear shuttling, siRNA-p120ctn transfection was used to reduce p120ctn expression (Fig 10Ci). Subsequently, siRNA p120ctn transfected DU-145 or scramble-transfected cells were treated with EGF for 24 hours. siRNA p120ctn transfected DU-145 cells failed to exhibit nuclear Kaiso expression over a 24-hour period of EGF stimulation compared to scramble-transfected cells, which showed nuclear Kaiso (Fig 10Cii). Further, quantification of fluorescent intensity of Kaiso expression revealed that Kaiso localization remained cytoplasmic in si-p120 treated cells, compared to predominantly nuclear expression in scramble-treated cells, after exposure to EGF (Fig 10D). These findings suggest the important role for $p120^{ctn}$ in Kaiso nuclear localization, and highlight a novel signaling cascade that regulates Kaiso subcellular localization in prostate cancer cell lines.

Figure 11

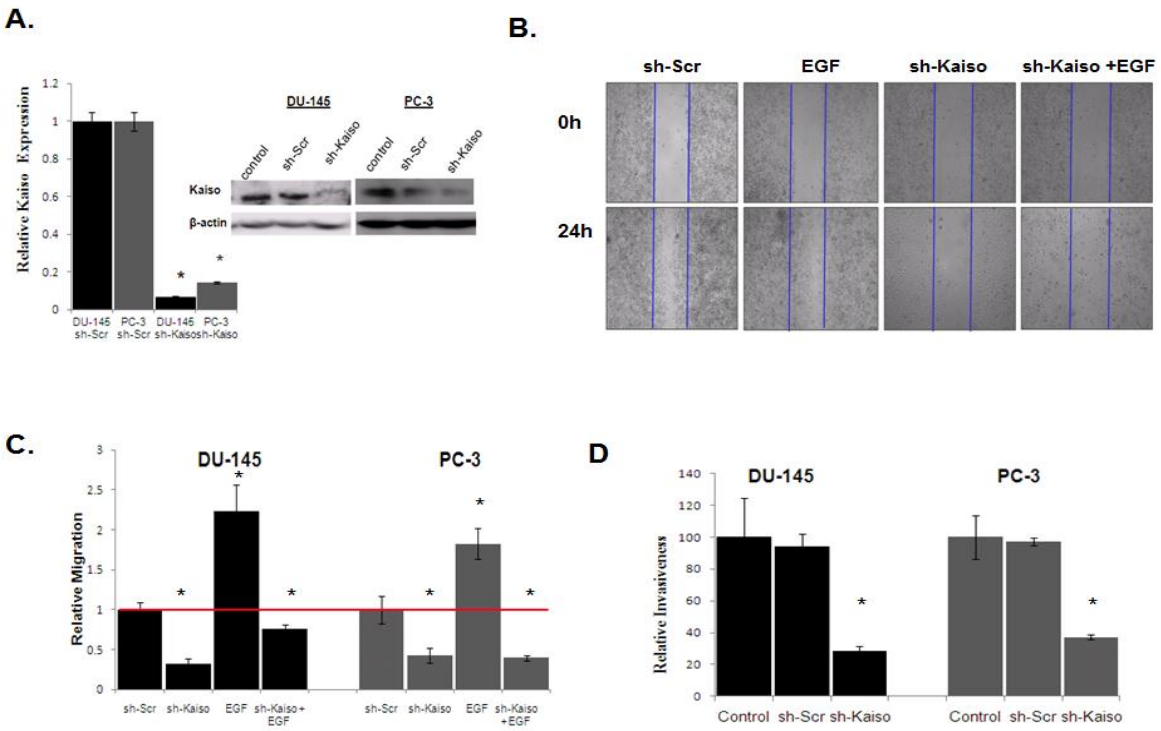

Fig 11. ***Kaiso is required for EGF induced cell migration and invasion.*** *A,* shRNA Kaiso downregulated Kaiso levels at mRNA as determined by qRT-PCR with Kaiso specific TaqMan primers and HPRT1 as the loading control or protein levels by immunoblot. β-actin served as loading control *B,* shRNA DU-145 or PC-3 cells were wounded and treated with EGF for 24 hours. Blue vertical bars indicate the starting area migration on Day 0. Photos were taken at 100X magnification and DU-145 images serve as representative images of both DU-145 and PC-3 cell lines. *C,* Quantification of area migrated in presence or absence of EGF stimulation in shRNA DU-145 or PC-3 cells compared to scrambled control si-Scr show that Kaiso depletion significantly decreased cell migration. Data was normalized to control (red bar). *C,* shRNA DU-145 and PC-3 cells were plated on Matrigel-coated filters and the invasive cells were fixed, stained with crystal violet, and counted. shRNA Kaiso cells show decreased invasiveness compared to sh-Scr and controls. All data presented are the mean of three independent experiments ±s.e.*P<0.05.

Promotion by Kaiso of EGFR-Induced Prostate Cancer Cell Migration and Invasion To further define the function of Kaiso in prostate cancer cells, DU-145 and PC-3 cells were stably transduced with a plasmid vector containing the sh-Kaiso silencing sequence (Fig 11A). Both sh-Kaiso DU-145 and sh-Kaiso PC-3 clones exhibited delayed migration, even in the presence of EGF stimulation, as measured by wound-healing assays (Fig 11 B,C). These results show that Kaiso is a mediator of EGFR-induced migration of prostate cancer cells. For cancer cells to invade surrounding tissue, the cells must degrade the underlying basement membrane. To determine the function of Kaiso in invasion by prostate cancer cells, sh-Kaiso PC-3 and sh-DU-145 were

seeded onto a filter coated with Matrigel and compared to cells exposed to the vector only. Suppression of endogenous Kaiso expression resulted in inhibition of cell invasion, resulting in a reduction in the ability of the cells to invade through Matrigel (Fig 11 D).

Figure 12

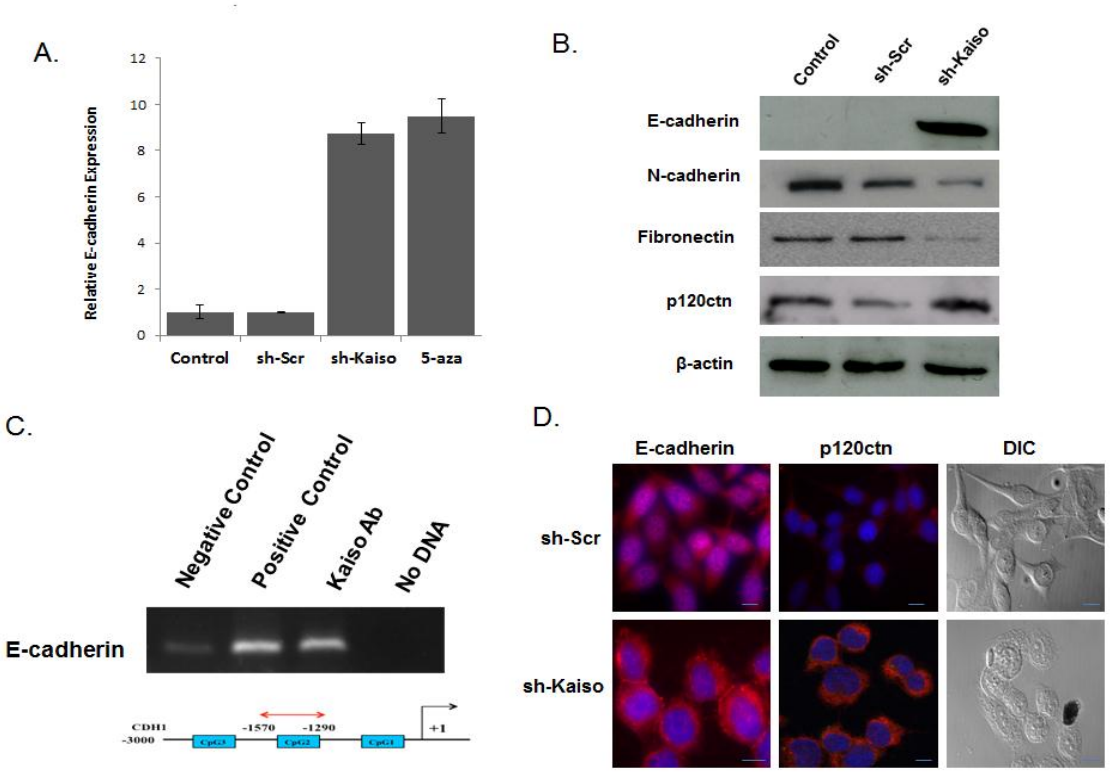

Fig 12. ***Kaiso regulates E-cadherin expression.*** *A,* E-cadherin mRNA levels was determined by qRT-PCR in sh-Kaiso PC-3 cells, sh-Scr (vector only) and control cell treated with demethylating agent, 5-aza-2'-deoxycytidine (5-aza) utilizing E-cadherin TaqMan specific primer with HPRT1 as the loading control. Data was normalized to control (n=4) ± s.e. *B,* sh-Kaiso PC-3 cells, sh-Scr (vector only) and control lysates were immunoblotted with an anti-E-cadherin, anti-N-cadherin antibody, anti-fibronectin antibody, and anti-p120ctn antibody. β-actin served as loading control. Shown is one of two representative blot series. *C.* Chromatin sample from PC-3 cells was subjected to ChIP by mouse IgG (lane 1) and specific antibodies against RNA pol II (lane 2) and Kaiso (6F/6F8, ChIP grade, Lane 3). Mouse IgG was used as a negative control. Lane 4 was no DNA negative control. ChIP products were analyzed by real-time PCR specific E-cadherin primer set (-1290 to-1570) to amply methylated region. *D,* E-cadherin and p120ctn localization was determined by immunofluorescence in sh-Kaiso or sh-Scr PC-3 cells utilizing anti-E-cadherin (Red) and Dapi nuclear stain (Blue). Arrows indicate E-cadherin staining at cell-cell junctions. DIC images demonstrate an altered cellular morphology in sh-Kaiso PC-3 compared to sh-Scr PC-3 cells (Bar,25 μM).

Repression of E-cadherin by Kaiso in prostate cancer cells

In various cancer types, increased cell migration and invasion has been attributed to growth factor induced loss of E-cadherin or to hypermethylation of the E-cadherin promoter [16, 17]. Since Kaiso has high affinity for methylated dinucleotide sequences and is regulated by EGFR, we next sought to determine if suppression of Kaiso restored E-cadherin expression in sh-Kaiso PC-3 cells. Control PC-3 cells and vector only cells show no E-cadherin expression, as previously reported [17]. sh-Kaiso PC-3 cells, however, show 8-fold increased expression of E-cadherin mRNA, as measured by qRT-PCR. Furthermore, the level of re-expression was comparable to that of PC-3 cells exposed to the demethylating agent, 5-aza-2'-deoxycytidine (5-aza) (Fig 12A). There was also an increase in epithelial markers E-cadherin and p120ctn expression, and a decrease in mesenchymal markers N-cadherin and fibronectin expression at the protein level, as determined by immunoblots (Fig 12B). To determine whether Kaiso directly binds to E-cadherin we performed ChIP assay. Immunoprecipitated DNA was incubated with anti-Kaiso antibody, anti-RNA pol II (positive control) or IgG antibody (negative control). and subjected to PCR with specific primers designed to amplify the Kaiso (mCGmCG) binding sites in the E-cadherin promoter region. Our results show that the Kaiso antibody (not negative control IgG antibody) enriched a mCGmCG fragment within the E-cadherin promoter (Fig 12C). These results demonstrate that Kaiso can bind to directly to methylated regions in the E-cadherin promoter in PC-3 cells. It is well recognized that membrane expression of E-cadherin regulates cell polarity and increases cell-cell cohesiveness limiting the migratory ability of tumor cells [10, 19]. Therefore we performed immunofluorescence for E-cadherin and p120ctn in sh-Kaiso PC-3 cells, compared to vector only sh-Scr PC-3 cells. sh-Kaiso cells exhibited E-cadherin at cell-cell contacts as well as increased p120ctn, which is rate limiting for E-cadherin stability [20, 21], at the cellular membrane (Fig 12D). Furthermore, sh-Kaiso PC-3 cells also exhibited more of an epithelial morphology compared to the mesenchymal morphology exhibited by sh-Scr PC-3 cells (Fig 12C). Collectively, these results suggest that EGFR-regulated expression and subcellular re-localization of Kaiso promotes methylation-related gene silencing of E-cadherin.

CONCLUSION

Collectively, these studies in highlight the influence of the tumor microenvironment on prostate cancer progression and suggest that tumor cell plasticity is necessary to successfully complete the step of metastasis. Furthermore these studies highlight Kaiso cytoplasmic-to-nuclear localization, which correlates with many clinicopathological features of aggressive prostate cancer progression, is responsible for hypermethylation induced epithelial-to-mesenchymal transition associated plasticity. The fact that we found that Kaiso is regulated through EGFR activity provides additional mechanistic insight into the underlining signaling pathway that apparently mediates this process. Because a large number of tumor/metastasis suppressor genes are silenced as a result of methylation, Kaiso could be a central regulator of many key events that contribute to tumorigenesis and aggressiveness. Targeting of growth factor receptors has shown minimal therapeutic effects

for prostate cancers, however targeting of downstream mediators, such as Kaiso, could be a rational approach for developing a new target for directed therapies.

MATERIALS AND METHODS

Cell culture, antibodies and reagents.

Human prostate cancer cell lines DU-145 and PC-3 were obtained from the ATCC and were routinely cultured in DMEM medium supplemented with 10% FBS (Gibco, Paisley, Scotland), and antibiotics in a humidified atmosphere of 5% $C0_2$ in air. In these conditions the duplication period of the cells is 36 h.

DU-145 EGFR overexpressing cells (DU-145 WT) were generated by transfecting DU-145 cells with retroviral-containing EGFR constructs [44]. Primary antibodies were obtained as follows: Kaiso 6F clone (Abcam, Boston, Massachusetts); p120ctn, E-cadherin, N-cadherin and those for tyrosine residues Y228, Y96, Y290 of p120ctn (BD Biosciences , Oregon). Mouse secondary antibodies, Alexa 488, 594, and 625, were obtained from Invitrogen (Oregon). Human EGF was obtained from BD Biosciences (Kentucky). The EGFR-specific tyrosine kinase inhibitor, PD153035, was purchased from CalBiochem (California). Other reagents were obtained from Sigma (Missouri).

The human prostate cancer cell lines, $ARCAP_E$, $ARCaP_M$, and the HS-27a bone stromal cells were utilized in this study and purchased from ATCC (Manasss, VA). Isolation and characterization of the human prostate cancer RFP-ARCaP cell lines has been reported [48]. Red Fluorescent Protein (RFP) transfected cells were maintained in G418 (350 mg/ml) prior to experimentation. All cell lines were grown in a 5% CO_2 incubator at 37˚C in media consisting of T-medium (Invitrogen, Carlsbad, CA) supplemented with 5% (v/v) fetal bovine serum and 1% Penicillin–Streptomycin.

Co-cultures

Initial co-cultures performed as previously described [12, 39] with modifications. Co-cultures consisted of 50 000 cells/cm^2 of HS-27a bone marrow stromal cells and 2000 cells/cm^2 prostate cancer cells. Co-cultures were maintained in serum-free T-media, and plated on tissue culture dishes.

Clongenic Assay

Cells were plated at low densities in six-well plates for 24 hr and then were irradiated with the appropriate radiation dose. Twenty-four hours later, the media were changed and cells were incubated until they formed colonies having at least 50 or more cells. Seventeen days later colonies were rinsed with PBS, stained with methanol/crystal violet dye, and counted. The colony formation ability was calculated as a ratio of the number of colonies formed, divided by the total number of cells plated, times the plating efficiency Ai. For experiments with cocultures, cells were initially incubated on a mat of stromal cells for 24 h and radiated, 4 h later

clongenic assay was performed. For antibody based experiments using anti-E-Cadherin (15 µg/ml, DECMA or SHEP8-7, Sigma) and integrin alpha-v (20 µg/ml, CNT095) antibody, cancer cells were treated with respective antibodies for 24 h prior to plating them on a mat of stromal cells.

Radiation

External beam radiation was delivered on a 600 Varian linear accelerator (Varian Medical Systems, Inc.Palo Alto, CA) with a 6 MV photon beam. A 40 x 40 cm field size was utilized and Petri dishes were placed on 1.5 cm of superflab bolus. Monitor units (MU) were calculated to deliver the dose to a depth of dmax at a dose rate of 600 MU/min.

Immunohistochemistry

The prostate cancer tissue microarrays were obtained from US Biomax (Maryland) or from the UAB Tissue Bank. The use of tissue was approved by the Institutional Review Board of both Tuskegee University and University of Alabama at Birmingham (UAB). Immunohistochemistry was performed using the anti-Kaiso clone 6F (Upstate Biotechnology, New York) as previously described. Duplicate microarrays were stained for evaluation by immunohistochemistry [45]. Briefly, cells were examined, by a pathologist , separately for membranous, cytoplasmic, and nuclear staining for Kaiso and classified with respect to the intensity of immunostaining, with the percent of cells determined at each staining intensity from 0 to +4 [46]. To permit numerical analysis the proportion of cells at each intensity can be multiplied by that intensity. Statistical analyses were performed using Pearson's Chi-Square test to analyze the relationships between cytoplasmic and nuclear expression of Kaiso and clinicopathological factors.

Immunoblotting

Cells were grown to 80% confluency in six-well plates. Lysates were prepared from cultured cells in a solution containing 50 mM Tris, pH 7.5; 120 mM NaCl; 0.5% Nonidet p-40; 40 µM phenylmethylsulfonylfluoride (PMSF); 50 µg/ml leupeptin; and 50 µg/ml aprotinin (all from Sigma, Missouri). Cells were allowed to lyse for 1 hour on ice. The lysed cells were centrifuged, and the resulting supernatants were extracted and quantitated by use of a Bradford assay. Lysates (30 µg of protein) were separated by 7.5% SDS PAGE, immunoblotted, and analyzed by chemiluminescence (Amersham Biosciences, New Jersey).

Immunofluorescence microscopy

Cells (3×10^5) were grown for 2 days or to 80% confluency on glass coverslips. Cells were then fixed with Methanol alone or 4% paraformaldehyde, permeabilized with 100 mM Tris-HCl, pH 7.4; 150 mM NaCl; 10 mM EGTA; 1% Triton X-100; 1 mM PMSF; and 50 µg/ml aprotinin (all from Sigma). and subsequently blocked with 5% bovine serum albumin (BSA) for 1 hour at room temperature. Identical results were obtained

with both methods. Samples were incubated with indicated primary antibodies diluted in blocking buffer at 4°C overnight. FITC-conjugated secondary antibody (BD Biosciences, California) was added. Cells were then treated with 4'-6-diamidino-2-phenylindole for nuclear staining and analyzed with a DSU confocal microscope (Olympus, New York). To determine the relative intensities, the total area of each image was measured as well as the threshold intensity for each channel utilizing Metamorph Imaging Software (Molecular Devices, Inc., California). Differences between the two intensities were then determined by Excel. Bar graphs represent n = 4 images sectioned and individually analyzed for total area. All quantitative data were normalized to appropriate control images.

Quantitative real-time PCR (qRT-PCR)

RNA was extracted from prostate cancer cells using TRIzol (Invitrogen). cDNA was prepared using Superscript III First Strand cDNA Synthesis kits (Invitrogen) and detected by Kaiso-specific TaqMan. Hypoxanthine-guanine phosphoribosyltransferase (HRPT1) (Applied Biosystems, California) was used to normalize all RNA samples. RNA analyses were performed in triplicate, and fold change was calculated using the 2 -ΔCt value method.

RNAi

Transient transfection of p120ctn siRNA (Santa Cruz, CA) (100 nM or 150 nM) and stable transfection with a shRNA construct specific for human Kaiso (Origene Technologies, Rockville, Maryland) were performed. For siRNA p120ctn transfections 4 ml portion of Lipofectamine 2000 (Invitrogen, California, USA) was diluted in 200 ml of Opti-MEM and incubated for 5 min at room temperature. The diluted siRNA and Lipofectamine 2000 were mixed and incubated for 20 min at room temperature. Complexes were added to each well and incubated for 24 h. Media were changed and incubated for an additional 24 h. For siRNA p120 transfections, cells were lysed according to established protocols.

To generate stable sh-RNA Kasio cells, the HuSH 29-mer for Kaiso was provided in the pRFP-C-RS plasmid driven by the U6-RNA promoter. Plasmid DNA pRFP-C-RS, containing puromycin resistant gene, expressing Kaiso-specific shRNA and scrambled shRNA were transfected into DU-145 or PC-3 cells using Lipofectamine 2000 (Invitrogen)... The medium was replaced by T-medium containing 2 μg/ml puromycin for selection of antibiotic-resistant colonies over a period of 3 weeks. The puromycin-resistant cells were further selected by use of red fluorescence protein (RFP) as a marker to enrich for cells expressing shRNA. shKaiso cells were plated at clonal densities, and >20 clones were chosen to determine the degree of knockdown. Clones with the lowest Kaiso levels were kept for further analysis.

Cell migration

Migration of cells was assessed by their capacity to move into an acellular area; this was accomplished with a two-dimensional (2D) wound-healing assay, as previously described [47]. With cells at 70–80% confluence, a denuded area was generated in the middle of each well with a rubber policeman. The cells were then exposed to EGF (0 or 10 ng/mL) and incubated for 24 hours. The distance that cells moved was determined and quantified in Metamorph imaging software. All measurements were normalized to values for controls.

Invasion assay

Cell invasiveness was determined by the capacity of cells to migrate across a layer of extracellular matrix, Matrigel, in a Boyden Chamber. Briefly, 20,000 cells were plated in the Matrigel-containing chamber in a serum-free medium containing 1% BSA for 24 hours; this was then replaced with a serum-free medium for an additional 24 hours. The number of cells that invaded through the matrix over a 48 hour-period was determined by counting, on the bottom of the filter, cells that stained with crystal violet. All experiments were performed in triplicate.

Statistical analysis

For all experiments, statistics were performed with Microsoft Excel or Graphpad prism software. Independent Student's t-test was utilized to determine statistical differences between experimental and control values. Tissue correlations were performed with Matlab (Mathworks Inc., Natick, MI, USA). p-values < 0.05 were considered statistically significant.

REFERENCES

1. Lehmann, U., et al., *Epigenetic inactivation of microRNA gene hsa-mir-9-1 in human breast cancer.* J Pathol, 2008. **214**(1): p. 17-24.
2. Lopes, E.C., et al., *Kaiso contributes to DNA methylation-dependent silencing of tumor suppressor genes in colon cancer cell lines.* Cancer Res, 2008. **68**(18): p. 7258-63.
3. Yoon, H.G., et al., *N-CoR mediates DNA methylation-dependent repression through a methyl CpG binding protein Kaiso.* Mol Cell, 2003. **12**(3): p. 723-34.
4. Daniel, J.M. and A.B. Reynolds, *The catenin p120(ctn) interacts with Kaiso, a novel BTB/POZ domain zinc finger transcription factor.* Mol Cell Biol, 1999. **19**(5): p. 3614-23.
5. Prokhortchouk, A., et al., *The p120 catenin partner Kaiso is a DNA methylation-dependent transcriptional repressor.* Genes Dev, 2001. **15**(13): p. 1613-8.
6. Dai, S.D., et al., *Cytoplasmic Kaiso is associated with poor prognosis in non-small cell lung cancer.* BMC Cancer, 2009. **9**: p. 178.
7. Ackland, M.L., et al., *Epidermal growth factor-induced epithelio-mesenchymal transition in human breast carcinoma cells.* Lab Invest, 2003. **83**(3): p. 435-48.
8. Jawhari, A.U., M.J. Farthing, and M. Pignatelli, *The E-cadherin/epidermal growth factor receptor interaction: a hypothesis of reciprocal and reversible control of intercellular adhesion and cell proliferation.* J Pathol, 1999. **187**(2): p. 155-7.
9. Yates, C., A. Wells, and T. Turner, *Luteinising hormone-releasing hormone analogue reverses the cell adhesion profile of EGFR overexpressing DU-145 human prostate carcinoma subline.* Br J Cancer, 2005. **92**(2): p. 366-75.
10. Xu, J., et al., *Prostate cancer metastasis: role of the host microenvironment in promoting epithelial to mesenchymal transition and increased bone and adrenal gland metastasis.* Prostate, 2006. **66**(15): p. 1664-73.
11. Zhau, H.E., et al., *Epithelial to mesenchymal transition (EMT) in human prostate cancer: lessons learned from ARCaP model.* Clin Exp Metastasis, 2008. **25**(6): p. 601-10.
12. Yates, C.C., et al., *Co-culturing human prostate carcinoma cells with hepatocytes leads to increased expression of E-cadherin.* Br J Cancer, 2007. **96**(8): p. 1246-52.
13. Wells, A., C. Yates, and C.R. Shepard, *E-cadherin as an indicator of mesenchymal to epithelial reverting transitions during the metastatic seeding of disseminated carcinomas.* Clin Exp Metastasis, 2008. **25**(6): p. 621-8.
14. Saha, B., et al., *Unmethylated E-cadherin gene expression is significantly associated with metastatic human prostate cancer cells in bone.* Prostate, 2008. **68**(15): p. 1681-8.
15. Li, L.N., et al., *Differential sensitivity of colorectal cancer cell lines to artesunate is associated with expression of beta-catenin and E-cadherin.* Eur J Pharmacol, 2008. **588**(1): p. 1-8.
16. Sung, S.Y., et al., *Coevolution of prostate cancer and bone stroma in three-dimensional coculture: implications for cancer growth and metastasis.* Cancer Res, 2008. **68**(23): p. 9996-10003.
17. Howlett, A.R., et al., *Cellular growth and survival are mediated by beta 1 integrins in normal human breast epithelium but not in breast carcinoma.* J Cell Sci, 1995. **108 (Pt 5)**: p. 1945-57.
18. Fornaro, M., et al., *Fibronectin protects prostate cancer cells from tumor necrosis factor-alpha-induced apoptosis via the AKT/survivin pathway.* J Biol Chem, 2003. **278**(50): p. 50402-11.
19. Li, G., K. Satyamoorthy, and M. Herlyn, *N-cadherin-mediated intercellular interactions promote survival and migration of melanoma cells.* Cancer Res, 2001. **61**(9): p. 3819-25.
20. Bisanz, K., et al., *Targeting ECM-integrin interaction with liposome-encapsulated small interfering RNAs inhibits the growth of human prostate cancer in a bone xenograft imaging model.* Mol Ther, 2005. **12**(4): p. 634-43.

21. Xie, H., et al., *In vitro invasiveness of DU-145 human prostate carcinoma cells is modulated by EGF receptor-mediated signals.* Clin Exp Metastasis, 1995. **13**(6): p. 407-19.
22. Turner, T., et al., *EGF receptor signaling enhances in vivo invasiveness of DU-145 human prostate carcinoma cells.* Clin Exp Metastasis, 1996. **14**(4): p. 409-18.
23. Gan, Y., et al., *Differential roles of ERK and Akt pathways in regulation of EGFR-mediated signaling and motility in prostate cancer cells.* Oncogene. **29**(35): p. 4947-58.
24. Traish, A.M. and A. Morgentaler, *Epidermal growth factor receptor expression escapes androgen regulation in prostate cancer: a potential molecular switch for tumour growth.* Br J Cancer, 2009. **101**(12): p. 1949-56.
25. Daniel, J.M., et al., *The p120(ctn)-binding partner Kaiso is a bi-modal DNA-binding protein that recognizes both a sequence-specific consensus and methylated CpG dinucleotides.* Nucleic Acids Res, 2002. **30**(13): p. 2911-9.
26. Daniel, J.M., *Dancing in and out of the nucleus: p120(ctn) and the transcription factor Kaiso.* Biochim Biophys Acta, 2007. **1773**(1): p. 59-68.
27. Mariner, D.J., M.A. Davis, and A.B. Reynolds, *EGFR signaling to p120-catenin through phosphorylation at Y228.* J Cell Sci, 2004. **117**(Pt 8): p. 1339-50.
28. Kallakury, B.V., C.E. Sheehan, and J.S. Ross, *Co-downregulation of cell adhesion proteins alpha- and beta-catenins, p120CTN, E-cadherin, and CD44 in prostatic adenocarcinomas.* Hum Pathol, 2001. **32**(8): p. 849-55.
29. Li, L.C., et al., *Methylation of the E-cadherin gene promoter correlates with progression of prostate cancer.* J Urol, 2001. **166**(2): p. 705-9.
30. Soubry, A., et al., *Expression and nuclear location of the transcriptional repressor Kaiso is regulated by the tumor microenvironment.* Cancer Res, 2005. **65**(6): p. 2224-33.
31. Kelly, K.F., et al., *NLS-dependent nuclear localization of p120ctn is necessary to relieve Kaiso-mediated transcriptional repression.* J Cell Sci, 2004. **117**(Pt 13): p. 2675-86.
32. Park, J.I., et al., *Kaiso/p120-catenin and TCF/beta-catenin complexes coordinately regulate canonical Wnt gene targets.* Dev Cell, 2005. **8**(6): p. 843-54.
33. Shuch, B., et al., *Racial disparity of epidermal growth factor receptor expression in prostate cancer.* J Clin Oncol, 2004. **22**(23): p. 4725-9.
34. Hatcher, D., et al., *Molecular mechanisms involving prostate cancer racial disparity.* Am J Transl Res, 2009. **1**(3): p. 235-48.
35. Timofeeva, O.A., et al., *Enhanced expression of SOS1 is detected in prostate cancer epithelial cells from African-American men.* Int J Oncol, 2009. **35**(4): p. 751-60.
36. Kelly, K.F., et al., *Nuclear import of the BTB/POZ transcriptional regulator Kaiso.* J Cell Sci, 2004. **117**(Pt 25): p. 6143-52.
37. Cozzolino, M., et al., *p120 Catenin Is Required for Growth Factor-dependent Cell Motility and Scattering in Epithelial Cells.* Mol Biol Cell, 2003. **14**(5): p. 1964-77.
38. Zhang, P.X., et al., *p120-catenin isoform 3 regulates subcellular localization of Kaiso and promotes invasion in lung cancer cells via a phosphorylation-dependent mechanism.* Int J Oncol. **38**(6): p. 1625-35.
39. Yates, C., et al., *Novel three-dimensional organotypic liver bioreactor to directly visualize early events in metastatic progression.* Adv Cancer Res, 2007. **97**: p. 225-46.
40. Mimori, K., et al., *Coexpression of matrix metalloproteinase-7 (MMP-7) and epidermal growth factor (EGF) receptor in colorectal cancer: an EGF receptor tyrosine kinase inhibitor is effective against MMP-7-expressing cancer cells.* Clin Cancer Res, 2004. **10**(24): p. 8243-9.
41. Klingelhofer, J., et al., *Epidermal growth factor receptor ligands as new extracellular targets for the metastasis-promoting S100A4 protein.* FEBS J, 2009. **276**(20): p. 5936-48.
42. Reinhold, W.C., et al., *Detailed DNA methylation profiles of the E-cadherin promoter in the NCI-60 cancer cells.* Mol Cancer Ther, 2007. **6**(2): p. 391-403.

43. Zou, D., et al., *Epigenetic silencing in non-neoplastic epithelia identifies E-cadherin (CDH1) as a target for chemoprevention of lobular neoplasia.* J Pathol, 2009. **218**(2): p. 265-72.

44. Wells, A., et al., *Ligand-induced transformation by a noninternalizing epidermal growth factor receptor.* Science, 1990. **247**(4945): p. 962-4.

45. Manne, U., et al., *Re: loss of tumor marker-immunostaining intensity on stored paraffin slides of breast cancer.* J Natl Cancer Inst, 1997. **89**(8): p. 585-6.

46. **Grizzle, W.**, et al., eds. *Factors Affecting Immunohistochemical Evaluation of Biomarker Expression in Neoplasia.* John Walker's *Methods in Molecular Medicine - Tumor Marker Protocols*, ed. M.H.a.Z. Walaszek. 1998, Humana Press, Inc., : NJ. 161-179.

47. Yates, C.C., et al., *Delayed and deficient dermal maturation in mice lacking the CXCR3 ELR-negative CXC chemokine receptor.* Am J Pathol, 2007. **171**(2): p. 484-95.

48. He, H., et al., *Progressive epithelial to mesenchymal transitions in ARCaP(E) prostate cancer cells during xenograft tumor formation and metastasis.* Prostate, 2009. **70**(5): p. 518-528.

49. Ackland ML, Newgreen DF, Fridman M, Waltham MC, Arvanitis A, Minichiello J, Price JT, Thompson EW (2003) Epidermal growth factor-induced epithelio-mesenchymal transition in human breast carcinoma cells. *Lab Invest* **83:** 435-48

50. Cozzolino M, Stagni V, Spinardi L, Campioni N, Fiorentini C, Salvati E, Alema S, Salvatore AM (2003) p120 Catenin Is Required for Growth Factor-dependent Cell Motility and Scattering in Epithelial Cells. *Mol Biol Cell* **14:** 1964-77

51. Dai SD, Wang Y, Miao Y, Zhao Y, Zhang Y, Jiang GY, Zhang PX, Yang ZQ, Wang EH (2009) Cytoplasmic Kaiso is associated with poor prognosis in non-small cell lung cancer. *BMC cancer* **9:** 178

52. Daniel JM (2007) Dancing in and out of the nucleus: p120(ctn) and the transcription factor Kaiso. *Biochimica et biophysica acta* **1773:** 59-68

53. Daniel JM, Reynolds AB (1999) The catenin p120(ctn) interacts with Kaiso, a novel BTB/POZ domain zinc finger transcription factor. *Molecular and cellular biology* **19:** 3614-23

54. Daniel JM, Spring CM, Crawford HC, Reynolds AB, Baig A (2002) The p120(ctn)-binding partner Kaiso is a bi-modal DNA-binding protein that recognizes both a sequence-specific consensus and methylated CpG dinucleotides. *Nucleic acids research* **30:** 2911-9

55. Gan Y, Shi C, Inge L, Hibner M, Balducci J, Huang Y Differential roles of ERK and Akt pathways in regulation of EGFR-mediated signaling and motility in prostate cancer cells. *Oncogene* **29:** 4947-58

56. **Grizzle W**, Myers R, Manne U, Stockard C, Harkins L, Srivastava S (eds) (1998) *Factors Affecting Immunohistochemical Evaluation of Biomarker Expression in Neoplasia.* Humana Press, Inc., : NJ

57. Hatcher D, Daniels G, Osman I, Lee P (2009) Molecular mechanisms involving prostate cancer racial disparity. *Am J Transl Res* **1:** 235-48

58. Jawhari AU, Farthing MJ, Pignatelli M (1999) The E-cadherin/epidermal growth factor receptor interaction: a hypothesis of reciprocal and reversible control of intercellular adhesion and cell proliferation. *The Journal of pathology* **187:** 155-7

59. Kallakury BV, Sheehan CE, Ross JS (2001) Co-downregulation of cell adhesion proteins alpha- and beta-catenins, p120CTN, E-cadherin, and CD44 in prostatic adenocarcinomas. *Hum Pathol* **32:** 849-55

60. Kelly KF, Otchere AA, Graham M, Daniel JM (2004a) Nuclear import of the BTB/POZ transcriptional regulator Kaiso. *Journal of cell science* **117:** 6143-52

61. Kelly KF, Spring CM, Otchere AA, Daniel JM (2004b) NLS-dependent nuclear localization of p120ctn is necessary to relieve Kaiso-mediated transcriptional repression. *Journal of cell science* **117:** 2675-86

62. Klingelhofer J, Moller HD, Sumer EU, Berg CH, Poulsen M, Kiryushko D, Soroka V, Ambartsumian N, Grigorian M, Lukanidin EM (2009) Epidermal growth factor receptor ligands as new extracellular targets for the metastasis-promoting S100A4 protein. *FEBS J* **276:** 5936-48

63. Lehmann U, Hasemeier B, Christgen M, Muller M, Romermann D, Langer F, Kreipe H (2008) Epigenetic inactivation of microRNA gene hsa-mir-9-1 in human breast cancer. *The Journal of pathology* **214:** 17-24

64. Li LC, Zhao H, Nakajima K, Oh BR, Ribeiro Filho LA, Carroll P, Dahiya R (2001) Methylation of the E-cadherin gene promoter correlates with progression of prostate cancer. *The Journal of urology* **166:** 705-9

65. Lopes EC, Valls E, Figueroa ME, Mazur A, Meng FG, Chiosis G, Laird PW, Schreiber-Agus N, Greally JM, Prokhortchouk E, Melnick A (2008) Kaiso contributes to DNA methylation-dependent silencing of tumor suppressor genes in colon cancer cell lines. *Cancer research* **68:** 7258-63

66. Manne U, Myers RB, Srivastava S, Grizzle WE (1997) Re: loss of tumor marker-immunostaining intensity on stored paraffin slides of breast cancer. *Journal of the National Cancer Institute* **89:** 585-6

67. Mariner DJ, Davis MA, Reynolds AB (2004) EGFR signaling to p120-catenin through phosphorylation at Y228. *Journal of cell science* **117:** 1339-50

68. Mimori K, Yamashita K, Ohta M, Yoshinaga K, Ishikawa K, Ishii H, Utsunomiya T, Barnard GF, Inoue H, Mori M (2004) Coexpression of matrix metalloproteinase-7 (MMP-7) and epidermal growth factor (EGF) receptor in colorectal cancer: an EGF receptor tyrosine kinase inhibitor is effective against MMP-7-expressing cancer cells. *Clin Cancer Res* **10:** 8243-9

69. Park JI, Kim SW, Lyons JP, Ji H, Nguyen TT, Cho K, Barton MC, Deroo T, Vleminckx K, Moon RT, McCrea PD (2005) Kaiso/p120-catenin and TCF/beta-catenin complexes coordinately regulate canonical Wnt gene targets. *Dev Cell* **8:** 843-54

70. Prokhortchouk A, Hendrich B, Jorgensen H, Ruzov A, Wilm M, Georgiev G, Bird A, Prokhortchouk E (2001) The p120 catenin partner Kaiso is a DNA methylation-dependent transcriptional repressor. *Genes & development* **15:** 1613-8

71. Reinhold WC, Reimers MA, Maunakea AK, Kim S, Lababidi S, Scherf U, Shankavaram UT, Ziegler MS, Stewart C, Kouros-Mehr H, Cui H, Dolginow D, Scudiero DA, Pommier YG, Munroe DJ, Feinberg AP, Weinstein JN (2007) Detailed DNA methylation profiles of the E-cadherin promoter in the NCI-60 cancer cells. *Molecular cancer therapeutics* **6:** 391-403

72. Shuch B, Mikhail M, Satagopan J, Lee P, Yee H, Chang C, Cordon-Cardo C, Taneja SS, Osman I (2004) Racial disparity of epidermal growth factor receptor expression in prostate cancer. *J Clin Oncol* **22:** 4725-9

73. Soubry A, van Hengel J, Parthoens E, Colpaert C, Van Marck E, Waltregny D, Reynolds AB, van Roy F (2005) Expression and nuclear location of the transcriptional repressor Kaiso is regulated by the tumor microenvironment. *Cancer research* **65:** 2224-33

74. Timofeeva OA, Zhang X, Ressom HW, Varghese RS, Kallakury BV, Wang K, Ji Y, Cheema A, Jung M, Brown ML, Rhim JS, Dritschilo A (2009) Enhanced expression of SOS1 is detected in prostate cancer epithelial cells from African-American men. *International journal of oncology* **35:** 751-60

75. Traish AM, Morgentaler A (2009) Epidermal growth factor receptor expression escapes androgen regulation in prostate cancer: a potential molecular switch for tumour growth. *British journal of cancer* **101:** 1949-56

76. Turner T, Chen P, Goodly LJ, Wells A (1996) EGF receptor signaling enhances in vivo invasiveness of DU-145 human prostate carcinoma cells. *Clin Exp Metastasis* **14:** 409-18

77. Wells A, Welsh JB, Lazar CS, Wiley HS, Gill GN, Rosenfeld MG (1990) Ligand-induced transformation by a noninternalizing epidermal growth factor receptor. *Science* **247:** 962-4

78. Wells A, Yates C, Shepard CR (2008) E-cadherin as an indicator of mesenchymal to epithelial reverting transitions during the metastatic seeding of disseminated carcinomas. *Clinical & experimental metastasis* **25:** 621-8

79. Xie H, Turner T, Wang MH, Singh RK, Siegal GP, Wells A (1995) In vitro invasiveness of DU-145 human prostate carcinoma cells is modulated by EGF receptor-mediated signals. *Clin Exp Metastasis* **13:** 407-19

80. Yates C, Shepard CR, Papworth G, Dash A, Beer Stolz D, Tannenbaum S, Griffith L, Wells A (2007a) Novel three-dimensional organotypic liver bioreactor to directly visualize early events in metastatic progression. *Advances in cancer research* **97:** 225-46

81. Yates C, Wells A, Turner T (2005) Luteinising hormone-releasing hormone analogue reverses the cell adhesion profile of EGFR overexpressing DU-145 human prostate carcinoma subline. *British journal of cancer* **92:** 366-75

82. Yates CC, Shepard CR, Stolz DB, Wells A (2007b) Co-culturing human prostate carcinoma cells with hepatocytes leads to increased expression of E-cadherin. *British journal of cancer* **96:** 1246-52

83. Yates CC, Whaley D, Kulasekeran P, Hancock WW, Lu B, Bodnar R, Newsome J, Hebda PA, Wells A (2007c) Delayed and deficient dermal maturation in mice lacking the CXCR3 ELR-negative CXC chemokine receptor. *The American journal of pathology* **171:** 484-95

84 Yoon HG, Chan DW, Reynolds AB, Qin J, Wong J (2003) N-CoR mediates DNA methylation-dependent repression through a methyl CpG binding protein Kaiso. *Mol Cell* **12:** 723-34

85 Zhang PX, Wang Y, Liu Y, Jiang GY, Li QC, Wang EH p120-catenin isoform 3 regulates subcellular localization of Kaiso and promotes invasion in lung cancer cells via a phosphorylation-dependent mechanism. *International journal of oncology* **38:** 1625-35

86. Zou D, Yoon HS, Perez D, Weeks RJ, Guilford P, Humar B (2009) Epigenetic silencing in non-neoplastic epithelia identifies E-cadherin (CDH1) as a target for chemoprevention of lobular neoplasia. *The Journal of pathology* **218:** 265-72

KEY RESEARCH ACCOMPLISHMENTS

1. **Tumor Stroma induces Tumor plasticity in prostate cancer cells.**
    - **a.** Tumor-Associated stroma induces a MErT , with increased E-cadherin expression in prostate cancer cells.
    - b. Bone or prostate stroma decreases sensitivity of Prostate cancer cell lines to radiation treatment.
    - c. Bone stromal causes and EMT-MET transition of prostate cancer cells.
    - d. Manuscript published in Journal of Onocology

2. **Kaiso as Biomarker for Invasive Prostate cancer**
    - a. Overexpression of Kaiso was determined to be associated with prostate cancer progression in large cohort of tumor samples. With African American patients displaying significantly higher expression. (This was not in our original proposal, and an unexpected, but very interesting finding from our prosed staining for Kaiso in prostate tissue.
    - b. Cytoplasmic to nuclear localization of Kaiso is associated with invasive and metastatic prostate cancer and this correlates with tumor grade and clinical stage.
    - c. EGFR signaling regulates cytoplasmic to nuclear shuttling of Kaiso via p120ctn.
    - d. Kaiso promotes increased migration and invasion, with direct binding to methylated sequences in E-cadherin promoter, thus promoting EMT
    - e. In sum we highlighted the an entire signaling network through which induced Kaiso localization is associated with aggressive prostate cancer characteristics.
    - f. Manuscript published in American Journal of Pathology

REPORTABLE OUTCOMES:

ABSTRACTS

"Influence of the Tumor Microenvironment on Prostate Cellular Behavior". **Dr. Clayton Yates**, Invited Speaker, 5th Annual National Symposium on Prostate Cancer, Clark Atlanta University, Atlanta, AL, March 15-17, 2009.

Tumor-Stromal Interactions Influence Radiation Sensitivity in Epithelial versus Mesenchymal Prostate Cancer Cells Sajni Josson, Starlette Sharp, Ritu Aneja, Ruoxiang Wang, Timothy Turner, Leland W.K Chung, **Clayton Yates,** University of Michigan, NCIBI workshop, Invited Speaker. 2010.

"Nuclear Kaiso Indicates Aggressive Prostate Cancers and Promotes Migration and Invasiveness of Prostate Cancer Cells ". Jacqueline Jones, Jianjun Zhou, Honghe Wang, Shana Hardy, David Austin, Qinghua He, Timothy Turner, Alan Wells, William Grizzle, Clayton Yates . Department of Defense Prostate 2011 Impacting Meeting, Sheraton Orlando, FL

PUBLICATIONS (Peer reviewed)

1. Sajni Josson, Starlette Sharp, Ritu Aneja, Ruoxiang Wang, Timothy Turner, Leland W.K Chung, **Clayton Yates** "Tumor-Stromal Interactions Influence Radiation Sensitivity in Epithelial- versus Mesenchymal-Like Prostate Cancer Cells," Journal of Oncology, vol. 2010, Article ID 232831, 10 pages, 2010. PMID: 20798867

2. Sajni Josson, Cynthia S. Anderson, Shian-Ying Sung, Peter A. S. Johnstone, Hiroyuki Kubo, Chia-Ling Hsieh, Rebecca Arnold, Murali Gururajan, **Clayton Yates**, and Leland W. K. Chung " Inhibition of ADAM9 expression induces epithelial phenotypic alterations and sensitizes human prostate cancer cells to radiation and chemotherapy" The Prostate PMID: 20672324

3. Jacqueline Jones*, Honghe Wang*, Jianjun Zhou, Shana Hardy, David Austin, Qinghua He, Timothy Turner, Alan Wells, William Grizzle, **Clayton Yates "**Nuclear Kaiso Indicates Aggressive Prostate Cancers and Promotes Migration and Invasiveness of Prostate Cancer Cells " Am J Pathol. 2012 Sep 10. pii: S0002-9440(12)00605-0. doi: 10.1016/j.ajpath.2012.08.008. [Epub ahead of print] PMID:22974583

4. Jianjun Zhou, Honghe Wang, Virginetta Cannon, Karen Marie Scott, Hongbin Song, **Clayton Yates** "Side population rather than CD133+ cells distinguishes enriched tumorigenicity in hTERT-immortalized primary prostate cancer cell" Molecular Cancer 2011 Sep 14;10(1):112. PMID: 21917149 **[Highly Accessed]**

5. **Clayton Yates**, "Prostate Tumor Cell Plasticity: A Consequence of the Microenvironment" Adv Exp Med Biol. 2011;720:81-90.PMID: 21901620

Provisional Patent Filled –see appendix below

APPENDIX

Research Article

Tumor-Stromal Interactions Influence Radiation Sensitivity in Epithelial- versus Mesenchymal-Like Prostate Cancer Cells

Sajni Josson,[1,2] Starlette Sharp,[3] Shian-Ying Sung,[1] Peter A. S. Johnstone,[4] Ritu Aneja,[4,5] Ruoxiang Wang,[1] Murali Gururajan,[2] Timothy Turner,[3] Leland W. K. Chung,[1,2] and Clayton Yates[1,3]

[1] *Department of Urology, Emory School of Medicine, Atlanta, GA 30311, USA*
[2] *Cedars-Sinai Medical Center, Los Angeles, CA 90048, USA*
[3] *Department of Biology and Center for Cancer Research, Tuskegee University, Carver Research Foundation, Tuskegee, AL 36088, USA*
[4] *Department of Radiation Oncology, Emory School of Medicine, Atlanta, GA 30322, USA*
[5] *Department of Biology, Georgia State University, Atlanta, GA 30303, USA*

Correspondence should be addressed to Clayton Yates, cyates@tuskegee.edu

Received 15 March 2010; Revised 12 May 2010; Accepted 12 May 2010

Academic Editor: Claudia D. Andl

HS-27a human bone stromal cells, in 2D or 3D coultures, induced cellular plasticity in human prostate cancer $ARCaP_E$ and $ARCaP_M$ cells in an EMT model. Cocultured $ARCaP_E$ or $ARCaP_M$ cells with HS-27a, developed increased colony forming capacity and growth advantage, with $ARCaP_E$ exhibiting the most significant increases in presence of bone or prostate stroma cells. Prostate (Pt-N or Pt-C) or bone (HS-27a) stromal cells induced significant resistance to radiation treatment in $ARCaP_E$ cells compared to $ARCaP_M$ cells. However pretreatment with anti-E-cadherin antibody (SHEP8-7) or anti-alpha v integrin blocking antibody (CNT095) significantly decreased stromal cell-induced radiation resistance in both $ARCaP_E$- and $ARCaP_M$-cocultured cells. Taken together the data suggest that mesenchymal-like cancer cells reverting to epithelial-like cells in the bone microenvironment through interaction with bone marrow stromal cells and reexpress E-cadherin. These cell adhesion molecules such as E-cadherin and integrin alpha v in cancer cells induce cell survival signals and mediate resistance to cancer treatments such as radiation.

1. Introduction

Prostate cancer is the most frequent tumor in men, afflicting African American males to a greater degree than Caucasians. Morbidity and mortality are mainly attributable to metastasis; yet the mechanisms associated with progression are largely unknown. Localized carcinomas are readily removed surgically, but once a tumor has established metastases, current therapies are not curative and prolong survival by only a few years. Metastasis occurs through a multistep process, where metastatic cells must intravasate local tissues and enter into and survive in the blood stream. These cells then extravasate into the secondary tissue and initiate and maintain micrometastases at distant sites, with the end result being the development of a metastatic tumor [1, 2]. During each step of this process, cancer cells exhibit transdifferentiation properties that allow both the spatial and temporal expression of epithelial and mesenchymal properties in response to microenvironment signals and its own basic survival needs (e.g., motility and invasion versus proliferation). Thus, a model of cellular transitions, as opposed to a continual progression to permanent differentiation state, is emerging as a significant mechanism during metastasis. A greater understanding of these mechanisms will result in clinical improvements and a better control of the metastasis process.

Epithelial-mesenhymal transition (EMT) was first described during development [3, 4]; however an EMT-like phenotypic change has been observed in a number of solid tumors [5–7]. This transition is typically characterized by a loss in E-cadherin and cytokeratin expression. EMT in cancer, as in development, is associated with an increase in cell proliferation [8, 9] and the acquisition of a mesenchymal phenotype that includes vimentin, N-cadherin,

and osteopontin expression. In both normal development EMT and cancer-associated EMT, the loss of E-cadherin is critical to the differentiation and maintenance of the epithelial phenotype and provides a structural link between adjacent cellular cytoskeletons, which is important for tissue architecture. Cells that have undergone EMT (E-cadherin negative mesenchymal cells) subsequently become more migratory and invasive and proceed to traverse underlying basement membranes, with an acquired ability to intravaste the surrounding local tissue and gain access to vascular conduits. As such, the loss of E-cadherin is rate limiting for EMT [10, 11]. Recent reports from this laboratory and others have described a mesenchymal to epithelial reverting transition (MErT) to occur, where mesenchymal-like prostate cancer cell lines reexpress E-cadherin to become epithelial-like, and reestablish cellular adhesion during colonization within the liver tumor microenvironment [12, 13]. These findings are shared in clinical metastases of various cancer origins including breast, colon, and bladder, where robust membrane expression of E-cadherin was observed, and the paired more differentiated primary tumors were E-cadherin negative [6, 14]. Thus, a reversion of the mesenchymal phenotype appears to be important in latter stages of metastasis.

Numerous studies have shown that the underlying influence of these cellular transitions is a consequence of tumor-stromal interactions [15, 16]. Coculture studies have found that the survival and proliferation of cancer cells are intimately linked to the soluble factors in the microenvironment, such as EGF, TGF-β, IGF-*I* that contribute to survival and the subsequent formation of macrometastasis [17–20]. However, these factors are not likely to have a direct effect during initial metastatic colonization, and thus heterotypic and homotypic cellular adhesion has been proposed to provide the necessary survival signals for successful colonization [21, 22]. Current state-of-the-art technology does not provide the necessary resolution to determine at the single cell level in patients or experimental *in vivo* systems, individual cells that have successfully colonized the secondary site. However, numerous reports have firmly established that cancer-stromal interactions *in vitro* or in three-dimensional (3D) assays accurately mimic the drug sensitivity/resistance behavior of those cells found within solid tumors *in vivo* in a preclinical or clinical setting [23]. Thus, we employed a novel coculture assay to determine the cellular plasticity of cancer cells promoted by the bone stroma and the effect of tumor-stromal interactions on irradiation therapy in prostate cancer.

The ARCaP model is the only robust prostate cancer bone metastatic model which demonstrates epithelial to mesenchymal transition(EMT). The ARCaP progression model consists of $ARCaP_E$ (epithelial) and $ARCaP_M$ (mesenchymal), where the $ARCaP_E$ cells have a bone metastatic potential of 12.5% and the $ARCaP_M$ cells have a bone metastatic potential of 100%. The $ARCaP_E$ and $ARCaP_M$ cells express the classical markers of EMT [24, 25]. Herein we present findings that $ARCaP_M$ cells undergo MErT when cocultured within the bone microenvironment in 3D and 2D cultures. Additionally, $ARCaP_E$ cells that retained an epithelial phenotype exhibited a measurable growth advantage and retained ability to form colonies, however only under coculture conditions with bone stroma. Furthermore, blocking the ability of $ARCaP_E$ or $ARCaP_M$ cells from E-cadherin-mediated cell-cell adhesion or integrin alpha v beta-associated adhesion significantly affected ARCaP cell survival within bone stroma and sensitized these cells to radiation treatment.

2. Methods

2.1. Cell Culture. The human prostate cancer cell lines, $ARCAP_E$, $ARCaP_M$, the HS-27a bone stromal cells (ATCC, Manasss, VA) and the Pt-N or Pt-C human prostate stromal cell. Isolation and characterization of the human prostate cancer RFP-ARCaP cell lines has been reported [26]. Red Fluorescent Protein- (RFP-) transfected cells were maintained in G418 (350 mg/mL) prior to experimentation. All cell lines were grown in a 5% CO_2 incubator at 37°C in media consisting of T-medium (Invitrogen, Carlsbad, CA) supplemented with 5% (v/v) fetal bovine serum and 1% Penicillin-Streptomycin.

2.2. Cocultures. Initial cocultures were performed as previously described [12, 13] with modifications. Cocultures consisted of 50 000 cells/cm^2 of HS-27a bone marrow stromal cells and 2000 cells/cm^2 prostate cancer cells. Cocultures were maintained in serum-free T-media and plated on tissue culture dishes.

2.3. Clonogenic Assay. Cells were plated at low densities in six-well plates for 24 hours and then were irradiated with the appropriate radiation dose. Twenty-four hours later, the media were changed and cells were incubated until they formed colonies having at least 50 or more cells. Seventeen days later colonies were rinsed with PBS, stained with methanol/crystal violet dye, and counted. The colony formation ability was calculated as a ratio of the number of colonies formed, divided by the total number of cells plated, times the plating efficiency [(# of colonies formed ÷ total # cells plated) × plating efficiency]. For experiments with cocultures, cells were initially incubated on a mat of stromal cells for 24 hours and radiated; 4 hours later clonogenic assay was performed. For antibody-based experiments using anti-E-cadherin (15 μg/mL, DECMA or SHEP8-7, Sigma) and anti-integrin alpha-v (20 μg/mL, CNT095) antibody, cancer cells were treated with respective antibodies for 24 hours prior to plating them on a mat of stromal cells.

2.4. Radiation. External beam radiation was delivered on a 600 Varian linear accelerator (Varian Medical Systems, Inc.Palo Alto, CA) with a 6 MV photon beam. A 40 × 40 cm field size was utilized and Petri dishes were placed on 1.5 cm of superflab bolus. Monitor units (MUs) were calculated to deliver the dose to a depth of dmax at a dose rate of 600 MU/min.

2.5. Statistical Analysis. Representative findings are shown for all experiments, which were performed in triplicate, repeated a minimum of three times. Student's t-test was used to determine the statistical significance between groups.

3. Results

3.1. ARCaP EMT Model Undergoes a Mesenchymal-to-Epithelial Reverting Transition (MErT). Recently, the ARCaP model has been described to closely mimic the pathophysiology of advanced clinical human prostate cancer bone metastasis [25]. The $ARCaP_E$ cells were derived from single-cell dilutions of the ARCaP cells. These cells exhibit a cuboidal-shaped epithelial morphology with high expression of epithelial markers, such as cytokeratin 18 and E-cadherin. The lineage-derived $ARCaP_M$ cells have a spindle-shaped mesenchymal morphology and phenotype. $ARCaP_M$ cells have decreased expression of E-cadherin and cytokeratins 18 and 19 but increased expression of N-cadherin and vimentin. These cells have decreased cell adhesion and increased metastatic propensity to bone and adrenal glands [27]. The morphologic and phenotypic changes observed in the $ARCaP_M$ cells closely resemble those of cells undergoing EMT.

Previously, we have demonstrated a Mesenchymal to Epithelial *reverse* Transition (MErT) of metastatic prostate cancer cell lines within an experimental coculture model and confirmed in patients with liver metastasis [13, 28]. Our findings have recently been confirmed in prostate cancer bone metastasis where E-cadherin and β-catenin were robustly expressed in late stage carcinomas [29]. Therefore we sought to identify the significance of the bone microenvironment within the experimental ARCaP model. To assess cellular plasticity of the ARCaP EMT model, we coultured ARCaP cells with HS-27a cells in 3D RWV (rotary wall vessel) system for 3 days. $ARCaP_E$ cells formed larger prostate organoids than $ARCaP_M$ cells (data not shown). Upon immunohistochemical examination of organoids, we observed that both $ARCaP_E$ and $ARCaP_M$ express E-cadherin and lack N-cadherin expression (Figure 1(a)). To further examine the influence of tumor-stroma interactions over a multiday period we utilized a similar 2D cocultures method. Utilizing immunoctyochemical analysis, we observed a lack E-cadherin and robust N-cadherin staining after 1 day in both $ARCAP_E$ and $ARCaP_M$ cocultures. However by day 4, both $ARCaP_E$ and $ARCaP_M$ cells formed tumor nest that express E-cadherin and lack N-cadherin staining (Figure 1(b)). It is worthy to note that $ARCaP_M$ tumor nest appeared to develop at much smaller extent, compared to $ARCaP_E$ cocultures.

Since $ARCaP_E$ cells formed larger tumor nest and spheroids when cocultured with HS-27a cells compared to $ARCaP_M$ cells, we sought to further assess if HS-27a cells preferentially stimulated the growth of $ARCaP_E$ cells versus $ARCaP_M$ cells. Utilizing GFP-transfected HS-27a bone marrow stromal cells and RFP-transfected $ARCaP_E$ or $ARCaP_M$ cells (Figure 2(a)), we examined the proliferative ability of ARCaP cells in homotypic and coculture conditions. Growth of RFP-transfected $ARCaP_E$ and $ARCaP_M$ cells, respectively, was quantified by relative fluorescent units (RFU) of transfected cell lines over a 6-day period in homotypic cultures and coculture conditions (Figure 2(a)). As previously reported, homotypic cultured $ARCaP_M$ shows significant growth compared to $ARCaP_E$ homotypic cultures; however cocultures reversed this trend with $ARCaP_E$ cells demonstrating the most significant growth (Figure 2(b)). We also confirmed these findings in $ARCaP_E$ cells in coculture using clonogenic assay. Although $ARCaP_M$ cells have a higher plating efficiency than $ARCaP_E$ cells, $ARCaP_E$ cells exhibited an 8-fold increase in their ability to form colonies after coculture compared to 1.35-fold increase of cocultured $ARCaP_M$ cells (Figure 2(c)). Phase-contrast microscopy of colonies after coculture shows that $ARCaP_M$ colonies appear loosely adherent, while $ARCaP_E$ cells are compact and interact physically with few of the bone stromal fibroblast (Figure 2(d)). Taken together, these results demonstrate that $ARCaP_M$ cells reexpress E-cadherin when grown with bone stromal cells for longer periods. Additionally, $ARCaP_E$ cells which have high levels of E-cadherin gain enhanced growth and self-renewal ability when cocultured with bone stromal cells.

3.2. Stromal Cells Influence Radiation Treatment in Prostate Cancer Cells. Mesenchymal cancer cells have been thought to be more tumorigenic, aggressive, and resistant to treatments when compared to epithelial cancer cells [30]. A similar trend was observed in both $ARCaP_E$ and $ARCaP_M$ cells after (4 Gy) irradiation treatment. $ARCaP_M$ homotypic cancer cells are more resistant to radiation treatment compared to $ARCaP_E$ homotypic cancer cells (Figure 3(a)). However, $ARCaP_M$ cocultures did not affect the radiation sensitivity of $ARCaP_M$ cancer cells. The highly sensitive $ARCaP_E$ cells exhibit a significant increased resistance to radiation therapy, up to 3-fold, as result of their interaction with bone stromal cells (Figure 3(a), $P < .01$).

To further assess the role of the prostate stromal cells on tumor-stromal interactions influencing ARCaP cellular behavior, we cocultured paired prostate stromal fibroblasts isolated either from normal (Pt-N) or from cancer-associated regions (Pt-C) [31]. Again, $ARCaP_E$ cells cocultured with (Pt-N) or (Pt-C) exhibited a 7-fold and 8-fold increase in colony formation, respectively (Figure 3(b), $P < .01$). We also saw a similar trend in a growth analysis assay (data not shown). However when measuring clonogenic ability after radiation treatment, $ARCaP_E$ cells cocultured with either Pt-N or Pt-C had increased radiation resistance, with a 2-fold difference observed between homotypic cultured cells. Although a significant increase in clonogenic formation was observed in Pt-C versus Pt-N cocultures ($P < .05$), this did not significantly effect the radiation sensitivity of $ARCaP_M$ cells (Figures 3(c)). Taken together, both bone and prostate stromal cell have a grown inductive effect on $ARCaP_E$ cancer cells and mediate radiation resistance (up to 2-3 fold) in epithelial cancer phenotype, but not in $ARCaP_M$ mesenchymal cancer cells.

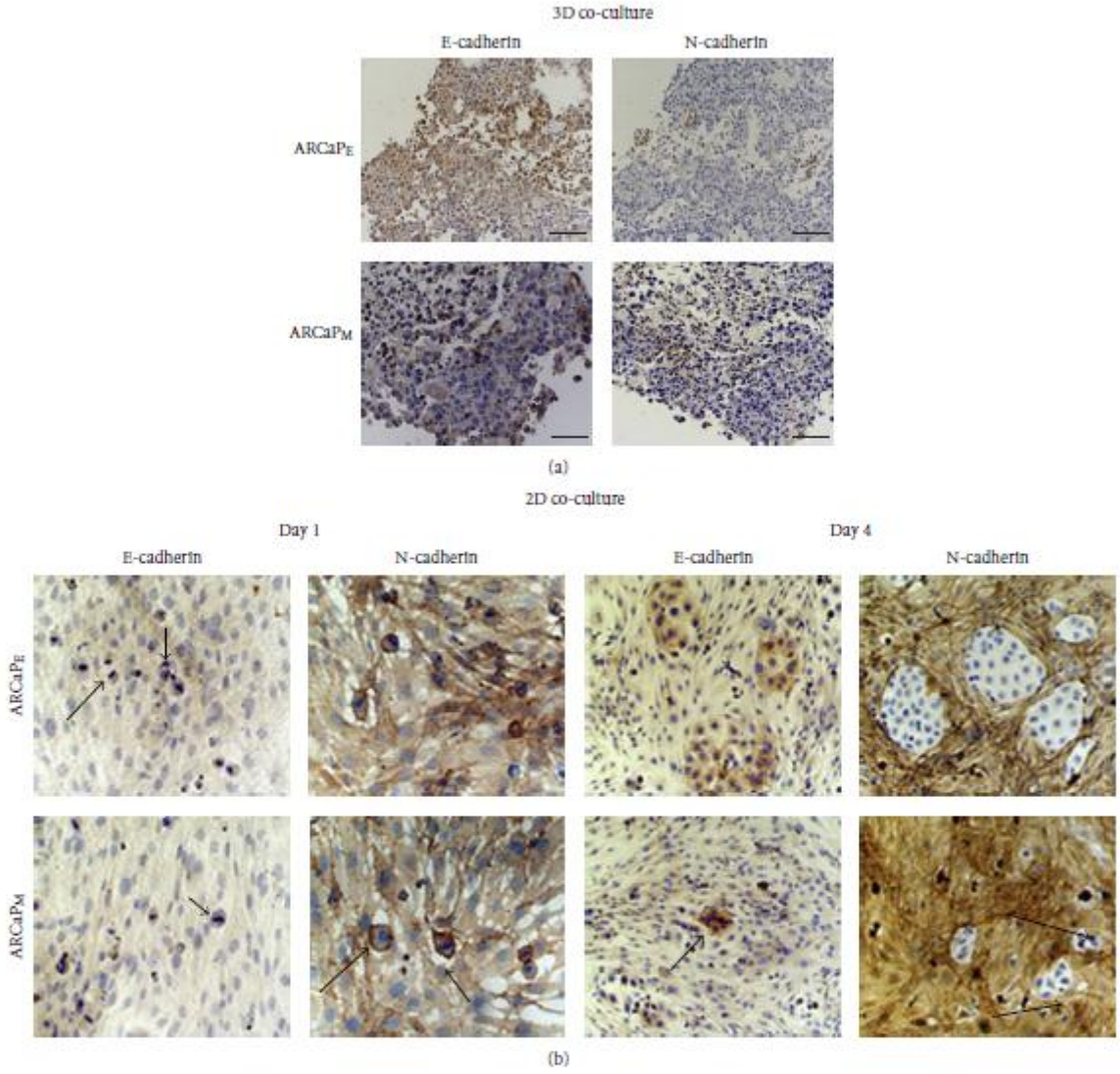

FIGURE 1: 3D cocultures of ARCaP$_E$ or ARCaP$_M$ with HS-27a cells show E-cadherin expression. (a) 1×10^7 ARCaP$_E$ or ARCaP$_M$ were cocultured with HS-27a cells in RWV for 3 days. Immunohistochemistry of organoids was stained with anti-E-cadherin or N-cadherin antibody. (b) 2D Cocultures of HS-27a were preformed utilizing a total of 50,000 cm^2/HS-27a fibroblasts, after which 20,000 cm^2 ARCaP$_E$ or ARCaP$_M$ were seeded on top of the fibroblast monolayer. The cocultures were maintained in serum-free medium for 1 or 4 days. Immunocytochemistry of cocultures over these time periods was performed utilizing anti-E-cadherin and N-cadherin antibodies. Shown are the EMT/MET of ARCaP$_E$cells (top panels) and MErT of ARCaP$_M$cells (bottom panels).

3.3. Blocking Adhesive Contact Effects Radiation Sensitivity of Cocultured ARCaP Cells. The importance of cell adhesion (i.e., cell-cell and cell-ECM adhesion) on the survival of disseminated cancer cells has been well documented as a requirement for colonization and survival within the metastatic microenvironment [32–34]. Therefore we utilized a well-known E-cadherin blocking antibody (SHEP8-7) and a pan-integrin antibody (CNT095) that targets human alpha-v-integrin and also was shown to block prostate tumor growth within bone [35]. Since ARCaP$_E$ cells express high levels of the epithelial marker E-cadherin, and ARCaP$_M$ cells can be microenvironmentally induced to express E-cadherin, we tested whether either of these blocking antibodies would affect the colony forming ability of either ARCaP$_E$ or

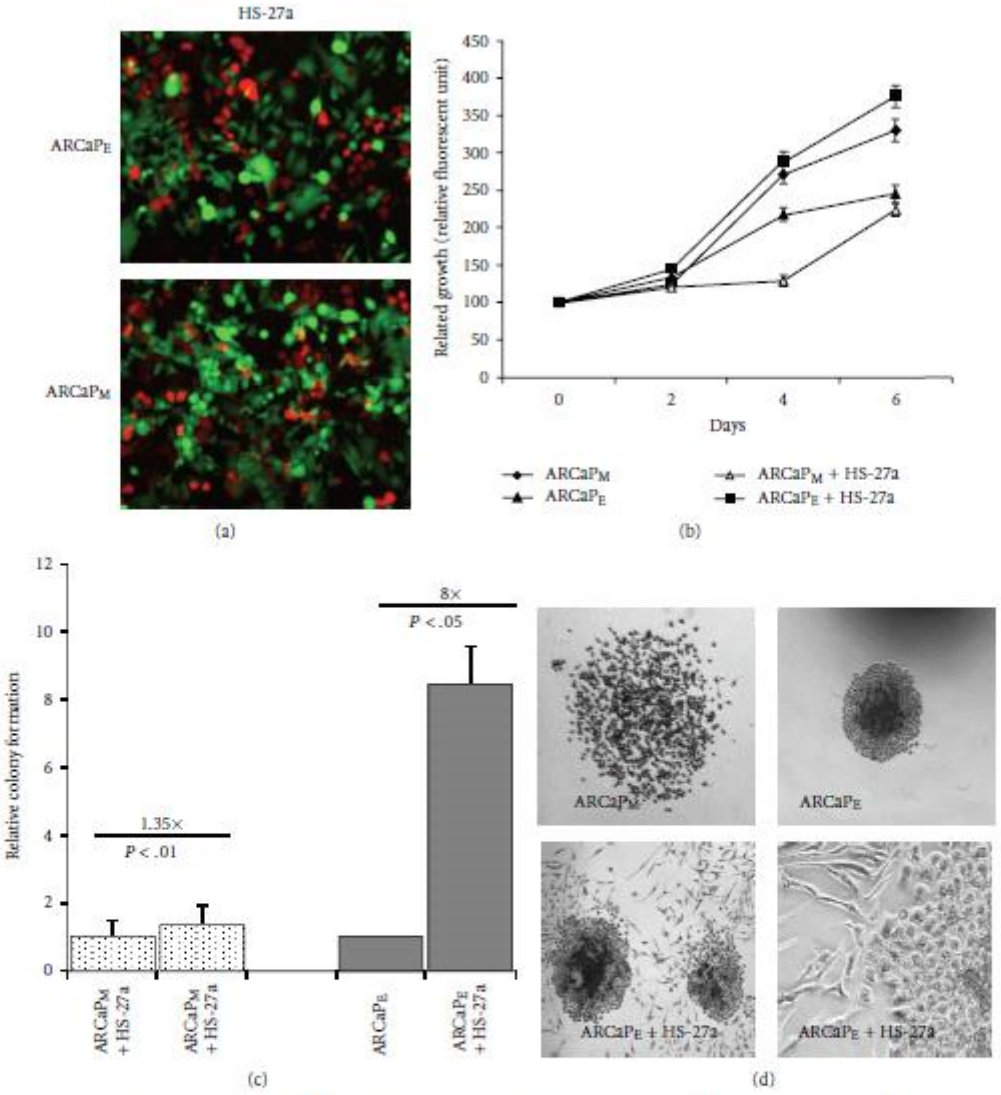

FIGURE 2: ARCaP$_E$ cells show a growth and colony forming capacity advantage in presence of HS-27a cells. (a) and (b) ARCaP$_M$ cells were cocultured in the presence of GFP-HS-27a cells over a 6-day period. Growth of RFP. ARCaP$_E$ or ARCaP$_M$ human prostate cancer cells was assessed by RFUs (relative fluorescent units) in the presence cocultures over a 6-day period. Results are means ± SE of three independent experiments. *$P < .05$ (students t-test) compared to cell number at day 1 ± SEM. (c) Clonogenic colony forming capacity of ARCaP$_E$ and ARCaP$_M$ prostate cancer cell after coculture ± SEM. ARCaP$_M$ data were normalized to ARCaP$_M$ control, and ARCaP$_E$ data were normalized to ARCaP$_E$ control (Note HS-27a induced slightly (1.35x) the growth of ARCaP$_M$ cells but markedly (8x) the growth of ARCaP$_E$ cells.). (d) ARCaP$_E$ or ARCaP$_M$ cells were cocultured with HS-27a cells. Shown are phase contrast images of colonies formed in the clonogenic assay.

ARCaP$_M$ bone stroma-cocultured cells. Pretreatment with E-cadherin antibody did not affect the colony forming capacity of either ARCaP$_E$ or ARCaP$_M$ homotypic cultured cells; however it significantly reduced the ability of ARCaP$_M$-($P < .001$) and ARCaP$_E$- ($P < .01$) coultured cells to form colonies (Figure 4). Additionally, E-cadherin blocking antibody pretreatments further increased sensitivity to radiation treatment of ARCaP$_M$ cells in homotypic and cocultured conditions, similarly ($P < .01$). E-cadherin blocking antibody-pretreated ARCaP$_E$ cells showed the most significant increased sensitivity to radiation treatment in homotypic compared cocultured conditions ($P < .001$), however a significant reduction in colony formation, to a lesser extent, was observed in ARCaP$_E$ cocultured cells

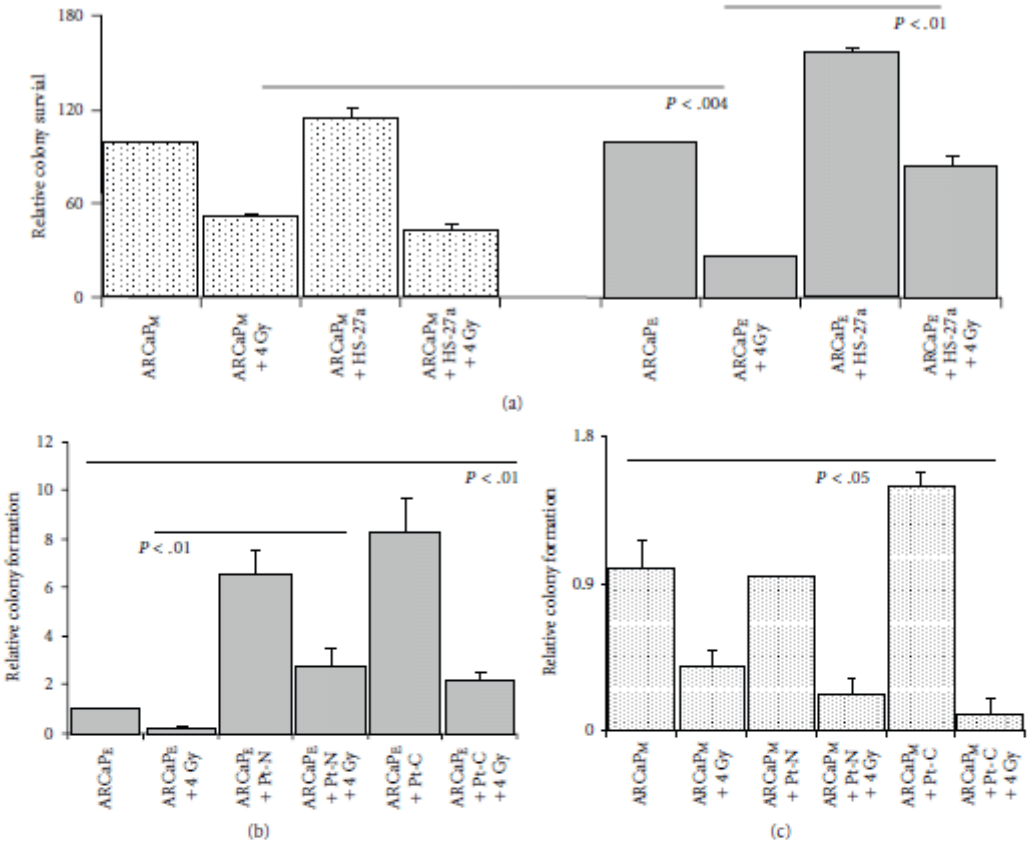

FIGURE 3: Cocultured $ARCaP_E$ cells gain cell colony forming capacity and radiation resistance when grown with bone and prostate stromal cells. (a) $ARCaP_E$ or $ARCaP_M$ cocultured cells were irradiated 24 hours after coculture with HS-27a cells and cancer cell colony forming capacity was assayed using clonogenic assay. Results are means ± SE of three independent experiments. $ARCaP_M$ experimental data are normalized to $ARCaP_M$ control and $ARCaP_E$ experimental data are normalized to $ARCaP_E$ control (a). $ARCaP_E$ cells cocultured with prostate stromal fibroblasts Pt-C (Cancer associated fibroblasts) or Pt-N (Normal/benign fibroblasts) were irradiated and compared to nonirradiated cocultures. Cell colony forming capacity was assayed by clonogenic assay. Data are normalized to $ARCaP_E$ control levels. (b) $ARCaP_M$ cells cocultured with Pt-C or Pt-N were irradiated and compared to nonirradiated cocultures (c). Cell colony forming capacity was assayed by clonogenic assay. Data are normalized to $ARCaP_M$ control levels.

(Figure 4, $P < .01$). Therefore, targeting E-cadherin limited both epithelial and mesenchymal cells ability to form colonies after coculture with bone stromal cells.

To determine the influence of intergin alpha v cell adhesion with bone microenvironment, we performed similar clonogenic formation assay. Pretreatment with CNT095 antibody significantly decreased the clonogenic ability of both $ARCaP_M$ and $ARCaP_E$ cells in homotyic cultures (Figure 5, $P < .001$). Additionally, CNT095 significantly decreased bone stroma-induced radiation resistance in cancer cells in both $ARCaP_M$ ($P < .001$) and $ARCaP_E$ ($P < .001$) cancer cells, with the most significant reduction in cocultured conditions ($P < .001$) (Figure 5). Taken together, these results suggest that bone stroma-induced radiation resistance is mediated through both E-cadherin and integrin alpha v beta signaling in epithelial and mesenchymal cells. Thus, E-cadherin and integrin alpha v beta appear to present novel targets for metastatic and radiation resistant cells.

4. Discussion

It is well documented in prostate and others cancers that EMT is associated with initial transformation from encapsulated to invasive carcinomas. The mesenchymal phenotype, which is required for dissemination, has been suggested to revert to an epithelial phenotype in distant metastasis [13, 14, 29, 36]. This has been evidenced in the primary tumors which lack E-cadherin expression and, showing nuclear β-catenin expression, show strong membrane staining for both E-cadherin and β-catenin in metastatic liver [13] or bone microenvironment [28, 29]. We have previously shown, in commonly utilized prostate cancer cells lines DU-145 and

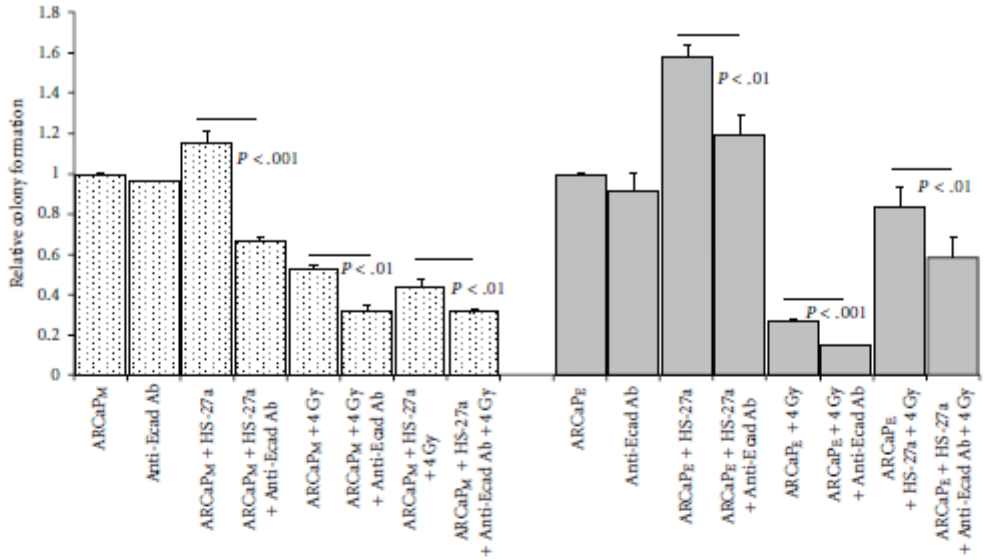

FIGURE 4: Effect of Anti-E-cadherin antibody on tumor-stroma interactions. A. $ARCaP_M$ and $ARCaP_E$, cells were pretreated with Anti-E-cadherin antibody (SHEP8-7), cocultured with HS-27a stromal cells for 24 hours, and radiated with 4 Gy. Cell colony forming capacity was assayed using clonogenic assay. $ARCaP_M$ data are normalized to $ARCaP_M$ control levels, and $ARCaP_E$ data are normalized to $ARCaP_E$ control levels.

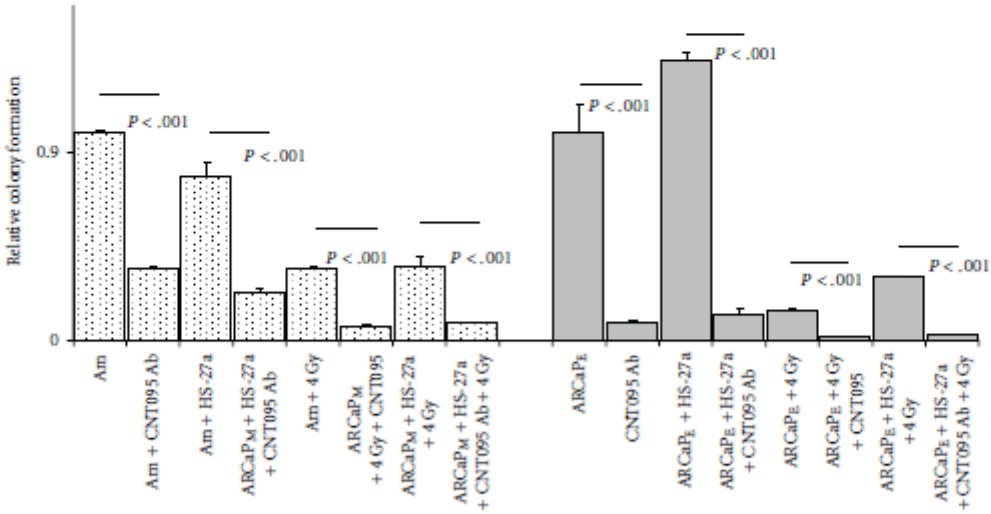

FIGURE 5: Effect of Anti-alpha v integrin (CNT095) on tumor-stroma interactions. $ARCaP_M$ and $ARCaP_E$, cells were pretreated with CNT095 antibody was cocultured with HS-27a stromal cells for 24 hours, and radiated with 4 Gy. Cell colony forming capacity was assayed using clonogenic assay. $ARCaP_M$ data are normalized to $ARCaP_M$ control levels, and $ARCaP_E$ data are normalized to $ARCaP_E$ control levels.

PC-3, that reexpression of E-cadherin and reversion of the mesenchymal phenotype is a rate limiting for metastatic seeding of primary rat hepatocytes [13]. Since bone metastasis is most prevalent in prostate cancers, we sought to extent these finding utilizing the ARCaP model, which is the first prostate cancer EMT model demonstrating histomorphological features and classical markers in a lineage-derived series of cells, to determine the functional relationship of this cellular transition. Whether this is accomplished through exposure to soluble growth factors or the bone microenvironment, the end result decreased differentiation with increased metastatic potential [25, 27, 37].

Our initial results show that $ARCaP_M$ cells maintained in 3D Rotary Wall Vessel (RWV) or 2D cocultures underwent

MErT when cocultured with HS-27a bone stromal cells, as shown through expression of E-cadherin and of N-cadherin expression (Figures 1(a) and 1(b)). Moreover $ARCaP_E$ cells show a significant enhancement in colony formation (8×) and significant growth pattern comparable to $ARCaP_M$ (1.35×) cocultures (Figures 2(b) and 2(c)). A recent report has shown through RFP cell tracking that selected $ARCaP_E$ clones after *in vivo* inoculation into the bone microenvironment gives rise to both $ARCaP_E$ and $ARCaP_M$ populations [37]. These findings coupled with our observed reversion of $ARCaP_M$ cells to $ARCAP_E$ like cells suggest that tumor-stromal-induced cellular plasticity gives rise to distinct populations of cancer cells within bone microenvironment, the mesenchymal phenotype and its kinetic characteristics (motility/invasive), and the epithelial characteristics necessary for secondary tumor development. The fact that the $ARCaP_M$ cells have an increase propensity for metastasis compared to $ARCaP_E$ cells suggest that dissemination from the primary tumor mass requires the mesenchymal phenotype. However a mesenchymal to epithelial transition is associated with initial metastatic seeding and subsequent formation of a cohesive tumor mass within the bone microenvironment. This hypothesis is supported in a bladder cancer model, where lineage-derived series of EMT-transformed mesenchymal-like cells exhibit increased lung metastasis *in vivo*; however secondary tumor formation is predominantly enhanced by the presence of epithelial cells compared to mesenchymal cells [38].

Since epithelial reversion enhances the growth of tumor cells in bone microenvironment, and this is observed in multiple experimental models and clinical metastases, there is a question of whether this transition is required for metastatic seeding and therefore an avenue for therapeutic intervention(s). To gain insight into the importance of this reversion, we utilized ionizing radiation on $ARCaP_E$ and $ARCaP_M$ homotypic and cocultured cells. Our results show that $ARCaP_E$ homotypic cultures when compared to $ARCaP_M$ homotypic cultures are more sensitive to radiation treatment (Figure 3(a)). However in the presence of bone or prostate stromal cells, $ARCaP_E$ cells gained increased radiation resistance, with increased proliferative and colony forming capacity (Figures 2(b) and 2(c)). This phenomenon was not observed in the $ARCaP_M$ cocultures. To determine the underlining causes of this observation, we hypothesized that cell-cell interactions through E-cadherin or cell-ECM interactions through integrins may mediate the stromal induced proliferative effect and radiation resistance in $ARCaP_E$ cancer cells. Using E-cadherin neutralizing antibody (SHEP8-7) and pan-anti-integrin alpha v antibody (CNT095), we were able to significantly block the stromal induced colony forming ability on $ARCaP_E$ cancer cells (Figures 4 and 5). Additionally, both antibodies significantly blocked the radiation resistance of $ARCaP_E$ in cocultured conditions (Figures 4 and 5). The E-cadherin neutralizing antibody also had an effect on homotypic $ARCaP_M$-radiated cells and $ARCaP_M$ cells within cocultures (Figure 4). Thus it appears that blocking bone stroma-induced reexpression of E-cadherin in $ARCaP_M$ in the presence of bone stromal cells reduced the colony forming capacity of these cells (Figure 4). The decreased radiation sensitivity of E-cadherin expressing cells compared to cells lacking E-cadherin expression has recently been demonstrated in a cocultured model of MCF-7 (E-cad positive) and MDA-MB-231 (E-cad negative) cells with normal and radiation-induced senescent fibroblast [39], where radiation in MCF-7 cells showed enhanced resistance to radiation treatment compared to MDA-MB-231 cells. These findings are consent with our model of a reepithelization requirement within tumor microenvironment.

CNT095 antibody was toxic to both $ARCaP_M$ and $ARCaP_E$ homotypic and cocultured cells. Additionally CNT095 increased radiation sensitivity, even to a greater extent than E-cadherin neutralizing antibody treatment (Figure 5). These findings are consistent with our results of CTN095 treatment that causes a significantly reduced number of tumors generated by C4-2B cells, along with a concomitant increase of cortical bone in mice (unpublished data). Although C4-2B cells have not been observed to undergo EMT, this would suggest that targeting the cell-ECM *in vitro* and *in vivo* could be limiting the cell cohesiveness necessary for metastatic tumor formation.

Targeting of cell adhesion as a therapeutic approach has been proposed previously. E-cadherin neutralizing antibody (SHEP8-7) has been shown to sensitize multicellular spheroids to microtubule binding therapies in the taxane family in HT29 human colorectal adenocarcinoma cells [23]. A more recent observation is that survival of androgen receptor-expressing differentiated prostate cells is dependent on E-cadherin and PI3K, but not on androgen, AR, or MAPK [40]. Given the predominate role for PI3K in cell survival and reports that PI3K is rapidly recruited to cell membrane to stabilize E-cadherin junctions [40] and that PI3K activation requires integrin alpha v activity [41] suggests that PI3K is possibly responsible for the increased growth and colony formation gained within the tumor microenvironment. Thus in the absence of stimulating growth factors, it is possible that E-cadherin/PI3K or integrin alpha v/PI3K is involved in a signaling cascade that is initiated by the tumor microenvironment, at least during initial metastatic seeding.

In conclusion, our data demonstrate that the E-cadherin and integrin alpha nctional adhesive interaction is a possible adjuvant therapy avenue for patients treated with radiation. Although an in-depth *in vivo* exploration of targeting epithelial-like versus mesenchymal-like cells is necessary to translate these findings to the clinical situation, our results indeed raise critical questions as to how we view prostate cancer metastasis and subsequently target metastatic tumor cells for therapy. Additionally, we have generated an *in vitro* model, that closely mimics the clinical situation, to delineate in a stepwise manner the dynamic tumor-host interaction(s) that promote cellular plasticity in the later stages of metastasis. The identification of further key molecules driving MErT in this system holds promise for the development of preventative and therapeutic strategies to minimize metastatic disease.

Acknowledgments

The project described was supported by Grant nos. PC073977 Department of Defense and PO-1 CA-098912 NIH/NCI. The authors would like to thank Drs. Hayien Zhau, Daquig Wu, and Wolfgang Cerwinka for insightful comments and discussions.

References

[1] A. F. Chambers, A. C. Groom, and I. C. MacDonald, "Dissemination and growth of cancer cells in metastatic sites," *Nature Reviews Cancer*, vol. 2, no. 8, pp. 563–572, 2002.

[2] P. M. Comoglio and L. Trusolino, "Invasive growth: from development to metastasis," *Journal of Clinical Investigation*, vol. 109, no. 7, pp. 857–862, 2002.

[3] J. M. Veltmaat, C. C. Orelio, D. Ward-Van Oostwaard, M. A. Van Rooijen, C. L. Mummery, and L. H. K. Defize, "Snail is an immediate early target gene of parathyroid hormone related peptide signaling in parietal endoderm formation," *The International Journal of Developmental Biology*, vol. 44, no. 3, pp. 297–307, 2000.

[4] B. Ciruna and J. Rossant, "FGF signaling regulates mesoderm cell fate specification and morphogenetic movement at the primitive streak," *Developmental Cell*, vol. 1, no. 1, pp. 37–49, 2001.

[5] J. C. Machado, C. Oliveira, R. Carvalho et al., "E-cadherin gene (CDH1) promoter methylation as the second hit in sporadic diffuse gastric carcinoma," *Oncogene*, vol. 20, no. 12, pp. 1525–1528, 2001.

[6] J. P. Thiery, "Epithelial-mesenchymal transitions in tumor progression," *Nature Reviews Cancer*, vol. 2, no. 6, pp. 442–454, 2002.

[7] R. C. Bates and A. M. Mercurio, "The epithelial-mesenchymal transition (EMT) and colorectal cancer progression," *Cancer Biology and Therapy*, vol. 4, no. 4, pp. 365–370, 2005.

[8] T. Brabletz, A. Jung, S. Reu et al., "Variable β-catenin expression in colorectal cancers indicates tumor progression driven by the tumor environment," *Proceedings of the National Academy of Sciences of the United States of America*, vol. 98, no. 18, pp. 10356–10361, 2001.

[9] I. Poser, D. Domínguez, A. G. de Herreros, A. Varnai, R. Buettner, and A. K. Bosserhoff, "Loss of E-cadherin expression in melanoma cells involves up-regulation of the transcriptional repressor Snail," *The Journal of Biological Chemistry*, vol. 276, no. 27, pp. 24661–24666, 2001.

[10] A. M. Lowy, J. Knight, and J. Groden, "Restoration of E-cadherin/β-catenin expression in pancreatic cancer cells inhibits growth by induction of apoptosis," *Surgery*, vol. 132, no. 2, pp. 141–148, 2002.

[11] G. Strathdee, "Epigenetic versus genetic alterations in the inactivation of E-cadherin," *Seminars in Cancer Biology*, vol. 12, no. 5, pp. 373–379, 2002.

[12] C. Yates, C. R. Shepard, G. Papworth et al., "Novel three-dimensional organotypic liver bioreactor to directly visualize early events in metastatic progression," *Advances in Cancer Research*, vol. 97, pp. 225–246, 2007.

[13] C. C. Yates, C. R. Shepard, D. B. Stolz, and A. Wells, "Co-culturing human prostate carcinoma cells with hepatocytes leads to increased expression of E-cadherin," *British Journal of Cancer*, vol. 96, no. 8, pp. 1246–1252, 2007.

[14] B. Saha, B. Chaiwun, S. S. Imam et al., "Overexpression of E-cadherin protein in metastatic breast cancer cells in bone," *Anticancer Research*, vol. 27, no. 6 B, pp. 3903–3908, 2007.

[15] H. S. Oh, A. Moharita, J. G. Potian et al., "Bone marrow stroma influences transforming growth factor-β production in breast cancer cells to regulate c-myc activation of the preprotachykinin-1 gene in breast cancer cells," *Cancer Research*, vol. 64, no. 17, pp. 6327–6336, 2004.

[16] N. A. Bhowmick and H. L. Moses, "Tumor-stroma interactions," *Current Opinion in Genetics and Development*, vol. 15, no. 1, pp. 97–101, 2005.

[17] M. L. Ackland, D. F. Newgreen, M. Fridman et al., "Epidermal growth factor-induced epithelio-mesenchymal transition in human breast carcinoma cells," *Laboratory Investigation*, vol. 83, no. 3, pp. 435–448, 2003.

[18] C. D. Andl, T. Mizushima, H. Nakagawa et al., "Epidermal growth factor receptor mediates increased cell proliferation, migration, and aggregation in esophageal keratinocytes in vitro and in vivo," *The Journal of Biological Chemistry*, vol. 278, no. 3, pp. 1824–1830, 2003.

[19] A. P. Armstrong, R. E. Miller, J. C. Jones, J. Zhang, E. T. Keller, and W. C. Dougall, "RANKL acts directly on RANK-expressing prostate tumor cells and mediates migration and expression of tumor metastasis genes," *Prostate*, vol. 68, no. 1, pp. 92–104, 2008.

[20] V. A. Odero-Marah, R. Wang, G. Chu et al., "Receptor activator of NF-κB Ligand (RANKL) expression is associated with epithelial to mesenchymal transition in human prostate cancer cells," *Cell Research*, vol. 18, no. 8, pp. 858–870, 2008.

[21] M. D. Mason, G. Davies, and W. G. Jiang, "Cell adhesion molecules and adhesion abnormalities in prostate cancer," *Critical Reviews in Oncology/Hematology*, vol. 41, no. 1, pp. 11–28, 2002.

[22] X. Qian, T. Karpova, A. M. Sheppard, J. McNally, and D. R. Lowy, "E-cadherin-mediated adhesion inhibits ligand-dependent activation of diverse receptor tyrosine kinases," *The EMBO Journal*, vol. 23, no. 8, pp. 1739–1748, 2004.

[23] S. K. Green, M. C. I. Karlsson, J. V. Ravetch, and R. S. Kerbel, "Disruption of cell-cell adhesion enhances antibody-dependent cellular cytotoxicity: implications for antibody-based therapeutics of cancer," *Cancer Research*, vol. 62, no. 23, pp. 6891–6900, 2002.

[24] H. E. Zhau, C.-L. Li, and L. W. K. Chung, "Establishment of human prostate carcinoma skeletal metastasis models," *Cancer*, vol. 88, no. 12, pp. 2995–3001, 2000.

[25] J. Xu, R. Wang, Z. H. Xie et al., "Prostate cancer metastasis: role of the host microenvironment in promoting epithelial to mesenchymal transition and increased bone and adrenal gland metastasis," *Prostate*, vol. 66, no. 15, pp. 1664–1673, 2006.

[26] H. He, X. Yang, A. J. Davidson et al., "Progressive epithelial to mesenchymal transitions in $ARCaP_E$ prostate cancer cells during xenograft tumor formation and metastasis," *Prostate*, vol. 70, no. 5, pp. 518–528, 2010.

[27] H. E. Zhau, V. Odero-Marah, H.-W. Lue et al., "Epithelial to mesenchymal transition (EMT) in human prostate cancer: lessons learned from ARCaP model," *Clinical & Experimental Metastasis*, vol. 25, no. 6, pp. 601–610, 2008.

[28] A. Wells, C. Yates, and C. R. Shepard, "E-cadherin as an indicator of mesenchymal to epithelial reverting transitions during the metastatic seeding of disseminated carcinomas," *Clinical & Experimental Metastasis*, vol. 25, no. 6, pp. 621–628, 2008.

[29] B. Saha, P. Kaur, D. Tsao-Wei et al., "Unmethylated E-cadherin gene expressionis significantly associated with metastatic

The American Journal of Pathology, Vol. 181, No. 5, November 2012

http://dx.doi.org/10.1016/j.ajpath.2012.08.008

Tumorigenesis and Neoplastic Progression

Nuclear Kaiso Indicates Aggressive Prostate Cancers and Promotes Migration and Invasiveness of Prostate Cancer Cells

Jacqueline Jones,* Honghe Wang,* Jianjun Zhou,* Shana Hardy,* Timothy Turner,* David Austin,* Qinghua He,† Alan Wells,‡ William E. Grizzle,§ and Clayton Yates*

From the Department of Biology, Center for Cancer Research, and the Department of Chemical Engineering,† Tuskegee University, Tuskegee, Alabama; the Department of Pathology, Pittsburgh Veterans Affairs Medical Center, and the Department of Pathology,‡ University of Pittsburgh, Pittsburgh, Pennsylvania; and the Department of Pathology,§ University of Alabama at Birmingham School of Medicine, Birmingham, Alabama*

Kaiso, a p120 catenin-binding protein, is expressed in the cytoplasmic and nuclear compartments of cells; however, the biological consequences and clinical implications of a shift between these compartments have yet to be established. Herein, we report an enrichment of nuclear Kaiso expression in cells of primary and metastatic prostate tumors relative to the normal prostate epithelium. Nuclear expression of Kaiso correlates with Gleason score ($P < 0.001$) and tumor grade ($P < 0.001$). There is higher nuclear expression of Kaiso in primary tumor/normal matched samples and in primary tumors from African American men ($P < 0.0001$). We further found that epidermal growth factor (EGF) receptor up-regulates Kaiso at the RNA and protein levels in prostate cancer cell lines, but more interestingly causes a shift of cytoplasmic Kaiso to the nucleus that is reversed by the EGF receptor–specific kinase inhibitor, PD153035. In both DU-145 and PC-3 prostate cancer cell lines, Kaiso inhibition (short hairpin RNA-Kaiso) decreased cell migration and invasion even in the presence of EGF. Further, Kaiso directly binds to the E-cadherin promoter, and inhibition of Kaiso in PC-3 cells results in increased E-cadherin expression, as well as re-establishment of cell–cell contacts. In addition, Kaiso-depleted cells show more epithelial morphology and a reversal of the mesenchymal markers N-cadherin and fibronectin. Our findings establish a defined oncogenic role of Kaiso in promoting the progression of prostate cancer. *(Am J Pathol 2012, 181:1835–1846; http://dx.doi.org/10.1016/j.ajpath.2012.08.008)*

Prostate cancer is the most commonly diagnosed malignancy in men, with African American men experiencing a rate 60% higher than white patients. At the time of diagnosis, approximately 50% of men have clinically advanced disease.[1] The molecular mechanisms associated with tumor development are the result of genetic and epigenetic changes that promote tumor cell growth. DNA methylation, the most common epigenetic change, results from changes in cytosine methylation, typically at cytosine-guanine dinucleotides (CpG), or from changes in DNA-associated proteins. Recently, it was proposed that methylation alone is insufficient to silence transcription[2] and that recognition of methylated DNA by two classes of proteins, those with a methyl-CpG binding domain and those with C2H2 zinc fingers, such as Kaiso, are required for transcriptional inactivation. Methyl-CpG binding proteins recognize 5-methylcytosine and act as intermediates between the transcriptional machinery and methylated DNA. Of the methyl-binding proteins, Kaiso has a 10-fold higher affinity and represses transcription in part by recruiting the N-CoR corepressor.[2]

Kaiso, first identified as a p120 catenin (ctn)-binding protein,[3] is a member of the broad complex, tramtrak, brio-a-brac/pox virus, and zinc finger superfamily. Structurally, Kaiso contains a carboxyl-terminal region with

Supported by the Department of Defense Prostate Cancer Research Program (PC073977 to C.Y.), the NIH/Research Centers for Minority Research (RCMI) (G12 RR03059-21A1 to C.Y.), a pilot project of the NIH/National Cancer Institute (U54 CA119623 to C.Y.), and a Veterans Affairs (VA) Merit Award.

Accepted for publication August 1, 2012.

J.J. and H.W. contributed equally to this work.

Supplemental material for this article can be found at http://ajp.amjpathol.org or at http://dx.doi.org/10.1016/j.ajpath.2012.08.008.

Address reprint requests to Clayton Yates, Ph.D., Department of Biology and Center for Cancer Research, Tuskegee University, Carver Research Foundation, Room 22, Tuskegee, AL 36088. E-mail: cyates@mytu.tuskegee.edu

three zinc finger motifs of the C2H2 type and recognizes clusters of methylated CpG dinucleotides as well as sequence-specific Kaiso binding sites.[4] Several lines of evidence from both *in vitro* and *in vivo* models suggest a number of tumor suppressor genes, frequently silenced by hypermethylation, such as *HIC1*, *MTA2*, E-cadherin (*CDH1*), and matrilysin (*MMP7*) have been linked to Kaiso transcriptional regulation.[5,6] A clinical role for Kaiso also has been proposed. Immunohistochemical analysis in various tissue types shows that Kaiso is expressed in both the cytoplasmic and/or nuclear compartments. Studies in lung cancer show that Kaiso expression correlates with clinicopathologic characteristics of malignant tumors. However, functional studies using Kaiso antibody or the shRNA–depletion strategy resulted in enhanced proliferation and invasiveness.[6] Surprisingly, an opposite role for Kaiso was implicated in colorectal studies, in which down-regulation of Kaiso expression resulted in decreased proliferation and an overall antitumor effect.[6] Because Kaiso expression has been determined in multiple tumor types, additional studies are required to provide a detailed description of Kaiso expression and function in individual epithelial tumors.

Growth factors such as epidermal growth factor (EGF) have been well established to promote cell motility, invasion, and metastasis in multiple tumors. This promotes genetic and epigenetic changes that lead to a down-regulation of E-cadherin, via receptor tyrosine kinase signaling, and/or promoter hypermethylation. As a result, epithelial cells undergo an epithelial-to-mesenchymal transition, in which cells are directed to assume a less-differentiated phenotype with the acquired ability for metastasis. Previously, we showed that E-cadherin can be re-expressed through direct pharmacologic abrogation of EGF receptor (EGFR) signaling[7] or within the metastatic tumor microenvironment,[8] resulting in less invasive and more cohesive cells. However, whether Kaiso has a functional role and specific involvement in EGFR-associated epithelial-to-mesenchymal transition has not been explored. Herein, we show that Kaiso is highly expressed in primary prostate tumors and lymph node metastases, with significant increases for African Americans compared with white patients in high-grade tumors. Furthermore, a cytoplasmic-to-nuclear shift occurs in tumors and this correlates with increasing tumor grade and Gleason score. We further identified that EGF induces nuclear localization of Kaiso, which subsequently is associated with an increase in cell migration and invasion and suppression of tumor suppressor E-cadherin expression. These results show that Kaiso functions in an oncogenic manner, in which aberrant localization in the nucleus is essential for prostate cells to acquire the ability to metastasize.

Materials and Methods

Cell Culture, Antibodies, and Reagents

Human prostate cancer cell lines LNCaP, DU-145, and PC-3 were obtained from the ATCC and routinely were cultured in Dulbecco's modified Eagle's medium supplemented with 10% fetal bovine serum (Gibco, Paisley, Scotland) and antibiotics in a humidified atmosphere of 5% CO_2 in air. In these conditions the duplication period of the cells is 36 hours.

DU-145 EGFR-overexpressing cells [wild type (WT) DU-145] were generated by transfecting DU-145 cells with retroviral-containing EGFR constructs.[7] Primary antibodies were obtained as follows: Kaiso 6F clone (Abcam, Boston, MA); anti-Kaiso clone 6F (Upstate Biotechnology, Billerica, MA); anti-Kaiso 12H (Santa Cruz, CA); p120ctn, E-cadherin, and N-cadherin (BD Biosciences, OR). Mouse secondary antibodies, Alexa 488, 594, and 625, were obtained from Invitrogen (OR). Human EGF was obtained from BD Biosciences (KY). The EGFR-specific tyrosine kinase inhibitor, PD153035, was purchased from CalBiochem (CA). Other reagents were obtained from Sigma-Aldrich (St. Louis, MO).

Immunohistochemistry

The prostate cancer tissue microarrays were obtained from US Biomax (Rockville, MD) or from the Anatomical Pathology Division at the University of Alabama at Birmingham. The use of tissue was approved by the Institutional Review Board of both Tuskegee University and the University of Alabama at Birmingham. Immunohistochemistry was performed using the anti-Kaiso clone 6F (Upstate Biotechnology) and 12H clone (Santa Cruz) as previously described. Duplicate microarrays were stained for evaluation by immunohistochemistry.[5] Briefly, cells were blindly scored by two pathologists with similar results. Individual specimens were scored separately for membranous, cytoplasmic, and nuclear staining for Kaiso and classified with respect to the intensity of immunostaining, with the percentage of cells determined at each staining intensity from 0 to +4.[9] To permit numeric analysis, the proportion of cells at each intensity can be multiplied by that intensity. Statistical analyses were performed using the Pearson χ^2 test to analyze the relationships between cytoplasmic and nuclear expression of Kaiso and clinicopathologic factors.

Immunoblotting

Cells were grown to 80% confluency in six-well plates. Lysates were prepared from cultured cells in a solution containing 50 mmol/L Tris, pH 7.5; 120 mmol/L NaCl; 0.5% Nonidet p-40; 40 μmol/L phenylmethylsulfonyl fluoride; 50 μg/mL leupeptin; and 50 μg/mL aprotinin (all from Sigma-Aldrich). Cells were allowed to lyse for 1 hour on ice. The lysed cells were centrifuged, and the resulting supernatants were extracted and quantitated by use of a Bradford assay. Lysates (30 μg of protein) were separated by 8% SDS PAGE, immunoblotted, and analyzed by chemiluminescence (Amersham Biosciences, NJ). Densitometry was performed using NIH ImageJ software version 1.46 (Bethesda, MD).

Immunoblotting of Subcellular Fractions

Subcellular fractionation of cells was performed as previously described.[10] Cytosolic and nuclear fractions, and the DU-145, DU-145 WT, and PC-3 cells were resuspended in a hypotonic buffer [10 mmol/L Tris (pH 7.5), 1.5 mmol/L $MgCl_2$, 10 mmol/L KCl, 1 mmol/L dithiothreitol, pepstatin, leupeptin] and homogenized using a glass douncer. The cells were centrifuged at 13,000 × *g* and the supernatant was collected (cytosolic fraction). The nuclei were resuspended in a high-salt buffer [20 mmol/L HEPES (pH 7.9), 25% glycerol, $MgCl_2$, 1.2 mol/L KCl, 0.2 mmol/L EDTA, 0.2 mmol/L phenylmethylsulfonyl fluoride, 1 mmol/L dithiothreitol] and rotated at 4°C. Lysates then were separated by 7.5% SDS PAGE, immunoblotted, and analyzed by chemiluminescence (Amersham Biosciences).

Immunofluorescence Microscopy

Cells (3×10^5) were grown to 80% confluency on glass coverslips. Cells then were fixed with methanol alone or 4% paraformaldehyde, permeabilized with 100 mmol/L Tris-HCl (pH 7.4), 150 mmol/L NaCl, 10 mmol/L EGTA, 1% Triton X-100, 1 mmol/L phenylmethylsulfonyl fluoride, and 50 μg/mL aprotinin (all from Sigma-Aldrich) and subsequently blocked with 5% bovine serum albumin for 1 hour at room temperature. Identical results were obtained with both methods. Samples were incubated with indicated primary antibodies diluted in blocking buffer at 4°C overnight. Fluorescein isothiocyanate–conjugated secondary antibody (BD Biosciences) was added. Cells then were treated with DAPI for nuclear staining and analyzed with a disk scanning unit confocal microscope (Olympus, Pittsburgh, PA). To determine the relative intensities, the total area of cytoplasmic and nuclear regions of each image was measured as well as the threshold intensity for each channel using Metamorph Imaging Software version 7.5 (Molecular Devices, Inc, Sunnyvale, CA). Differences between intensities then were determined by Excel (Microsoft, Redmond, WA). Bar graphs represent $n = 3$ images sectioned and individually analyzed for total area. All quantitative data were normalized to appropriate control images.

Quantitative RT-PCR

RNA was extracted from prostate cancer cells using TRIzol (Invitrogen). cDNA was prepared using Superscript III First Strand cDNA Synthesis kits (Invitrogen) and detected by Kaiso-specific TaqMan (Invitrogen). The housekeeping gene hypoxanthine-guanine phosphoribosyltransferase (HRPT1; Applied Biosystems, Carlsbad, CA) was used as an endogenous control for all RNA samples. RNA analyses were performed in triplicate, and fold change was calculated using the ΔΔCt value method.

RNA Interference

To generate stable short hairpin RNA (shRNA) Kaiso cells, the HuSH 29-mer for Kaiso was provided in the pRFP-C-RS plasmid driven by the U6-RNA promoter. Plasmid DNA pRFP-C-RS, containing puromycin-resistant gene, expressing Kaiso-specific shRNA, and scrambled shRNA were transfected into DU-145 or PC-3 cells using Lipofectamine 2000 (Invitrogen). The medium was replaced by T medium containing 2 μg/mL puromycin for selection of antibiotic-resistant colonies over a period of 3 weeks. The puromycin-resistant cells were further selected by use of red fluorescence protein as a marker to enrich for cells expressing shRNA. sh-Kaiso cells were plated at clonal densities, and more than 20 clones were chosen to determine the degree of knockdown. Clones with the lowest Kaiso levels were retained for further analysis.

Cell Migration

Migration of cells was assessed by their ability to move into an acellular area; this was accomplished with a two-dimensional wound-healing assay, as previously described.[11] With cells at 70% to 80% confluence, a denuded area was generated in the middle of each well with a rubber policeman. The cells then were exposed to EGF (0 or 10 ng/mL) and incubated for 24 hours in dialyzed media. The rate of migration was determined and quantified in Metamorph Imaging Software. All measurements were normalized to values for controls.

Invasion Assay

Cell invasiveness was determined by the capacity of cells to migrate across a layer of extracellular matrix, matrigel, in a Boyden chamber. Briefly, 20,000 cells were plated in the matrigel-containing chamber in serum-free medium containing 1% bovine serum albumin for 24 hours; this then was replaced with a serum-free medium for an additional 24 hours. The number of cells that invaded through the matrix over a 48 hour-period was determined by counting cells that stained with crystal violet on the bottom of the filter. All experiments were performed in triplicate.

Chromatin Immunoprecipitation Assay

Chromatin immunoprecipitation experiments were performed with the use of the ChIP-IT Kit (Active Motif, Carlsbad, CA). In brief, PC3 cells were fixed in 1% formaldehyde at room temperature for 10 minutes; the fixation reaction was stopped by adding a 1:10 volume of 10× glycine to the tube at room temperature for 5 minutes. The cell pellets were resuspended and incubated for 30 minutes in ice-cold lysis buffer with phenylmethylsulfonyl fluoride and proteinase inhibitor cocktail. The nuclear pellets were resuspended in shearing buffer, and chromatin was sheared to an average size of 200 to 1500 bp by sonication at 25% power for 10 pulses of 20 seconds

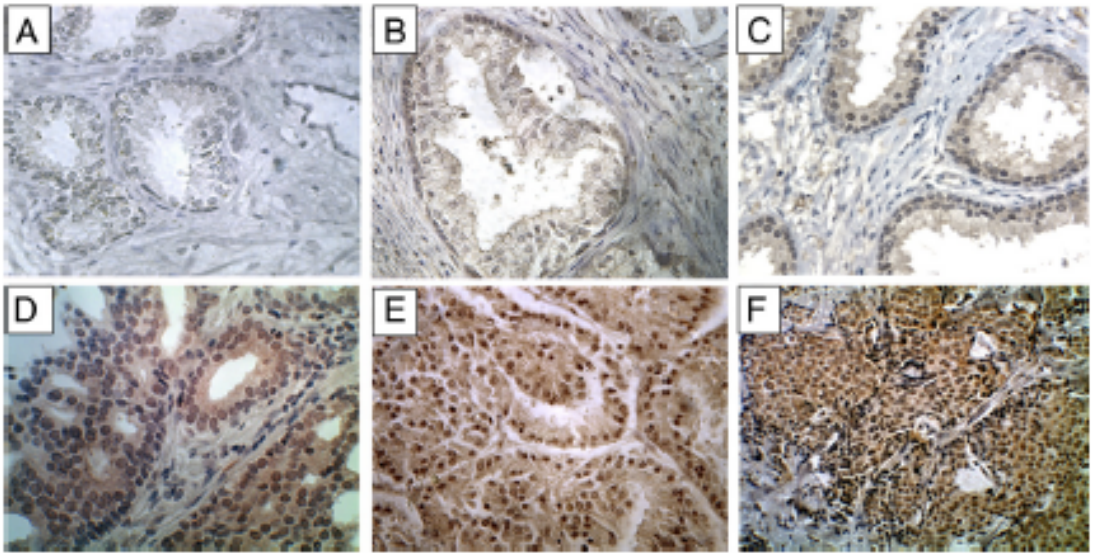

Figure 1. Abnormal nuclear expression of Kaiso in prostate cancer specimens. Representative data from immunohistochemical studies of 172 prostate cancer specimens are shown. A: Kaiso levels in a normal, healthy prostate with low staining seen in glandular epithelia. B: Kaiso expression in normal epithelia from adjacent PCa tumors showed discernible cytoplasmic staining in epithelia, and nuclear positivity in the basal cells. C: Kaiso expression in benign prostatic hyperplasia showed cytoplasmic positivity with low nuclear positivity. D: Kaiso expression in low grade 3 tumors showed a general up-regulation of Kaiso expression with cytoplasmic and nuclear positivity. E and F: High grade 9 and lymph node metastasis showed uniform intense nuclear expression of Kaiso. Original magnification: ×400.

each, with a 30-second rest on ice between each pulse. Chromatin (10 μL) was saved for input DNA control. Sheared chromatin was incubated in chromatin immunoprecipitation buffer with 25 μL of protein G magnetic beads and anti-Kaiso antibody (Abcam), mouse RNA Polymerase II (Active Motif), and rabbit IgG antibody (Active Motif) as a negative control on a rolling shaker at 4°C for 4 hours. The immunoprecipitated chromatin was purified from the chromatin-antibody mixture by several washing steps, and the chromatin-immunoprecipitated DNA was eluted in 50 μL of elution buffer AM2 (Active Motif). Cross-links were reversed by adding 50 μL of reverse cross-link buffer. After removing proteins by digestion with proteinase K, the purified DNA was used as templates for PCR analysis. The primers used were designed to amplify a 422-bp methylated fragment of the E-cadherin promoter (−1163 to −1585): 5'-AGGAGGCTGATAGAGGAGAACC-3' and 5'-GATTGAGACCATCCTGGCTAAC-3'.

Statistical Analysis

For all experiments, statistics were performed with Microsoft Excel or Prism software version 5.0 (GraphPad, La Jolla, CA). An independent Student's *t*-test was used to determine statistical differences between experimental and control values. Median scores were obtained from a subset of patients to statistically evaluate Kaiso expression. Tissue correlations were performed with Matlab (Mathworks, Inc, Natick, MI). *P* values <0.05 were considered statistically significant.

Results

Kaiso Expression and Subcellular Localization

To evaluate the expression and localization of Kaiso during prostate cancer progression, immunohistochemistry was used to evaluate samples from 172 patients, consisting of normal tissue (9 patients), benign prostatic hyperplasia (14 patients), adjacent normal tissue (17 patients), primary tumors (142 patients), and metastases (4 patients). There was low expression of the Kaiso protein in luminal cells of noncancerous samples (Figure 1A); expression was predominantly in the membrane or cytoplasm (Figure 1, B and C). There was, however, nuclear expression of Kaiso in the basal cells of adjacent normal tissue (Figure 1B). Scoring for nuclear Kaiso staining intensities 0 to 4 (as mentioned in *Materials and Methods*) between normal, low Gleason, and high Gleason are summarized in Table 1.

In contrast to previous reports, Kaiso expression was observed within the nucleus, with weak to moderate ex-

Table 1. Nuclear Kaiso Expression in Normal, Low Gleason, High Gleason, and Lymph Node Metastases Prostate Carcinomas

Kaiso	Normal (n = 26)*	Low Gleason (n = 52)	High Gleason (n = 50)	Mets
No score (0)	9			
Weak (0–1)	10	18	4	
Moderate (2–3)	7*	28	10	
Strong (3–4)		6	36	4

*Adjacent normal.

Table 2. Correlation of Kaiso Subcellular Localization with Clinical Features

Characteristics	All patients	Cytoplasmic Kaiso expression		P^a	Nuclear Kaiso expression		P^a
		≤0.53 (median)	>0.53		≤2.45 (median)	>2.45	
Total	142	70	72		73	69	
Age							
≤69.5 (median)	71	27	44	0.0072	35	36	0.6145
>69.5	71	43	28		38	33	
Grade							
≤2	70	39	31	0.1066	57	13	<0.001
>2	69	29	40		13	56	
Gleason score							
≤7	52	20	32	0.6394	29	23	<0.001
>7	50	17	33		10	40	
PSA, ng/mL	15	4	11	0.1587	3	12	0.058
≤17, median	15	5	10		8	7	

[a] P value for the correlation of the mean expression with clinical feature. P values were obtained with the χ^2 test. Statistics were not performed on samples without clinical information. Median scores were obtained for each subset.

pression in tumors with low Gleason scores (Figure 1D), and strong intense expression in tumors with high Gleason scores and in metastases (Figure 1, E and F). To determine the clinical significance of subcellular localization of Kaiso expression, we performed χ^2 analysis. Median values of scoring intensities were used to separate the low and high tumor grades and Gleason scores. Nuclear expression of Kaiso was found to correlate significantly with tumor grade of ≥2 ($P < 0.001$) and Gleason score of ≥7 ($P < 0.001$) (Table 2). Cytoplasmic expression was observed in tumor samples; however, correlations with clinicopathologic features were not found to be significant. Increased nuclear expression occurred in a stage-specific manner, with the largest differential expression between metastatic tumors and normal samples; however, differences between primary tumors and normal samples were significant as well (Figure 2A). Further characterization of nuclear Kaiso expression in high grade tumors of similar-age African American men ($n = 22$) and white ($n = 18$) primary tumors showed that African American patients expressed higher mean values of Kaiso ($P < 0.0001$) independent of grade and age (Figure 2B). Further Kaiso nuclear expression significantly correlated with race ($P = 0.0032$) (see Supplemental Table S1 at *http://ajp.amjpathol.org*).

To determine whether there is a shift in Kaiso localization in prostate tumors, matched normal and tumor samples were evaluated ($n = 13$). Cytoplasmic expression was decreased significantly in paired primary tumors compared with normal samples ($P < 0.0001$) (Figure 2C); however, there were significant increases in nuclear expression within the same patients ($P < 0.0001$) (Figure 2D). This analysis supports the idea that there is a progressive enhancement of abnormal Kaiso expression during prostate cancer progression and that the extent of abnormal expression correlates with progression.

Expression and Subcellular Localization of Kaiso in Prostate Cancer Cell Lines

Because there have been no reports of Kaiso expression in prostate cancer cell lines, its expression and localization were evaluated in LNCaP, DU-145, and PC-3 cells, and in a DU-145 subline (DU-145WT) that was genetically engineered to overexpress EGFR. DU-145 WT cells escape EGFR down-regulation and show enhanced invasiveness *in vitro*[12] and *in vivo*.[13] Quantitative RT-PCR showed that Kaiso levels were increased at the mRNA in DU-145 WT and PC-3 cells compared with LNCaP and DU-145 cells (see Supplemental Figure S1A at *http://ajp.amjpathol.org*). Confocal images show that Kaiso is located in both the cytoplasmic and nuclear compartments in all cell lines. However, the more aggressive

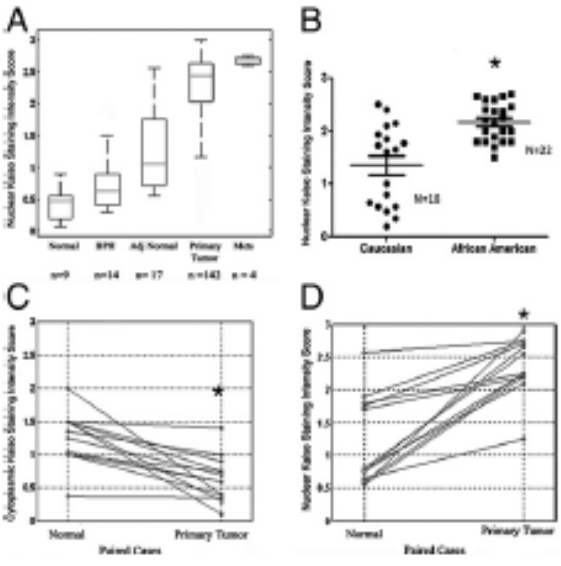

Figure 2. Quantitative analysis of nuclear Kaiso in prostate tumor progression. A: Nuclear expression of Kaiso was analyzed and presented in a box plot. Nuclear Kaiso levels increases monotonically from normal, benign prostatic hyperplasia (BPH), adjacent normal, primary tumor, and metastasis, with all four P values less than 0.05. ($P = 0.016$, normal and BPH; $P = 0.01$, BPH and adjacent normal; $P < 0.0001$, adjacent normal and malignant; and $P < 0.0001$, malignant and metastasis). B: Points represent nuclear Kaiso staining intensity of individual African American and white patients of similar age (ages, 67 to 80) and grade 3; bars represent the median value for the sample set. *$P < 0.0001$. Cytoplasmic Kaiso expression (C) and nuclear Kaiso expression (D) in paired (surrounding nontumor) normal and primary tumor tissue from $N = 13$ prostate cancer patients. *$P < 0.0001$.

DU-145WT and PC-3 cells showed increased presence of nuclear expression compared with LNCaP and DU-145 cells (see Supplemental Figure S1B at http://ajp.amjpathol.org), which was verified after quantification of fluorescent intensity in each compartment (see Supplemental Figure S1C at http://ajp.amjpathol.org). The influence of EGFR expression on Kaiso localization was shown further by the fact that subcellular fractions of DU-145 WT cells show increased nuclear expression, whereas DU-145 cells show low amounts of nuclear levels, which correlated with the confocal images (see Supplemental Figure S1D at http://ajp.amjpathol.org). Thus, it appears that the subcellular localization of Kaiso is associated with EGFR expression.

Activation of EGFR Signaling Results in Increased Kaiso Expression and Nuclear Localization

Various lines of evidence suggest the involvement of EGFR signaling in prostate cancer.[14,15] To identify EGFR as an upstream regulator of Kaiso, 10 ng/mL EGF, a concentration showing the most significant fold increase (data not shown), was used in a time-dependent assay over 24 hours. DU-145, DU-145 WT, and PC-3 lines showed incremental increases in Kaiso expression at the RNA level; DU145WT cells showed the greatest increase (fourfold) as early as 1 hour after EGF stimulation (Figure 3A). Increases in Kaiso expression also were observed at the protein level, as determined by immunoblots, with significant increases observed as early as 6 hours and sustained over 24 hours of exposure to EGF (Figure 3B).

Because we observed that increases in Kaiso expression are associated with a subcellular localization pattern in our patient cohort, we further determined if EGFR-induced increases in Kaiso expression coincided with a subcellular localization in our cell culture model. After only 0.5 hours, EGF caused perinuclear accumulation of previously dispersed Kaiso in DU-145 cells, with visible nuclear accumulation at 1 hour. After 24 hours, significant increases in both cytoplasmic and nuclear expression were observed, although nuclear expression was the most significant (Figure 3, C and D). DU-145WT and PC-3 cells, which endogenously express high levels of nuclear Kaiso, showed similar trends as DU-145 cells. Both cytoplasmic and nuclear Kaiso expression increased on

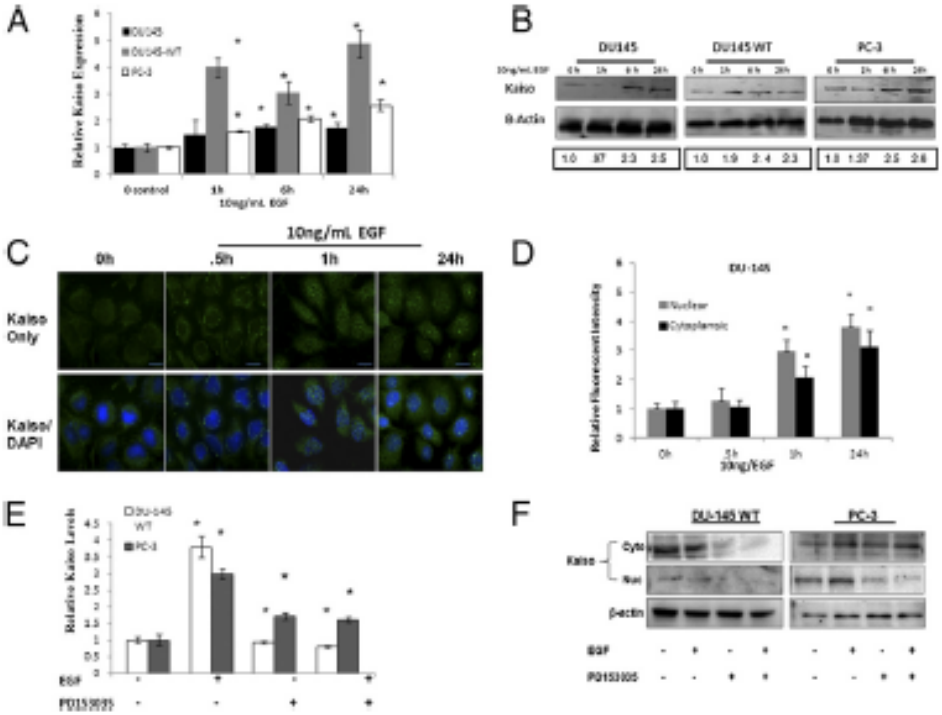

Figure 3 EGF induces Kaiso expression and cytoplasmic-to-nuclear localization in prostate cancer cell lines. A: DU145, DU145 WT, and PC-3 prostate cancer cell lines were treated with 10 ng/mL of EGF for 0, 1, 6, and 24 hours and assayed for mRNA Kaiso levels by quantitative RT-PCR with Kaiso-specific TaqMan primers and hypoxanthine-guanine phosphoribosyltransferase (HPRT) as the loading control. Data are normalized to control; $n = 4 \pm$ SE. $^{*}P < 0.05$. B: Kaiso protein levels in whole-cell lysates by immunoblot using anti-Kaiso antibody and anti-β-actin antibody as loading control. Images shown are representative of three individual experiments. Densitometry was performed on individual time intervals and compared with control. C: Kaiso subcellular localization (green) was determined by immunofluorescence. Note the colocalization of Kaiso in nuclear (green) with nuclear stain DAPI (blue) after EGF treatment in DU145 cells. Images shown are representative of three individual experiments. Scale bar = 25 μm. D: Bar-graph quantification of Kaiso intensity in the individual cytoplasmic and nuclear compartments of DU145 cells treated with 10 ng/mL of EGF compared with untreated control, shown is the mean ± SD of three individual experiments. Data were normalized to 0 hours control. $^{*}P < 0.05$. E: Kaiso mRNA levels were determined by quantitative RT-PCR, in the presence or absence of 10 ng/mL EGF or EGFR-specific kinase inhibitor, PD153035, in DU145 WT and PC-3 cells using Kaiso-specific TaqMan primers and HPRT as the loading control. Data were normalized to control; $n = 4 \pm$ SE. $^{*}P < 0.05$. F: Kaiso protein levels were determined by immunoblot in the cytoplasm and the nucleus in the presence or absence of 10 ng/mL EGF or EGFR-specific kinase inhibitor, PD153035, in DU145 WT and PC-3 cells. β-Actin served as loading control. Images shown are representative of three individual experiments. h, hours.

exposure to EGF, however, nuclear expression remained significantly higher throughout the exposure time periods (see Supplemental Figure S2, A and B, at *http://ajp.amjpathol.org*). To more clearly define the role of EGFR activation on increases in Kaiso expression and localization, we used an EGFR-specific kinase inhibitor, PD153035 (500 nmol/L), in the presence or absence of EGF. PD153035 significantly reduced mRNA Kaiso expression levels even after EGF pretreatment (Figure 3E). After subcellular fractionation and subsequent immunoblot of both DU-145 WT and PC-3 cells, we also observed that PD153035 significantly reduced expression of Kaiso in the cytoplasmic and nuclear compartments (Figure 3F; see also Supplemental Figure S2C at *http://ajp.amjpathol.org*), which is a reversal of the expression pattern observed in endogenously expressing and EGF-treated DU-145 WT and PC-3 cells. Thus, EGFR signaling positively affects Kaiso expression and subcellular localization.

Promotion by Kaiso of EGFR-Induced Prostate Cancer Cell Migration and Invasion

To further define the function of Kaiso in prostate cancer cells, DU-145 and PC-3 cells were stably transduced with a plasmid vector containing the sh-Kaiso silencing sequence (Figure 4A). Both sh-Kaiso DU-145 and sh-Kaiso PC-3 clones showed delayed migration, even in the presence of EGF stimulation, as measured by wound-healing assays (Figure 4, B and C). These results show that Kaiso is a mediator of EGFR-induced migration of prostate cancer cells. For cancer cells to invade surrounding tissue, the cells must degrade the underlying basement membrane. To determine the function of Kaiso in invasion by prostate cancer cells, sh-Kaiso PC-3 and sh-DU-145 were seeded onto a filter coated with Matrigel and compared with cells exposed to the vector only. Suppression of endogenous Kaiso expression resulted in inhibition of cell invasion, resulting in a reduction in the ability of the cells to invade through Matrigel (Figure 4D).

Repression of E-Cadherin by Kaiso in Prostate Cancer Cells

In various cancer types, increased cell migration and invasion has been attributed to growth factor–induced loss of E-cadherin or to hypermethylation of the E-cadherin promoter.[17,18] Because Kaiso has high affinity for methylated dinucleotide sequences and is regulated by EGFR (Figure 3A), we next sought to determine whether suppression of Kaiso restored E-cadherin expression in sh-Kaiso PC-3 cells. Control PC-3 cells and vector-only cells showed no E-cadherin expression, as previously reported.[18] sh-Kaiso PC-3 cells, however, show eightfold increased expression of E-cadherin mRNA, as measured by quantitative RT-PCR. Furthermore, the level of re-expression was comparable with that of PC-3 cells exposed to the demethylating agent 5-aza-2′-deoxycytidine (Fig-

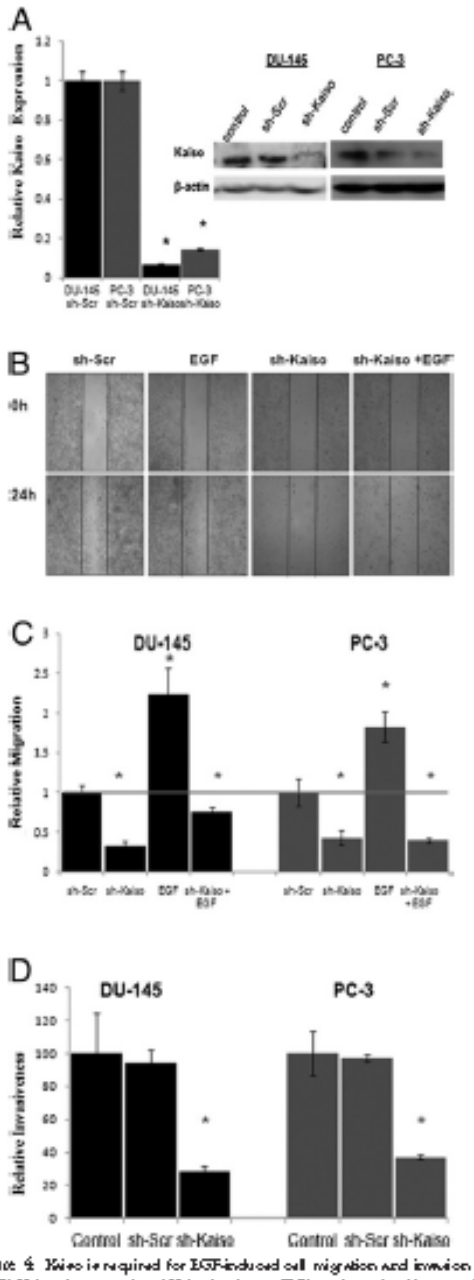

Figure 4 Kaiso is required for EGF-induced cell migration and invasion. A: shRNA Kaiso down-regulated Kaiso levels at mRNA as determined by quantitative RT-PCR with Kaiso-specific TaqMan primers and HPRT as the loading control or protein levels by immunoblot. B: β-actin served as loading control. shRNA DU145 or PC-3 cells were wounded and treated with EGF for 24 hours. Vertical bars indicate the starting area migration on day 0. Photographs were taken at ×100 magnification and DU145 images were as representative images of both DU145 and PC-3 cell lines. C: Quantification of area migrated in the presence or absence of EGF stimulation in shRNA DU145 or PC-3 cells compared with scrambled control sh-Scr show that Kaiso depletion significantly decreased cell migration. Data were normalized to control (gray bar). D: shRNA DU145 and PC-3 cells were plated on Matrigel-coated filters and the invasive cells were fixed, stained with crystal violet, and counted. shRNA Kaiso cells show decreased invasiveness compared with sh-Scr and controls. All data presented are the mean of three independent experiments ± SE. *P < 0.05.

ure 5A). There was also an increase in epithelial markers E-cadherin and p120ctn expression, and a decrease in mesenchymal markers N-cadherin and fibronectin expression at the protein level, as determined by immunoblots (Figure 5B). To determine whether Kaiso directly binds to E-cadherin, we performed a chromatin immunoprecipitation assay. Immunoprecipitated DNA was incubated with anti-Kaiso antibody, anti-RNA pol II (positive control), or IgG antibody (negative control), and subjected to PCR with specific primers designed to amplify the Kaiso (mCGmCG) binding sites in the E-cadherin promoter region. Our results showed that the Kaiso antibody (not negative control IgG antibody) enriched a mCGmCG fragment within the E-cadherin promoter (Figure 5C). These results show that Kaiso can bind directly to methylated regions in the E-cadherin promoter in PC-3 cells.

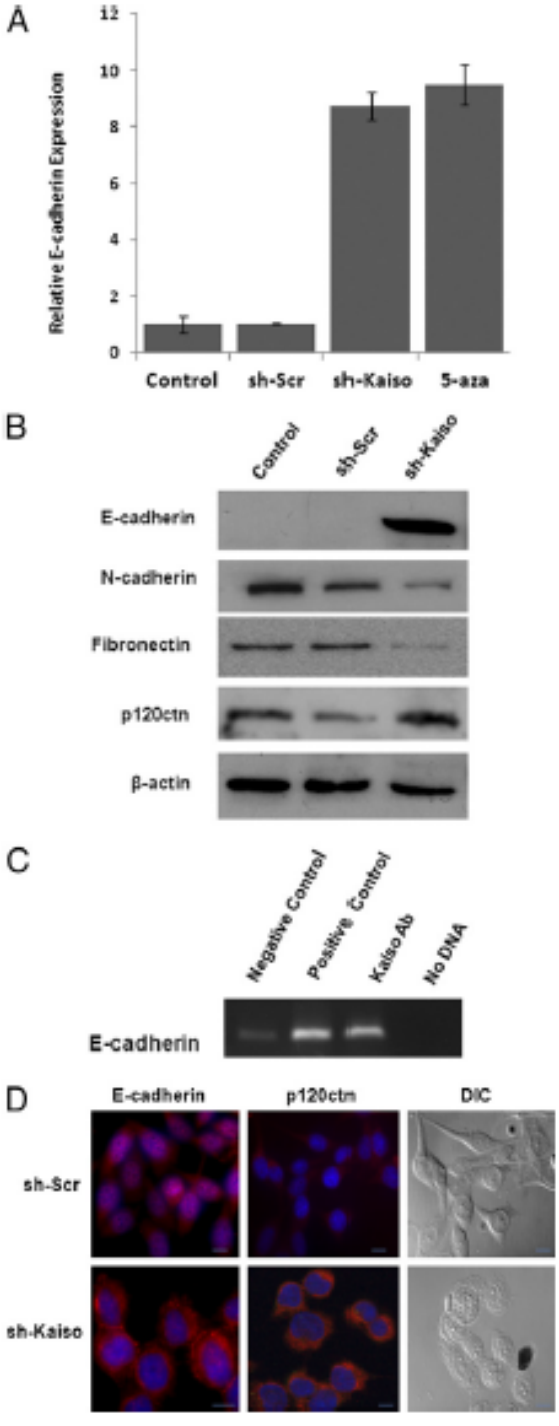

It is well recognized that membrane expression of E-cadherin regulates cell polarity and increases cell–cell cohesiveness, limiting the migratory ability of tumor cells.[10,19] Therefore, we performed immunofluorescence for E-cadherin and p120ctn in sh-Kaiso PC-3 cells compared with vector only sh-Scr PC-3 cells. sh-Kaiso cells showed E-cadherin at cell–cell contacts as well as increased p120ctn, which is rate limiting for E-cadherin stability,[20,21] at the cellular membrane (Figure 5D). Furthermore, sh-Kaiso PC-3 cells also showed more of an epithelial morphology compared with the mesenchymal morphology shown by sh-Scr PC-3 cells (Figure 5C). Collectively, these results suggest that EGFR-regulated expression and subcellular re-localization of Kaiso promotes methylation-related gene silencing of E-cadherin.

Discussion

Kaiso previously was observed to be localized predominately in the cytoplasm of various tumor types, including prostate cancer.[22] Herein, we observed positive nuclear expression of Kaiso in aggressive tumors from prostate cancer patients. This expression profile was reproducible, using two commercially available antibodies to both the 6F8 and 12H epitopes. Semiquantitative analysis of Kaiso expression shows that nuclear expression significantly correlates with increasing tumor grade and Gleason score. A correlation with nuclear expression and PSA levels also was observed, although it was not found to be significant, possibly owing to the limited number of patients with documented PSA information. Although a large number of patients showed nuclear positivity, we indeed

Figure 5 Kaiso regulates E-cadherin expression. A: E-cadherin mRNA levels were determined by quantitative RT-PCR in sh-Kaiso PC-3 cells, sh-Scr (vector only), and control cell treated with demethylating agent, 5-aza-2′-deoxycytidine (5-aza) using E-cadherin TaqMan-specific primer with HPRT1 as the loading control. Data were normalized to control (X = 0 ± SEE). B: sh-Kaiso PC-3 cells, sh-Scr (vector only), and control lysates were immunoblotted with an anti-E-cadherin, anti-N-cadherin antibody, anti-fibronectin antibody, and anti-p120ctn antibody. β-actin served as loading control. Shown is one of two representative blot series. C: Chromatin samples from PC-3 cells were subjected to chromatin immunoprecipitation by mouse IgG (lane 1) and specific antibodies against RNA pol II (lane 2) and Kaiso (6F/12H, ChIP grade, lane 3). Mouse IgG was used as a negative control. Lane 4 was no DNA negative control. Chromatin immunoprecipitation products were analyzed by real-time PCR-specific E-cadherin primer set (−120 to −170) to amplify the methylated region. D: E-cadherin and p120ctn localization was determined by immunofluorescence in sh-Kaiso or sh-Scr PC-3 cells using anti-E-cadherin (red) and DAPI nuclear stain (blue). Arrows indicate E-cadherin staining at cell–cell junctions. Differential interference contrast (DIC) images show an altered cellular morphology in sh-Kaiso PC-3 compared with sh-Scr PC-3 cells (bar = 25 μm). (D)

observed cytoplasmic expression within our patient cohort. Low levels of expression were observed in the cytoplasm in normal and benign patients. Critical analysis of a subpopulation of normal/tumor paired samples from 13 individual patients showed that although Kaiso expression was cytoplasmic in normal tissues, the corresponding malignant samples showed a shift to the nuclear compartment. Furthermore, colorectal tumors from the *Muc2*$^{-/-}$ *in vivo* mouse model also showed significant increases in Kaiso expression, as well as positive nuclear expression compared with normal matched control.[22] These findings further emphasize a role for nuclear Kaiso in tumorigenesis.

Various cell types have displayed subcellular localization of Kaiso in culture. A report by Soubry et al[22] showed that microenvironmental differences, such as two-dimensional versus three-dimensional Matrigel culture conditions or cell density, influences both subcellular localization and expression. Dense three-dimensional cultures of nontumorigenic MCF-10A cells over a multiday period, showed a cytoplasmic re-localization and eventual loss of Kaiso expression as cultures become dense, which also is associated with E-cadherin present at the membrane. HT29 or SW48 colon cancer cells, which display nuclear Kaiso, did not show a difference in Kaiso localization, even under hypoxic conditions. However, no single factor has been associated with localization of Kaiso in the cytoplasmic and nuclear compartments to date.[22,24,26] EGF, abundantly secreted in the primary tumor microenvironment,[26,27] is up-regulated during hypoxia,[28] and is a robust promoter of cell migration, invasion, and metastasis.[14,29] Commonly used DU-145 and PC-3 cells, and a DU-145 WT cell line, in which we overexpress EGFR,[14,20] reveal that the more aggressive DU-145 WT and PC-3 cells show increased Kaiso expression and nuclear localization, whereas LNCaP and DU-145 cells show lower levels and an increased ratio of cytoplasmic-to-nuclear Kaiso. Furthermore, this is independent of culture density. This would suggest that Kaiso subcellular localization, at least in part, is influenced by Kaiso levels within the cell. There are two lines of evidence in support of this hypothesis. First, we observed that EGF stimulation results in an increased expression and a cytoplasmic-to-nuclear expression shift in DU-145 cells. However, in the reverse experiment in DU-145 WT and PC-3 cells, blocking EGFR signaling resulted in a decrease in overall Kaiso levels in both the cytoplasmic and nuclear compartments. Second, Madin-Darby canine kidney epithelial cells and MCF-7 breast cancer cells, which both display Kaiso predominately in the cytoplasm, display immediate nuclear expression after overexpression with Kaiso cDNA in both cell lines.[21] The fact that activation or attenuation of EGFR signaling, as opposed to cell density alone, modulated Kaiso expression and localization is likely owing to reinforced autocrine signaling in the highly aggressive carcinoma cell lines compared with noncarcinoma and/or early stage carcinoma cell lines, which do not possess this feature. Although we did not determine whether Kaiso is phosphorylated in response to EGF, it appears that Kaiso is similar to other cancer-related transcription factors (ERK and ZEB1) that normally reside in the cytoplasm until they are signaled to translocate to the nucleus. These findings establish that expression and subcellular localization of Kaiso is at least partially influenced by EGFR.

We have found in prostate carcinoma lines that inhibition of the autocrine EGFR loop (and likely the EGFR-induced hepatocyte growth factor/c-met autocrine loop[28]), either by direct disruption of the signaling loop or by secondary site signaling *trans*-attenuation, results in E-cadherin re-expression and a re-localization of both p120ctn and E-cadherin to cell–cell contacts.[15,22,24] E-cadherin expression is down-regulated by two mechanisms: posttranslational modification[25] or hypermethylation of promoter.[26] In addition to E-cadherin, the proposed Kaiso target gene SA100A4 (mts-1) typically is silenced by methylation in epithelial tumors,[6,27] and has been implicated in EGFR-mediated cell migration as well.[15,25,29] Our results showed that shRNA-targeted depletion of Kaiso in both DU-145 and PC-3 cells showed decreased cell migration and invasion, even in the presence of EGF stimulation. Furthermore, sh-Kaiso PC-3 cells, which have a partially methylated E-cadherin promoter,[40] re-express E-cadherin at RNA and protein levels similar to those caused by exposure to the demethylating agent 5-aza-2′-deoxycytidine. Similar to findings in NIH3T3 cells,[6] we did observe that Kaiso directly binds to CpG-rich regions in the E-cadherin promoter. As a result of E-cadherin re-expression, sh-Kaiso cells also displayed morphologic changes, which coincided with decreases in the mesenchymal markers N-cadherin and fibronectin. Together these markers are of clinical importance in determining epithelial versus mesenchymal cells in various tumor types including prostate cancer.[41] We did not observe any changes in S100A4 or MMP expression in this model (data not shown), although both have been implicated in EGFR signaling. This is surprising, given that both SA100A4 and MMP-7 have been linked to Kaiso through methylation or consensus sequence binding.[12,27] However, collectively, our findings suggest that Kaiso is a promoter of cell migration through loss of cell–cell cohesiveness.

These observations provide a plausible explanation for a number of events during the progression to aggressiveness in epithelial tumors. For example, E-cadherin promoter is hypermethylated in most early stage lobular breast tumors; however, expression of E-cadherin protein is retained. It is only in late-stage tumors, which coincide with our observed nuclear Kaiso shift, that a lack of E-cadherin protein expression coincides with promoter hypermethylation.[42] More specifically, immunohistochemical staining displayed loss of p120ctn and E-cadherin expression at the leading edge of squamous cell carcinomas, which coincides with nuclear Kaiso positivity.[22] Although a Kaiso-p120ctn complex has been observed in the nucleus of other cell types,[16,24,42] similar to squamous cell carcinomas, nuclear p120ctn has not been observed in prostate tumors.[44,45] We did not observe nuclear p120ctn in any of the prostate cancer cell lines, even after EGF treatment (data not shown). Thus, the p120ctn-Kaiso relationship in the nucleus, at least in

prostate cancer, does not appear to contribute to aggressiveness.

The observation that Kaiso was increased in African American patients was intriguing. Several reports have shown that EGFR is overexpressed in African American prostate cancer patients.[45] In addition, SOS1, which is a regulator of EGFR expression and downstream signaling, also is increased in African American prostate cancer patients as well.[47] Because our findings show that Kaiso expression is positivity-influenced by EGFR activation, it is possible that overexpression of EGFR contributes to increased Kaiso levels in this patient population. Although this currently remains speculative, it does begin to provide more insight into why African American prostate cancer patients show more aggressive disease progression than do white patients in epidemiologic studies.[48,49] More work should be performed to further define this relationship, specifically in African American prostate cancer patients.

In summary, Kaiso cytoplasmic-to-nuclear localization correlates with many features of prostate cancer progression, including race. Epithelial-to-mesenchymal transition has been identified as a common mechanism underlying therapeutic resistance and has been linked to poor prognosis in many types of cancer, including prostate cancer.[50] The fact that we found that Kaiso is regulated through EGFR activity provides additional mechanistic insight into the signaling pathway that apparently contributes to aggressive prostate cancer. Because a large number of tumor/metastasis suppressor genes are silenced as a result of methylation, Kaiso could be a central regulator of many key events that contribute to tumorigenesis and aggressiveness. Targeting of growth factor receptors has shown minimal therapeutic effects for prostate cancers. Nevertheless, targeting of downstream mediators of metastasis, such as Kaiso, could be a rational approach for developing a new target for directed therapies.

Acknowledgment

We thank the members of the Yates laboratory for their comments and discussions.

References

1. Stangelberger A, Waldert M, Djavan B: Prostate cancer in elderly men. Rev Urol 2008, 10:111–119
2. Lopes EC, Valls E, Figueroa ME, Mazur A, Meng FG, Chiosis G, Laird PW, Schreiber-Agus N, Greally JM, Prokhortchouk E, Melnick A: Kaiso contributes to DNA methylation-dependent silencing of tumor suppressor genes in colon cancer cell lines. Cancer Res 2008, 68: 7258–7263
3. Yoon HG, Chan DW, Reynolds AB, Qin J, Wong J: N-CoR mediates DNA methylation-dependent repression through a methyl CpG binding protein Kaiso. Mol Cell 2003, 12:723–734
4. Daniel JM, Reynolds AB: The catenin p120(ctn) interacts with Kaiso, a novel BTB/POZ domain zinc finger transcription factor. Mol Cell Biol 1999, 19:3614–3623
5. Prokhortchouk A, Hendrich B, Jorgensen H, Ruzov A, Wilm M, Georgiev G, Bird A, Prokhortchouk E: The p120 catenin partner Kaiso is a DNA methylation-dependent transcriptional repressor. Genes Dev 2001, 15:1613–1618
6. Dai SD, Wang Y, Miao Y, Zhao Y, Zhang Y, Jiang GY, Zhang PX, Yang ZQ, Wang EH: Cytoplasmic Kaiso is associated with poor prognosis in non-small cell lung cancer. BMC Cancer 2009, 9:178
7. Wells A, Welsh JB, Lazar CS, Wiley HS, Gill GN, Rosenfeld MG: Ligand-induced transformation by a noninternalizing epidermal growth factor receptor. Science 1990, 247:962–964
8. Manne U, Myers RB, Srivastava S, Grizzle WE: Re: loss of tumor marker-immunostaining intensity on stored paraffin slides of breast cancer. J Natl Cancer Inst 1997, 89:585–586
9. Grizzle W, Myers R, Manne U, Stockard C, Harkins L, Srivastava S: Factors Affecting Immunohistochemical Evaluation of Biomarker Expression in Neoplasia. Edited by MHaZ Walaszek. New Jersey, Humana Press, Inc, 1998, pp 161–179
10. Graham TR, Zhau HE, Odero-Marah VA, Osunkoya AO, Kimbro KS, Tighiouart M, Liu T, Simons JW, O'Regan RM: Insulin-like growth factor-I-dependent up-regulation of ZEB1 drives epithelial-to-mesenchymal transition in human prostate cancer cells. Cancer Res 2008, 68:2479–2488
11. Yates CC, Whaley D, Kulasekeran P, Hancock WW, Lu B, Bodnar R, Newsome J, Hebda PA, Wells A: Delayed and deficient dermal maturation in mice lacking the CXCR3 ELR-negative CXC chemokine receptor. Am J Pathol 2007, 171:484–495
12. Daniel JM, Spring CM, Crawford HC, Reynolds AB, Baig A: The p120(ctn)-binding partner Kaiso is a bi-modal DNA-binding protein that recognizes both a sequence-specific consensus and methylated CpG dinucleotides. Nucleic Acids Res 2002, 30:2911–2919
13. Xie H, Turner T, Wang MH, Singh RK, Siegal GP, Wells A: In vitro invasiveness of DU-145 human prostate carcinoma cells is modulated by EGF receptor-mediated signals. Clin Exp Metastasis 1995, 13:407–419
14. Turner T, Chen P, Goodly LJ, Wells A: EGF receptor signaling enhances in vivo invasiveness of DU-145 human prostate carcinoma cells. Clin Exp Metastasis 1996, 14:409–418
15. Gan Y, Shi C, Inge L, Hibner M, Balducci J, Huang Y: Differential roles of ERK and Akt pathways in regulation of EGFR-mediated signaling and motility in prostate cancer cells. Oncogene 2010, 29:4947–4958
16. Traish AM, Morgentaler A: Epidermal growth factor receptor expression escapes androgen regulation in prostate cancer: a potential molecular switch for tumour growth. Br J Cancer 2009, 101:1949–1956
17. Li LC, Zhao H, Nakajima K, Oh BR, Ribeiro Filho LA, Carroll P, Dahiya R: Methylation of the E-cadherin gene promoter correlates with progression of prostate cancer. J Urol 2001, 166:705–709
18. Yates CC, Shepard CR, Stolz DB, Wells A: Co-culturing human prostate carcinoma cells with hepatocytes leads to increased expression of E-cadherin. Br J Cancer 2007, 96:1246–1252
19. Chunthapong J, Seftor EA, Khalkhali-Ellis Z, Seftor RE, Amir S, Lubaroff DM, Heidger PM Jr, Hendrix MJ: Dual roles of E-cadherin in prostate cancer invasion. J Cell Biochem 2004, 91:649–661
20. Reynolds AB, Carnahan RH: Regulation of cadherin stability and turnover by p120ctn: implications in disease and cancer. Semin Cell Dev Biol 2004, 15:657–663
21. Miao Y, Liu N, Zhang Y, Liu Y, Yu JH, Dai SD, Xu HT, Wang EH: p120ctn isoform 1 expression significantly correlates with abnormal expression of E-cadherin and poor survival of lung cancer patients. Med Oncol 2010, 27:880–886
22. Soubry A, van Hengel J, Parthoens E, Colpaert C, Van Marck E, Waltregny D, Reynolds AB, van Roy F: Expression and nuclear location of the transcriptional repressor Kaiso is regulated by the tumor microenvironment. Cancer Res 2005, 65:2224–2233
23. Prokhortchouk A, Sansom O, Selfridge J, Caballero IM, Salozhin S, Aithozhina D, Cerchietti L, Meng FG, Augenlicht LH, Mariadason JM, Hendrich B, Melnick A, Prokhortchouk E, Clarke A, Bird A: Kaiso-deficient mice show resistance to intestinal cancer. Mol Cell Biol 2006, 26:199–208
24. Kelly KF, Spring CM, Otchere AA, Daniel JM: NLS-dependent nuclear localization of p120ctn is necessary to relieve Kaiso-mediated transcriptional repression. J Cell Sci 2004, 117:2675–2686
25. Park JI, Kim SW, Lyons JP, Ji H, Nguyen TT, Cho K, Barton MC, Deroo T, Vleminckx K, Moon RT, McCrea PD: Kaiso/p120-catenin and TCF/beta-catenin complexes coordinately regulate canonical Wnt gene targets. Dev Cell 2005, 8:843–854

26. Amalinei C: [Reciprocal epithelio-stromal interactions in normal and neoplastic prostate]. Romanian. Rev Med Chir Soc Med Nat Iasi 2006, 110:391–398
27. Lin J, Freeman MR: Transactivation of ErbB1 and ErbB2 receptors by angiotensin II in normal human prostate stromal cells. Prostate 2003, 54:1–7
28. Fechner G, Muller G, Schmidt D, Garbe S, Hauser S, Vaupel P, Muller SC: Evaluation of hypoxia-mediated growth factors in a novel bladder cancer animal model. Anticancer Res 2007, 27:4225–4231
29. Angelucci A, Gravina GL, Rucci N, Millimaggi D, Festuccia C, Muzi P, Teti A, Vicentini C, Bologna M: Suppression of EGF-R signaling reduces the incidence of prostate cancer metastasis in nude mice. Endocr Relat Cancer 2006, 13:197–210
30. Yates C, Wells A, Turner T: Luteinising hormone-releasing hormone analogue reverses the cell adhesion profile of EGFR overexpressing DU-145 human prostate carcinoma subline. Br J Cancer 2005, 92: 366–375
31. Daniel JM, Ireton RC, Reynolds AB: Monoclonal antibodies to Kaiso: a novel transcription factor and p120ctn-binding protein. Hybridoma 2001, 20:159–166
32. Mamoune A, Kassis J, Kharait S, Kloeker S, Manos E, Jones DA, Wells A: DU145 human prostate carcinoma invasiveness is modulated by urokinase receptor (uPAR) downstream of epidermal growth factor receptor (EGFR) signaling. Exp Cell Res 2004, 299:91–100
33. Wells A, Yates C, Shepard CR: E-cadherin as an indicator of mesenchymal to epithelial reverting transitions during the metastatic seeding of disseminated carcinomas. Clin Exp Metastasis 2008, 25:621–628
34. Yates C, Shepard CR, Papworth G, Dash A, Beer Stolz D, Tannenbaum S, Griffith L, Wells A: Novel three-dimensional organotypic liver bioreactor to directly visualize early events in metastatic progression. Adv Cancer Res 2007, 97:225–246
35. Jawhari AU, Farthing MJ, Pignatelli M: The E-cadherin/epidermal growth factor receptor interaction: a hypothesis of reciprocal and reversible control of intercellular adhesion and cell proliferation. J Pathol 1999, 187:155–157
36. Graff JR, Herman JG, Lapidus RG, Chopra H, Xu R, Jarrard DF, Isaacs WB, Pitha PM, Davidson NE, Baylin SB: E-cadherin expression is silenced by DNA hypermethylation in human breast and prostate carcinomas. Cancer Res 1995, 55:5195–5199
37. Ogden SR, Wroblewski LE, Weydig C, Romero-Gallo J, O'Brien DP, Israel DA, Krishna US, Fingleton B, Reynolds AB, Wessler S, Peek RM Jr: p120 and Kaiso regulate Helicobacter pylori-induced expression of matrix metalloproteinase-7. Mol Biol Cell 2008, 19:4110–4121
38. Mimori K, Yamashita K, Ohta M, Yoshinaga K, Ishikawa K, Ishii H, Utsunomiya T, Barnard GF, Inoue H, Mori M: Coexpression of matrix metalloproteinase-7 (MMP-7) and epidermal growth factor (EGF) receptor in colorectal cancer: an EGF receptor tyrosine kinase inhibitor is effective against MMP-7-expressing cancer cells. Clin Cancer Res 2004, 10:8243–8249
39. Klingelhofer J, Moller HD, Sumer EU, Berg CH, Poulsen M, Kiryushko D, Soroka V, Ambartsumian N, Grigorian M, Lukanidin EM: Epidermal growth factor receptor ligands as new extracellular targets for the metastasis-promoting S100A4 protein. FEBS J 2009, 276:5936–5948
40. Reinhold WC, Reimers MA, Maunakea AK, Kim S, Lababidi S, Scherf U, Shankavaram UT, Ziegler MS, Stewart C, Kouros-Mehr H, Cui H, Dolginow D, Scudiero DA, Pommier YG, Munroe DJ, Reinberg AP, Weinstein JN: Detailed DNA methylation profiles of the E-cadherin promoter in the NCI-60 cancer cells. Mol Cancer Ther 2007, 6:391–403
41. Gravdal K, Halvorsen OJ, Haukaas SA, Akslen LA: A switch from E-cadherin to N-cadherin expression indicates epithelial to mesenchymal transition and is of strong and independent importance for the progress of prostate cancer. Clin Cancer Res 2007, 13:7003–7011
42. Zou D, Yoon HS, Perez D, Weeks RJ, Guilford P, Humar B: Epigenetic silencing in non-neoplastic epithelia identifies E-cadherin (CDH1) as a target for chemoprevention of lobular neoplasia. J Pathol 2009, 218:265–272
43. Kelly KF, Otchere AA, Graham M, Daniel JM: Nuclear import of the BTB/POZ transcriptional regulator Kaiso. J Cell Sci 2004, 117:6143–6152
44. Lu Q, Dobbs LJ, Gregory CW, Lanford GW, Revelo MP, Shappell S, Chen YH: Increased expression of delta-catenin/neural plakophilin-related armadillo protein is associated with the down-regulation and redistribution of E-cadherin and p120ctn in human prostate cancer. Hum Pathol 2005, 36:1037–1048
45. Kallakury BV, Sheehan CE, Winn-Deen E, Oliver J, Fisher HA, Kaufman RP Jr, Ross JS: Decreased expression of catenins (alpha and beta), p120 CTN, and E-cadherin cell adhesion proteins and E-cadherin gene promoter methylation in prostatic adenocarcinomas. Cancer 2001, 92:2786–2795
46. Shuch B, Mikhail M, Satagopan J, Lee P, Yee H, Chang C, Cordon-Cardo C, Taneja SS, Osman I: Racial disparity of epidermal growth factor receptor expression in prostate cancer. J Clin Oncol 2004, 22:4725–4729
47. Timofeeva OA, Zhang X, Ressom HW, Varghese RS, Kallakury BV, Wang K, Ji Y, Cheema A, Jung M, Brown ML, Rhim JS, Dritschilo A: Enhanced expression of SOS1 is detected in prostate cancer epithelial cells from African-American men. Int J Oncol 2009, 35:751–760
48. Evans S, Metcalfe C, Ibrahim F, Persad R, Ben-Shlomo Y: Investigating black-white differences in prostate cancer prognosis: a systematic review and meta-analysis. Int J Cancer 2008, 123:430–435
49. Berger AD, Satagopan J, Lee P, Taneja SS, Osman I: Differences in clinicopathologic features of prostate cancer between black and white patients treated in the 1990s and 2000s. Urology 2006, 67:120–124
50. Nauseef JT, Henry MD: Epithelial-to-mesenchymal transition in prostate cancer: paradigm or puzzle? Nat Rev Urol 2011, 8:428–439

Prostate Tumor Cell Plasticity: A Consequence of the Microenvironment

7

Clayton Yates

Abstract

During each step of prostate cancer metastasis, cancer displays phenotypic plasticity that is associated with the expression of both epithelial and mesenchymal properties or an epithelial to mesenchymal transition. This phenotypic transition is typically in response to microenvironment signals and is the basis for basic cancer cell survival (e.g. motility and invasion versus proliferation). In this review we discuss the loss and gain of E-cadherin expression as a marker of tumor plasticity throughout the steps of metastasis, and particularly focus on dynamic tumor–stromal interaction that induce a cancer cell-associated mesenchymal to epithelial reverting transition in the bone and liver microenvironments.

7.1 Epithelial to Mesenchymal Transition

Histological evidence of distinct neoplastic cell types within a tumor mass were observed as early as 1978 [1]. There are two main cell types; epithelial and mesenchymal cells, albeit most tumor cells are derived from epithelial origins, however in 1987 the term epithelial to mesenchymal transition (EMT) was utilized. This was subsequently followed by Elizabeth Hay in 1995 [2], with a cellular characterization of transitioned cells, that is still currently utilized to identify phenotypic subtypes within the tumor mass. Several hallmarks to phenotypically characterize these transitioned cells, such as cellular morphogenesis, change in shape, and tissue organization have all been associated with EMT. However, loss of cell–cell connectivity appears to an essential step feature. Normal epithelial cells comprise a sheet of cells that adhere laterally to each other by cell-to-cell junctions. In addition, epithelial cells have apical–basolateral polarization that is maintained through organization of the actin cytoskeleton, which has intimate interactions with cell membrane adhesion molecules such as cadherins, tight junctions, and certain integrins. This allows the polarized cells to maintain cell–cell junctions as a lateral belt, preventing robust cell motility, while remaining within the epithelial layer.

Mesenchymal-like cells, on the other hand, are spindle-shaped cells that exhibit end-to-end polarity,

C. Yates (✉)
Department of Biology and Center for Cancer Research, Tuskegee University, Tuskegee, AL 36088, USA
e-mail: cyates@mytu.tuskegee.edu

J.S. Rhim and R. Kremer (eds.), *Human Cell Transformation: Role of Stem Cells and the Microenvironment*, Advances in Experimental Medicine and Biology 720,
DOI 10.1007/978-1-4614-0254-1_7,

and have fibroblast morphology. Mesenchymal cells do not form an organized cell layer, nor do they have the same apical–basolateral organization, polarization of cell surface molecules, and the actin cytoskeleton as epithelial cells. Cell–cell contacts with neighboring mesenchymal cells are possible, however limited to focal adhesion only. As such this provides the freedom to migrate and interact with the surround extracellular matrix (ECM). Cell migration results from dynamic remodeling of actin into filamentous filopodia, lamellipodia, stress fibers. These cell protrusions lead to dynamic interactions with ECM substrates, which are mainly intergrins. The onset of these cell extensions are a prerequisite for maintenance of cell motility in normal and cancer cells, whether they are initiated spontaneously or induced by chemokines and growth factors. Coincidently, the migration mechanisms that occur in normal, non-neoplastic cells, such as embryonic morphogenesis, wound healing and immune-cell trafficking are identical to neoplastic cells [3, 4].

7.1.1 Epithelial to Mesenchymal Transition in Prostate Cancer

EMT has been shown to be a necessary step in the dissemination of cancer cell from the primary tumor mass. During this process there have been documented changes in the phenotypic expression of the cancer cells including a reduction in the cell adhesiveness. In-depth analysis showed that reduced or aberrant expression of cytokeratin levels, and cell–cell contacts related proteins are observed over multiple cancer types including breast and prostate cancer. Adhesive complexes such as ZO-1, desmoplakin, and E-cadherin are typically loss, and serve as a prerequisite for dissemination. The clinical significance of E-cadherin loss has also been well documented. Decreased expression of cell adhesion molecule E-cadherin has been largely observed to be inversely correlated clinical characteristic including grade, local invasiveness, and biochemical failure after salvage radiotherapy. Furthermore, patients with biochemical failure after prostatectomy and aberrant E-cadherin expression are likely to have subclinical disseminated disease [5]. Thus, the mechanisms responsible for such changes in adhesion complexes are of great interest.

Majority of the reports focused on of *E-cadherin* gene (*CDH1*), suggest that hypermethylation of the *E-cadherin* promoter [6, 7], is the main mode of downregulation, however a combination of mutations in one allele with loss or inactivation (by DNA methylation) of the remaining allele [8, 9] has been observed. However, in many types of cancer including breast and prostate cancers, E-cadherin expression is lost without mutations in the gene [10], due to transcriptional repression of *E-cadherin*. Concomitant with the loss of E-cadherin, N-cadherin levels increases during prostate carcinomas. This increased expression of N-cadherin has also been observed in invasive prostate cancer cell lines, and is associated with androgen deprivation [11]. The decreases in E-cadherin expression and increases in N-cadherin expression have been shown to be correlated with increased metastatic ability [12, 13]. Up-regulation of N-cadherin, and cadherin-11, and OB (osteoblasts) cadherin are typically associated with high-grade E-cadherin negative tumors. Other EMT-related changes included transition from cubodial morphology to a spindle-shaped fibroblastic morphology, and genotypic changes including loss of cytokeratin, and increased vimentin, snail, collagen I, thrombospondin-I, and other mesenchymal genes. However, the most consistent marker of EMT has been E-cadherin.

The relevance of EMT-associated markers is supported by studies describing how expression is regulated. Many transcription factors such as the family of zinc finger proteins of the Slug/Snail family, EF1/ZEB1, SIP-1, and the basic helix-loop-helix E12/E47 factor that interact with E-box sequences in the proximal E-cadherin promoter region triggering repression. Of these transcriptional repressors, forced expression of SNAIL is sufficient to induce EMT in $ARCAP_E$ and LnCaP prostate cancer cell lines [14], while Slug acts to only regulate cell proliferation [15]. However, recent reports have suggested in PC-3 cells that SNAIL inhibition alters common EMT markers, but does not affect invasiveness [16].

Other transcription factors are implicated as EMT mediators as well. TWIST, a highly conserved bHLH transcription factor, is upregulated in 90% of prostate cancer tissues. RNAi interference of TWIST expression significantly increased sensitivity to the anticancer drug taxol-induced cell death [17]. Furthermore, in addition to EMT, TWIST may also promote prostate cancer to bone metastasis by modulating prostate cancer cell-mediated bone remodeling via regulating the expression of a secretory factor, DKK-1, and enhancing osteomimicry of prostate cancer cells [18]. Thus, multiple factors contribute EMT in prostate cancer cells. Although the complex mechanisms that regulate the expression of multiple factors simultaneously in prostate cancer one common observation is that targeting individual factor is sufficient to reverse step wise events associated with EMT, thus providing targets for the development of therapeutics.

Decreased cell–cell adhesion in many cancers may not only be the result of direct transcriptional regulation. Soluble factors such as epidermal growth factor (EGF), scatter factor/hepatocyte growth factor (SF/HGF), and members of the transforming growth factor, TGFβ1, and basic fibroblast growth factor (bFGF) families have been shown to promote EMT in several model systems. Most all of these have been shown to influence the downregulate of E-cadherin expression with subsequent increased cell proliferation, dedifferentiation, and induction of cell motility [19–21]. As cancer-associated EMT is reversible, the loss of cell–cell connections creates a situation where decreased E-cadherin levels concede the tight junctions and enable apically secreted soluble growth factors to establish an autocrine loop with the basolaterally sequestered receptors. [22]. This feed-forward mechanism supports the maintenance of the mesenchymal phenotype. Although decreased levels of E-cadherin mRNA occurs at the transcriptional level, E-cadherin stability is a direct result of phosphorylated catenins. Extensive investigations have revealed that increased phosphorylation of the preferential catenins, β-catenin and p120, destabilize the cadherin complex thus inducing scattering of cancer cell lines to a more invasive phenotype [23]. We have showed that DU-145 and PC-3 cells express aberrant p120ctn and ß-catenin, and this is reversible through blockage of EGFR signaling [24]. In addition to disrupting the cell–cell junctions and enabling a more migratory phenotype, EGF upregulates secretion of matrix metalloproteinases that degrade the ECM aiding in tumor dissemination. EGF upregulates matrilysin (MMP-7) that mediates extracellular cleavage of E-cadherin, thereby further disrupting cell–cell adhesion and switching of prostate cells from a lesser to a highly invasive phenotype [25]. Thus ADAM10, ADAM9 knockdown increased E-cadherin and integrins and modulates epithelial phenotype and functional characteristics of prostate cancer cells [26], further emphasizes the vast number of pathways regulating E-cadherin expression.

Accumulating evidence suggest that growth factor-induced EMT is the result of transcriptional reprogramming and chromatin remodeling. Of the soluble growth factors mentioned, TGFß-1 is the most noted, however for the focus of this review we will focus on tyrosine kinase growth regulation of EMT. IGF-I stimulation of $ARCaP_E$ cells upregulates ZEB1 expression in prostate cancer cells exhibiting a phenotype and increased cell migration. The authors also demonstrated that this is mediated through activation of MAPK/ERK pathway [27]. Similarly EGF, which is a robust stimulator of the MAPK pathway, resulted in activation of new EMT-related marker receptor activator of NF-κB ligand (RANKL), and enhances bone resorption and bone turnover, facilitating successful bone metastasis [14]. Findings from our laboratory, support these observations in DU-145 and PC-3, both of which undergo enhanced EMT upon EGF stimulation [14, 28, 29].

It is important to note that in addition to transcriptional repression, DNA methylation of key tumor suppressor and EMT-related genes has been observed. In the case of E-cadherin, available cell culture models DU-145 and PC-3 do not exhibit methylation of E-cadherin, however this is not observed clinically, as E-cadherin is methylated in 70% of late-stage prostate [30].

More recently microRNAs (miRNAs), small non-coding RNAs regulating gene expression,

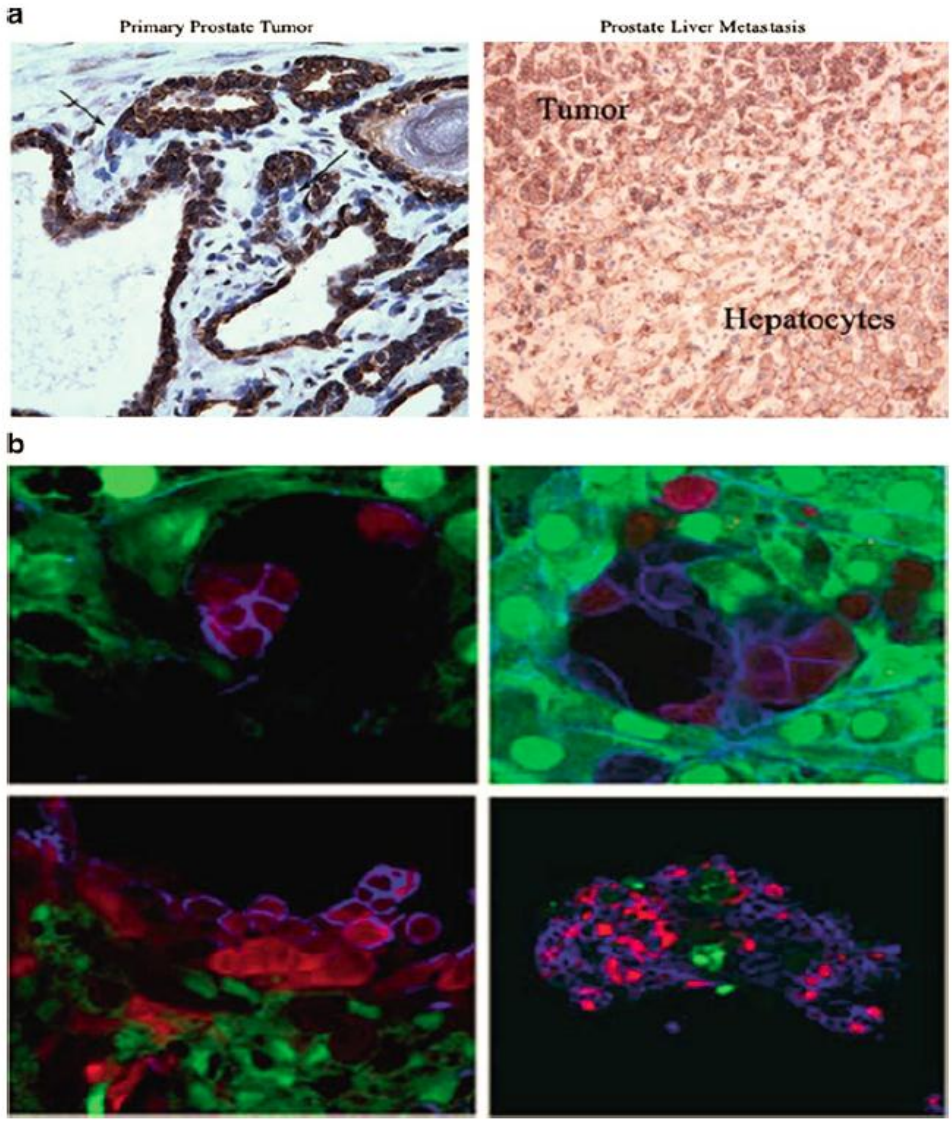

Fig. 7.1 Tumor cells exhibit phenotypic plasticity within the liver microenvironment. (**a**) Human primary prostate cancer (*left*) and metastases to liver (*right*) show expression of E-cadherin. Formalin-fixed, paraffin-embedded tissues were obtained from two well-defined prostate adenocarcinomas with liver metastasis, and stained with E-cadherin antibody. (**b**) Immunofluorescence of co-cultures shows subcellular location of E-cadherin re-expression. MCF-7 RFP (red) and GFP (*green*) primary rat hepatocytes were stained with human-specific anti-E-cadherin for a multiday period. *Top left* (Day 2), *top right* (Day 4), *bottom left* (Day 8), *bottom right* (Day 14). Cy5 secondary antibody (*blue*) was used for E-cadherin primary antibody

of co-culture. However, after long-term coculture (14 days) MCF-7 cells underwent three-dimensional organization. These findings are similar to our prostate cancer patient observations and provide the proof-of-principle that E-cadherin-associated EMT is the result of dynamic interactions of the tumor cell with its surrounding microenvironment.

Since we were able to observe stromal-induced reexpression of E-cadherin within the liver microenvironment, would suggest that a reepithelialization process is necessary for establishment

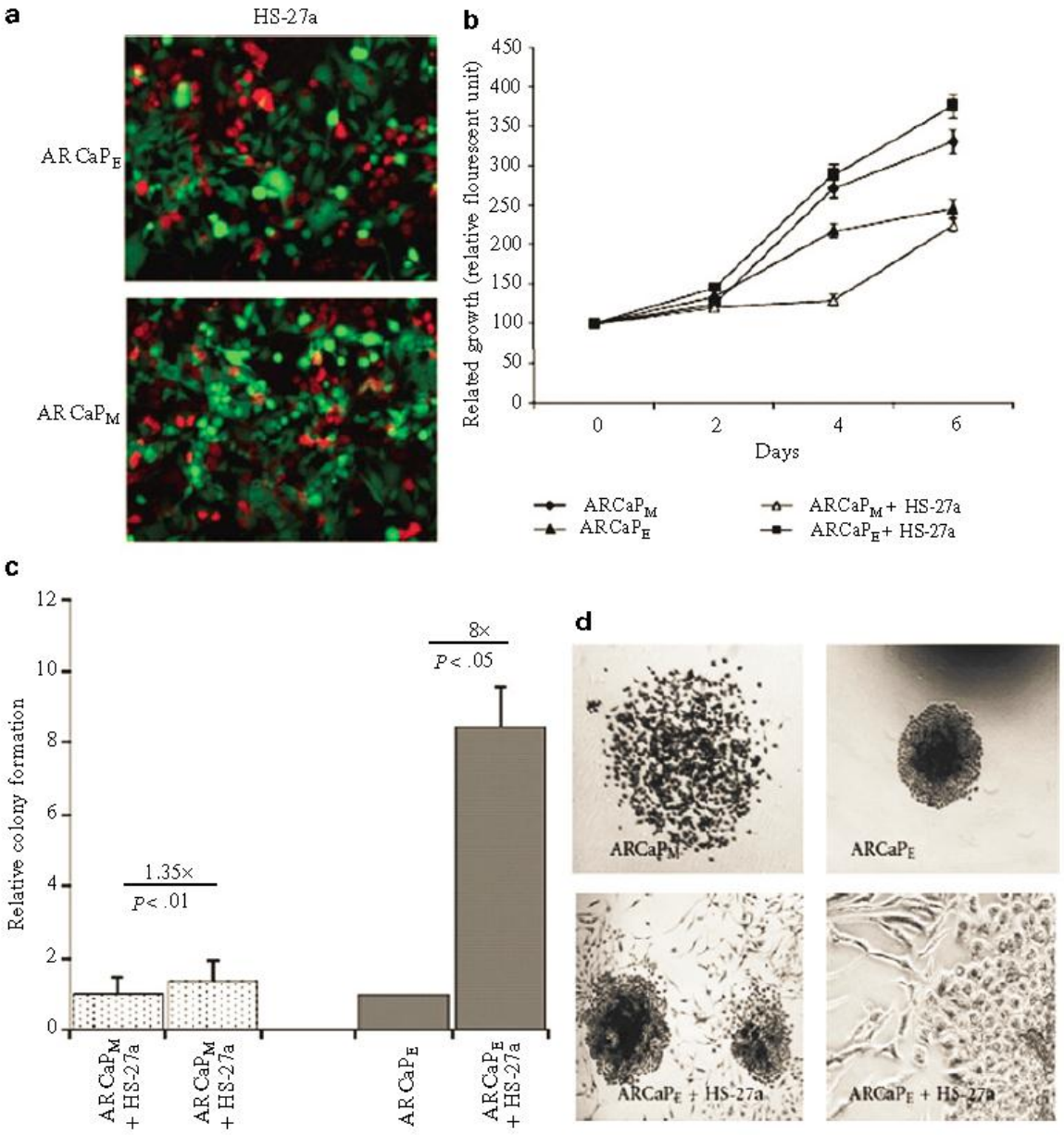

Fig. 7.2 ARCaP$_E$ cells show a growth and colony-forming capacity advantage in presence of HS-27a cells. (**a**) ARCaP$_M$ cells were cocultured in the presence of GFP-HS-27a cells over a 6-day period. Growth of RFP, ARCaP$_E$ or ARCaP$_M$ human prostate cancer cells was assessed by RFU (relative fluorescent units) in the presence cocultures over a 6-day period. Results are means ± SE of three independent experiments. *P, 0.05 (Student's t test) compared to cell number at day 1 ±SEM. (**b**) Clongenic colony-forming capacity of ARCaP$_E$ and ARCaP$_M$ prostate cancer cell after coculture ±SEM. ARCaP$_M$ data was normalized to ARCaP$_M$ control, and ARCaP$_E$ data was normalized to ARCaP$_E$ control. (**c**) Clonogenic colony forming capacity of ARCaP$_E$ and ARCaP$_M$ prostate cancer cell after coculture ± SEM. ARCaP$_M$ data were normalized to ARCaP$_M$ control, and ARCaP$_E$ data were normalized to ARCaP$_E$ control (Note HS-27a induced slightly (1.35×) the growth of ARCaP$_M$ cells but markedly (8×) the growth of ARCaP$_E$ cells). (**d**) ARCaP$_E$ or ARCaP$_M$ cells were cocultured with HS-27a cells. Shown are phase contrast images of colonies formed in the clonogenic assay

of secondary tumors. However, given the inherent differences in the stromal parenchyma of each organ, it is likely that multiple soluble factors can achieve similar effects.

For example, exogenous BMP-7 was able to induce E-cadherin of prostate tumors within the bone microenvironment, however failed to have any effect on tumors within the lymph nodes [40]. Furthermore, differential expression of a number of angiogenesis-associated genes and their proteins between prostate cancer metastasis to bone versus liver, and lymph nodes have been observed [41]. To determine if this is case with E-cadherin-associated EMT, we cocultured the ARCaP model with bone marrow stromal cells. Cocultured $ARCaP_M$ cells displayed a reversal of E-cadherin, and the more epithelial $ARCaP_E$ cells showing increased colony-forming capacity and growth advantage in presence of bone stromal cells [42]. Clinical evidence of E-cadherin expression in bone metastasis has been observed, and interesting is associated with a reversal of E-cadherin-specific methylation pattern [43].

7.3 Targeting Cell Adhesion for Therapeutic Intervention

Although we are just at the beginning of understanding the directive role of the stroma, more insight into how the stroma regulates tumor cells will lead to better therapies for late-stage metastatic disease. Multiple reports have suggested the benefits of targeting E-cadherin as a therapeutic approach. For example, E-cadherin neutralizing antibody (SHEP8-7) has been shown to sensitize multi-cellular spheroids to microtubule binding therapies in the taxane family in HT29 human colorectal adenocarcinoma cells [44]. A more recent observation that survival of androgen receptor-expressing differentiated prostate cells are dependent on E-cadherin and PI3K, but not on androgen, AR or MAPK [45]. Indeed this is the case because our findings suggest the blocking E-cadherin cell–cell interaction with E-cadherin neutralizing antibody, decreased both epithelial or mesenchymal-like prostate cells from reepithelialization and colonizing the bone microenvironment. The neutralizing antibody increases their sensitivity to radiation treatment [42]. Of further clinical benefit, recently a monoconal antibody to N-cadherin has been described as an effective treatment for prostate cancer limiting local invasion and metastasis both in vitro and in vivo [12]. Thus, blocking cellular adhesions appears to be a rationale strategy limiting prostate cancer metastasis.

7.4 Summary

In summary, we propose that the EMT required to "escape" from the primary tumor mass is transiently "reverted" during the initial stages of metastatic seeding, enabling the alien tumor cell to incorporate into the target tissue and derive survival signals thereof. Thus, tumor–stromal-interacts induce cellular plasticity gives rise to distinct populations of cancer cells within secondary site. This plasticity gives rise to distinct population, i.e. mesenchymal phenotype and its kinetic characteristics (motility/invasive), and the epithelial characteristics necessary for secondary tumor development. Our findings that epithelial cells are more successful in establishing secondary tumor suggest that dissemination from the primary tumor mass requires the mesenchymal phenotype, however a mesenchymal to epithelial transition is associated with initial metastatic seeding and subsequent formation of a cohesive tumor mass within the bone microenvironment (Fig. 7.3). Critical to our model of phenotypic mesenchymal-to-epithelial-reverting transitions is the underling signaling mechanisms that mediate this transition. Multiple-cell signaling pathways, most likely initiated by stromal-derived soluble factors, converge on an ever-expanding set of transcriptional and post-translation factors that epigenetically regulate specific proteins that ultimately serve as markers of the epithelial vs. mesenchymal phenotype. Understanding the events may offer new opportunity to target during and the reverting transition that appear to be essential to metastatic relapse.

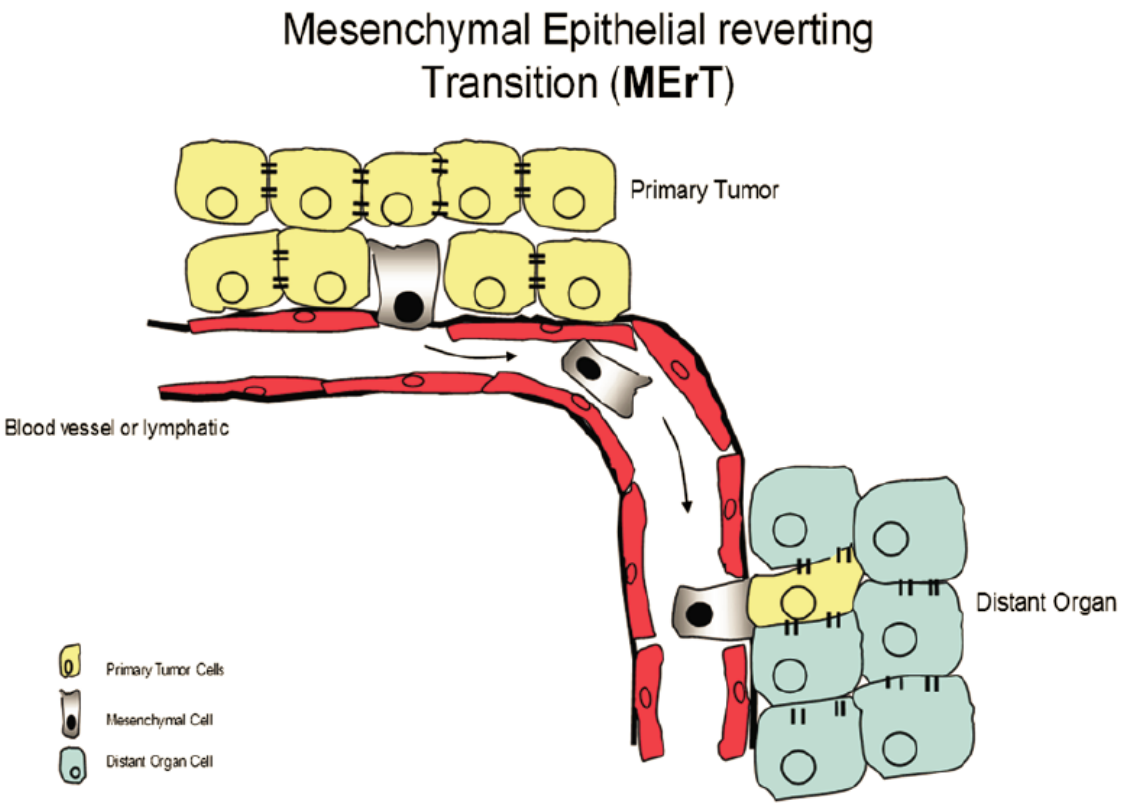

Fig. 7.3 Diagram of mesenchymal-to-epithelial reverting transition. Epithelial carcinomas cells and carcinoma cells undergo EMT, which involves a loss of adhesion and reinforcement of autocrine signaling that drive the cancer cell to escape the tumor mass and intravasate the blood or lymphatic vessels. At the secondary site mesenchymal cells extravasate the tissue parenchyma and phenotypic reversion occurs to form heterotypic interactions within foreign microenvironment, with subsequent development of micrometastases

Acknowledgments I would like to acknowledge all collaborators involved in the different phases of this work. This work was funded by grant from the Department of Defense Prostate Cancer Research Program (PC073977), and NIH/RCMI G12 RR03059-21A1.

References

1. Kahn LB, Uys CJ, Dale J, Rutherfoord S (1978) Carcinoma of the breast with metaplasia to chondrosarcoma: a light and electron microscopic study. Histopathology 2:93–106
2. Hay ED, Zuk A (1995) Transformations between epithelium and mesenchyme: normal, pathological, and experimentally induced. Am J Kidney Dis 26:678–690
3. Ehrlich JS, Hansen MD, Nelson WJ (2002) Spatiotemporal regulation of Rac1 localization and lamellipodia dynamics during epithelial cell-cell adhesion. Dev Cell 3:259–270
4. Akhtar N, Hudson KR, Hotchin NA (2000) Co-localization of Rac1 and E-cadherin in human epidermal keratinocytes. Cell Adhes Commun 7: 465–476
5. Ray ME, Mehra R, Sandler HM, Daignault S, Shah RB (2006) E-cadherin protein expression predicts prostate cancer salvage radiotherapy outcomes. J Urol 176:1409–1414, discussion 14
6. Hennig G, Behrens J, Truss M, Frisch S, Reichmann E, Birchmeier W (1995) Progression of carcinoma cells is associated with alterations in chromatin structure and factor binding at the E-cadherin promoter in vivo. Oncogene 11:475–484
7. Graff JR, Herman JG, Lapidus RG et al (1995) E-cadherin expression is silenced by DNA hypermethylation in human breast and prostate carcinomas. Cancer Res 55:5195–5199
8. Machado JC, Oliveira C, Carvalho R et al (2001) E-cadherin gene (CDH1) promoter methylation as the second hit in sporadic diffuse gastric carcinoma. Oncogene 20:1525–1528

9. Berx G, Becker KF, Hofler H, van Roy F (1998) Mutations of the human E-cadherin (CDH1) gene. Hum Mutat 12:226–237
10. Hirohashi S (1998) Inactivation of the E-cadherin-mediated cell adhesion system in human cancers. Am J Pathol 153:333–339
11. Jennbacken K, Tesan T, Wang W, Gustavsson H, Damber JE, Welen K (2010) N-cadherin increases after androgen deprivation and is associated with metastasis in prostate cancer. Endocr Relat Cancer 17:469–479
12. Tanaka H, Kono E, Tran CP et al (2010) Monoclonal antibody targeting of N-cadherin inhibits prostate cancer growth, metastasis and castration resistance. Nat Med 16:1414–1420
13. Tran NL, Nagle RB, Cress AE, Heimark RL (1999) N-cadherin expression in human prostate carcinoma cell lines. An epithelial-mesenchymal transformation mediating adhesion with stromal cells. Am J Pathol 155:787–798
14. Odero-Marah VA, Wang R, Chu G et al (2008) Receptor activator of NF-kappaB ligand (RANKL) expression is associated with epithelial to mesenchymal transition in human prostate cancer cells. Cell Res 18:858–870
15. Liu J, Uygur B, Zhang Z et al (2010) Slug inhibits proliferation of human prostate cancer cells via down-regulation of cyclin D1 expression. Prostate 70: 1768–1777
16. Emadi Baygi M, Soheili ZS, Schmitz I, Sameie S, Schulz WA (2010) Snail regulates cell survival and inhibits cellular senescence in human metastatic prostate cancer cell lines. Cell Biol Toxicol 26:553–567
17. Kwok WK, Ling MT, Lee TW et al (2005) Up-regulation of TWIST in prostate cancer and its implication as a therapeutic target. Cancer Res 65: 5153–5162
18. Yuen HF, Chan YP, Wong ML et al (2007) Upregulation of twist in oesophageal squamous cell carcinoma is associated with neoplastic transformation and distant metastasis. J Clin Pathol 60:510–514
19. Downing JR, Reynolds AB (1991) PDGF, CSF-1, and EGF induce tyrosine phosphorylation of p120, a pp 60src transformation-associated substrate. Oncogene 6:607–613
20. Hazan RB, Norton L (1998) The epidermal growth factor receptor modulates the interaction of E-cadherin with the actin cytoskeleton. J Biol Chem 273: 9078–9084
21. Andl CD, Mizushima T, Nakagawa H et al (2003) Epidermal growth factor receptor mediates increased cell proliferation, migration, and aggregation in esophageal keratinocytes in vitro and in vivo. J Biol Chem 278:1824–1830
22. Kassis J, Moellinger J, Lo H, Greenberg NM, Kim HG, Wells A (1999) A role for phospholipase C-gamma-mediated signaling in tumor cell invasion. Clin Cancer Res 5:2251–2260
23. Nakashiro K, Okamoto M, Hayashi Y, Oyasu R (2000) Hepatocyte growth factor secreted by prostate-derived stromal cells stimulates growth of androgen-independent human prostatic carcinoma cells. Am J Pathol 157: 795–803
24. Yates C, Wells A, Turner T (2005) Luteinising hormone-releasing hormone analogue reverses the cell adhesion profile of EGFR overexpressing DU-145 human prostate carcinoma subline. Br J Cancer 92:366–375
25. Davies G, Jiang WG, Mason MD (2001) HGF/SF modifies the interaction between its receptor c-Met, and the E-cadherin/catenin complex in prostate cancer cells. Int J Mol Med 7:385–388
26. Josson S, Anderson CS, Sung SY et al (2011) Inhibition of ADAM9 expression induces epithelial phenotypic alterations and sensitizes human prostate cancer cells to radiation and chemotherapy. Prostate 71(3):232–240
27. Graham TR, Zhau HE, Odero-Marah VA et al (2008) Insulin-like growth factor-I-dependent up-regulation of ZEB1 drives epithelial-to-mesenchymal transition in human prostate cancer cells. Cancer Res 68: 2479–2488
28. Yates C, Shepard CR, Papworth G et al (2007) Novel three-dimensional organotypic liver bioreactor to directly visualize early events in metastatic progression. Adv Cancer Res 97:225–246
29. Yates CC, Shepard CR, Stolz DB, Wells A (2007) Co-culturing human prostate carcinoma cells with hepatocytes leads to increased expression of E-cadherin. Br J Cancer 96:1246–1252
30. Li LC, Zhao H, Nakajima K et al (2001) Methylation of the E-cadherin gene promoter correlates with progression of prostate cancer. J Urol 166:705–709
31. Ma L, Teruya-Feldstein J, Weinberg RA (2007) Tumour invasion and metastasis initiated by microRNA-10b in breast cancer. Nature 449:682–688
32. Lehmann U, Hasemeier B, Christgen M et al (2008) Epigenetic inactivation of microRNA gene hsa-mir-9-1 in human breast cancer. J Pathol 214:17–24
33. Dalmay T, Edwards DR (2006) MicroRNAs and the hallmarks of cancer. Oncogene 25:6170–6175
34. Kong D, Li Y, Wang Z et al (2009) miR-200 regulates PDGF-D-mediated epithelial-mesenchymal transition, adhesion, and invasion of prostate cancer cells. Stem Cells 27:1712–1721
35. Wu TT, Sikes RA, Cui Q et al (1998) Establishing human prostate cancer cell xenografts in bone: induction of osteoblastic reaction by prostate-specific antigen-producing tumors in athymic and SCID/bg mice using LNCaP and lineage-derived metastatic sublines. Int J Cancer 77:887–894
36. Zhau HE, Li CL, Chung LW (2000) Establishment of human prostate carcinoma skeletal metastasis models. Cancer 88:2995–3001
37. Paget S (1889) The distribution of secondary growths in cancer of the breast. Cancer Metastasis Rev 8:98–101
38. Chung LW (2003) Prostate carcinoma bone-stroma interaction and its biologic and therapeutic implications. Cancer 97:772–778

Provisional Patient Application

Hogan Lovells

Hogan Lovells US LLP
Columbia Square
555 Thirteenth Street, NW
Washington, DC 20004
T +1 202 637 5600
F +1 202 637 5910
www.hoganlovells.com

June 30, 2011

VIA EMAIL: *fmgrant@tuskegee.edu*

Ms. Felecia Moss Grant, Assistant Director
Office of Grantsmanship & Compliance
Tuskegee University
103 Chappie James Center
Tuskegee Institute, Alabama 36088

Re: U.S. Provisional Application No.: 61/420,618
Title: BIOMARKERS FOR PROSTATE AND BREAST CANCER PATIENTS
Inventor(s): YATES, Clayton
Our Ref: 57193-0012PRO

Dear Ms. Grant

In furtherance to our letters dated March 8, 2011 in regards to the above-referenced application, this is a reminder that in order to get the benefit of this provisional applications, a PCT or other non-provisional application must be filed within one year of the filing date of this provisional applications, which is by **December 7, 2011**. Therefore, request your instructions by **November 7, 2011**.

We will continue to keep you advised regarding this application. In the meantime, should you have any questions, please do not hesitate to contact us.

Very truly yours,

Kevin G. Shaw

Counsel
kevin.shaw@hoganlovells.com
D +1 202 637 6466

Enclosure